Processing for properties

1 Processing for Properties

Han E. H. Meijer

Centre for Polymers and Composites (CPC), Eindhoven Polymer Laboratories, Eindhoven University of Technology, Eindhoven, The Netherlands

List of Symbols and Abbreviations

Ca	capillary number
d	membrane thickness
D	diffusion constant
De	Deborah number
D_{Ic}	critical thickness/interparticle distance
G	gas
G'	shear modulus
h	mold thickness
H	characteristic geometric dimension; channel depth
J	flux
L	liquid
M_c	molecular weight between crosslinks
M_e	molecular weight between entanglement points
N_1	first normal stress difference
p	viscosity ratio, pressure
P	permeability
R	drop radius
S	solubility
t	time
T	temperature
T_c	crystallization temperature
t_d	delay time
T_g	glass transition temperature
T_m	melting temperature
T_{eff}	effective temperature
T_{pol}	polymerization temperature
V	process velocity
v_p	piston velocity
x, y, z	Cartesian coordinates
α	selectivity or separation parameter
δ	gap height
$\dot{\gamma}$	shear rate
ε	dimensionless parameter in PTT model
η_c	viscosity of continuous phase
η_d	viscosity of dispersed phase
λ	fluid relaxation time
ξ	dimensionless parameter in PTT model
ρ	density
σ	stress
τ	shear stress
ABS	acrylonitrile–butadiene–styrene
BA	butylmethacrylate

BMC	bulk molding compounds
B.P.	Berghmans point
CA	cellulose acetate
CIPS	chemically induced phase separation
CTM	cavity transfer mixer
DIPS	diffusion-induced phase separation
DR	draw ratio
DSC	differential scanning calorimetry
EtOH	ethanol
FDM	finite difference method
FEM	finite element method
FIB	flow-induced birefringence
GAIM	gas-assisted injection molding
GMC	glassfiber (mats) reinforced compounds
GPC	gel permeation chromatography
HDPE	high density polyethylene
HIPS	high impact polystyrene
HPF	high performance fibers
HPPE	high performance polyethylene
IPN	interpenetrating network
LDA	laser Doppler anemometry
LDPE	low density polyethylene
MD	machine direction
MeOH	methanol
MFI	melt flow index
MMA	methylmethacrylate
MMIM	multi-material injection molding
NMP	*n*-methyl pyrrolidone
PAR	polyarylate
PC	polycarbonate
PEI	polyetherimide
PES	polyethersulfone
PETP	poly(ethylene terephthalate)
PH	polyhydroxyether
PIB	polyisobutene
PMMA	poly(methylmethacrylate)
PP	polypropylene
PPE	poly(phenylene-ether)
PS	polystyrene
PSF	polysulfone
PTT	Phan-Thien Tanner
PUR	polyurethane
REX	reactive extrusion
RIM	reaction injection molding
RMP	reactor modified polymers

ROA	rheo-optical analyzer
RRIM	reinforced reaction injection molding
RTM	resin transfer molding
SAXS	small angle X-ray scattering
SBR	styrene–butadiene rubber
SRIM	structural reaction injection molding
S	solid
St	styrene
STP	standard temperature and pressure
SUPG	streamline upwind method
TCE	trichloroethylene
TD	transverse direction
TIPS	temperature-induced phase separation
UHMWPE	ultrahigh molecular weight polyethylene
WAXS	wide angle X-ray scattering

1.1 Introduction

Given their intrinsically anisotropic nature [with strong intramolecular covalent bonds in the backbone, weak intermolecular interactions of secondary van der Waals and/or hydrogen bonds, and the physical network (entanglement) forces] polymers can be considered as the prime example of materials where neither the chemical structure nor the design solely determines the product's properties. As a consequence, in polymer technology the complete "chain of knowledge" is explored, from pure synthesis (organic chemistry), via catalysis, reactor technology (chemical engineering) and polymer design or the development of new polymeric systems (polymer chemistry and physics), to the final shaping process and product design (mechanical engineering). In the processing of polymers, the topic of this Volume, the whole, complex, deformation-temperature history proves to be relevant and, as a consequence, this research area is based on (relatively advanced) computational methods on the one hand and rheology on the other.

Most important for polymers is their ease of processability via automated mass production technologies. The prime example thereof is the injection molding process, where processability is exploited through freedom in materials choice and product design. Apart from related processes, e.g., (reinforced or structural) reactive molding, transfer molding, and pressing, the continuous processing techniques e.g., profile extrusion, film casting, film blowing, and blow molding, find extensive applications. Processes like these have attracted a great deal of attention, resulting in optimization processes with respect to controlled production and in the prediction of the influence of process parameters on the consistency and quality of the production process. This control results partly from (a large number of) experiments, yielding practical expertise, and partly from mathematical modeling (Chap. 2 of this Volume).

The trends in modeling nowadays are such that attention is focused on the prediction of product properties, given the material and production process selected, the processing conditions, and the final product design. Purely because of its great practical importance, the injection molding process has been chosen as the, given its complexity, not so much obvious, but certainly the most relevant process to be modeled. Substantial progress has been made in the last few years in predicting, e.g., the accuracy and dimensional stability, in the short and the long term, of injection molded products.

Polymers are rarely used in their virgin form. Mostly additives are used, from stabilizers and antioxidants, color pigments, and reinforcing agents, such as fillers and fibers, to dispersed rubber inclusions in order to obtain improved impact properties. Mixing in the molten state is, consequently, inherently part of polymer processing. The resulting morphology strongly determines the final properties (Chaps. 3 and 12 of this Volume), and interfacial design proves to be relevant for the final application (Chaps. 8 and 15 of this Volume). Reactions often occur during processing and the macromolecules forming the continuous phase, the compatibilizers at the interfaces, or the dispersed phase itself, are made in situ (Chaps. 6, 7, 8, and 9 of this Volume). Crystallizable polymers form heterogeneous structures upon crystallization and the temperature–deformation history strongly influences the resulting microstructure (Chaps. 4 and 5 of this Volume).

While the mechanical (and thermal) properties of polymeric materials, with modulus values of typically 3 GPa and strength values of 0.05 GPa, are generally far inferior

to those of competitive structural materials, like metals and ceramics, processing techniques have been developed to explore the maximum theoretical values of polymers if they are loaded not by their weak secondary bonds, but by their strong covalent bonds. Exceptional values for the modulus and strength of 150 and 4 GPa are now realized and, given their low density, the specific values for polymers are by far superior to those of the more classical structural materials. A prerequisite for obtaining these rather spectacular mechanical properties is full alignment of the chains, in order to be able to load the covalent bonds. The shape of the product is, necessarily, a fiber, and some of the properties are lost again if 2- or 3-dimensional structures have to be made using fiber-reinforced composites. Basically, two different techniques are available to orient the chains. The first starting with completely stiff molecules that, consequently, have to be spun from solutions to orient them in a dry, wet, or air-gap spinning operation, and second, a method based on flexible molecules that are stretched in the solid state (Chaps. 11 and 16 of this Volume). Thermotropic polymers can be regarded as intermediates between these extremes, and processability is introduced by generating flexibility in the molecular structure, either by alternating stiff and flexible segments ("spacers") in the main chain or by adding flexibility, or alternatively rigidity, to the polymer side chains. These examples already reveal the great potential of polymers, given the enormous flexibility in adjusting their basic structure, via chemistry, or alternatively by changing their morphology via physical or chemo-physical processes such as (reactive) blending or by introducing orientation.

For the group of functional polymers, special processing techniques have been developed, e.g., spin-coating, and different light-controlled in situ polymerization processes combined with selective dissolution methods (see Chap. 13 of this Volume). An area of great importance is that of the intrinsic conductive polymers which, being conjugated, without exception can be regarded as intractable from a processing point of view. However, new developments are also promising here, and interesting results have already been obtained (Chap. 14 of this Volume). Similar arguments hold for polymers (and their processing techniques) that are being developed for their optical properties. Apart from specific applications, e.g., the development of graded index optical fibers, the bulk properties are also investigated, and by controlling the microstructure, optical clarity can sometimes be combined with obtaining the intrinsic ultimate toughness of the polymers. For this purpose, specific processing routes have been developed, based on systems where reactive diluents are used to help processability and where, after molding or shaping, the reactive solvents are polymerized and thus converted into nonsolvents. The concomitant phase separation is often accompanied by phase inversion, and yields specific morphologies that cannot be realized by more conventional processing techniques (see Chap. 10 of this Volume).

In this introductory chapter, we will review some of these developments, focusing on how processing enhances the product's properties. The content of this chapter more or less follows that of Vol. 18 of this Series. It starts with a summary of what has been obtained to date with advanced modeling (Sec. 1.2). Attention is then given to structure development during flow. Apart from the classical fluid–fluid mixing, the TIPS, DIPS (Sec. 1.3) and CIPS (Sec. 1.4) processes (temperature, diffusion, and chemically induced phase separation processes, respectively) will be dealt

with in somewhat more detail and some remarks on crystallization during processing are made. That processing can be used to attain the ultimate properties in terms of stiffness and strength on the one hand and toughness on the other is clearly illustrated (Sec. 1.5). Finally, a short review on extruder modeling is given (Sec. 1.6) and some concluding remarks are made (Sec. 1.7).

1.2 Modeling Aspects

1.2.1 Introduction

The recent development of powerful and relatively cheap computer hardware, in the form of easily accessable workstations, which can eventually be combined via a high capacity ethernet to form complex networks, has evoked an explosive development of user-friendly computer software. The consequences of these developments in the area of modeling polymer processes have been substantial. Classically, processing handbooks were mainly based on qualitative reasoning and the solution of, bascially one-dimensional, differential equations, see, e.g., the textbooks of McKelvey (1962), Middleman (1968, 1977), Tadmor and Klein (1971), Bernhardt (1974), Ziabicki (1976), Funt (1976), Janssen (1978), Tadmor and Gogos (1979), Fenner (1970, 1979), Potente (1981), Rauwendaal (1986), and Macosko (1989). Nowadays, the combination of 3D continuum mechanics and computational mechanics in the analysis of polymer processes is attempted, see, e.g., the textbook on transport phenomena by Bird et al. (1960) and those on polymer processing by Petrie (1979), Pearson (1985), Pearson and Richardson (1983), Tucker (1989), Thomson et al. (1989), Isayev (1987, 1990), White (1990 a, b), and Agassant (1991), based on the 3D-material description in rheological textbooks by, e.g., Lodge (1964), Ferry (1980), Astarita and Marrucci (1974), Schowalter (1978), Janeschitz-Kriegl (1983), Crochet et al. (1984), Tanner (1985), Doi and Edward (1986), Bird et al. (1987), Larson (1988), Joseph (1990), and Macosko (1994).

As a result, present research is no longer so much aimed at the description of the process under consideration, but merely at the prediction of product properties resulting from the total preparation (e.g., compounding) and final shaping processes. In this respect, textbooks publications lag behind and most of this work is published in theses and in the open literature, where the combination of advanced rheology and computational methods in the analysis of polymer processes is attempted. Interestingly, in most cases the necessary assumptions made to enable careful analysis of the production process are less severe than the uncertainties in the input data, specifically in the constitutive equations. This holds not only for the (rheological) constitutive equation for the Cauchy stress tensor, which is the subject of the rheological textbooks mentioned earlier, but also for those for the density, the (anisotropic) heat conduction, nucleation-induced crystallization, and the kinetics of reactions and phase separation. In summary, those equations that describe the structure development in anisotropic, heterogeneous systems. As a consequence, a lot of basic research is devoted to a detailed study of the distinct processes that occur on a local scale. Implementation of these, generally microscopic, events in the macroscopic flow equations is not a straightforward task. Local processes could influence the continuum processes and vice versa. Generally, extra assumptions are needed, specifically on their possible mutual interactions. Moreover, polymer physics then becomes invol-

ved in the research area of polymer processing analysis and this not only makes the research necessarily multi-disciplinary, but also complicates the whole issue considerably. This holds especially for the rheology and the microrheology. Constitutive equations proposed for the description of polymer solutions and melts have been without exception tested only in weak, rotational, simple shear flows. It is known, however, that their descriptions of a material's behavior in strong, irrotational extension flows differ considerably (Walters, 1992; Hudson and Jones, 1993). Up to now, there has been no real possibility of testing the materials in these flows, although many attempts to design new equipment for the analysis of stretching flows have recently been undertaken. Examples include the Rheostrain, as developed by Vinogradov et al. (1970), Franck and Meissner (1984), and Munstedt (1975, 1979); a revival of the Rheotens, as promoted by Wagner (1994, 1996); the Rheometrics extensional rheometer, as developed by Meissner (1969, 1971, 1992), Meissner et al. (1981, 1982), Meissner and Hostettler (1992), and Li et al. (1990), all for polymer melts; while for polymer solutions we find the opposed tube device, as developed by Keller et al. (1987), Fuller et al. (1987), Mikkelsen et al. (1988), Schunk et al. (1990), and Schunk and Scriven (1990), and the constant strain rate test device, as investigated by McKinley (1995) and Van Nieuwkoop and Muller von Czernicki (1997). Only the future can show whether these new apparatuses will function properly. For the time being, in polymer processing, where typically complex flows prevail, which combine shear and elongational flow, researchers have to live with a multitude of constitutive equations, which should be tested in real practice. Nevertheless, some attempts have been made to test rheological equations in (generally 2D, isothermal) complex flow, using the so-called hybrid experimental numerical technique [see, e.g., Hendriks et al. (1990), Oomens et al. (1993), Baaijens (1994c), and Baaijens et al. (1994, 1995)].

1.2.2 Injection Molding

As an example of what can be obtained nowadays, we will focus for a start on the prediction of the properties of injection molded products. Given the relevance of this process for daily practice, over the years a lot of attention has been paid by different research groups all over the world to the modeling of injection molding [and related processes such as RIM (reaction injection molding), RRIM or SRIM (reinforced or structural RIM), RTM (Resin transfer molding), and pressing]. See, e.g., Hieber and Shen (1980), Hieber et al. (1983), and Chiang et al. (1991 a, b), who developed C-flow; Boshouwers and van der Werf (1988), who developed Inject-3; the CEMEF code originating from Agassant's group (see, e.g., Chap. 2 of this Volume); Polyflow as developed by Crochet's group [see, e.g., Crochet and Legat (1992), Fan and Crochet (1995)], based on which the code Polymold for injection molding was derived; Kennedy (1993) who developed Moldflow in its new release; Dupret and Vanderschuren (1988) and Couniot et al. (1993), who improved the Louvain-la-Neuve code; Papathanasiou and Kamal (1993) and Nguyen and Kamal (1993), who developed their viscoelastic code; and finally, the VIp code, as developed by our group, Sitters (1988), Douven (1991), Vos et al. (1991), Peters et al. (1994), Douven et al. (1995), Caspers (1995), and Zoetelief (1995).

All modern modeling is based on the so-called 2.5D approach, originally developed at Cornell University by Hieber and Shen. In this approach the temperature and veloc-

ity fields are solved in full 3D and the pressure equation in 2D, applying the lubrification approximation (Hieber and Shen, 1980; Hieber et al., 1983). A combined FEM/FDM (finite element/finite difference method) is used, with the finite elements applied in the midplane of the cavity and the finite differences added at every nodal point in the perpendicular direction. This elegant method combines the flexibility of the finite elements necessary to describe complex products, with the high resolution required in the off-plane direction, given the large gradients in temperature and velocity that are present here, without yielding unrealistic and thus unworkable computing times. Typically the influence of the process parameters was obtained from these analyses. Examples include the prediction of the position of the flow front, thus predicting air inclusions and yielding opportunities to optimize the position and number of the gates. Furthermore, the pressure and velocity field resulted, thus allowing for an evaluation of the machine size and clamping force to be used. Finally the temperature profiles were computed, thus yielding predictions for possible local hot spots, and more importantly, the cooling time and thus the process cycle time. These analyses could even be performed for products that have relatively complex shapes.

Accordingly, different groups developed similar codes, adding, for example, the possibility to analyze reactive molding, to process crystallizable materials, to predict fiber orientation, to simulate gas injection, etc. (Hayes, 1991; Liang et al., 1993; Saiu et al., 1992; Cintra and Tucker, 1994; Turng and Wang, 1991; Turng et al., 1993). The VIp code was developed as an extension of the above research in the direction of the prediction of product properties. Since these properties generally depend on the complete thermo-mechanical deformation history of every material element during flow, it proved to be of utmost importance to follow every individual "particle" during processing. This particle tracking required the solution of an extra equation, the equation of conservation of identity. This is a pure convection equation which is extremely difficult to solve accurately, and the results were experimentally checked by using tracers in the form of multicolors. In this way, multimaterial injection molding, where different materials are sequentially or simultaneously injected into the mold, could also be analyzed (Vos et al., 1991; Peters et al., 1994). Moreover, product properties, e.g., accuracy and dimensional stability (Sec. 1.2.3), prove to depend on the total density distribution on the one hand and the flow, temperature, and pressure-induced frozen-in stresses on the other (Sec. 1.2.4). The first requires a temperature and time history dependent constitutive equation for the density, e.g., the KAHR model (Kovacs et al., 1979), while the latter requires the temperature, time, and deformation history dependent constitutive equation for the stress tensor (Sec. 1.2.6). Different viscoelastic constitutive equations, of both the integral and differential type, were used. The problem is as mentioned, to find the correct material parameters for these equations (Sec. 1.2.5). Nevertheless, the first results look promising. This can be illustrated by the comparison of predicted experimentally determined values for different relevant quantities, using a simple strip only.

1.2.3 Dimensional Stability

In Fig. 1-1 the change with time of three important dimensions of this elementary strip are shown, yielding its dimensional (in)stability. The comparison of theory and experiment is amazing especially if it is realized that these changes in dimension depend

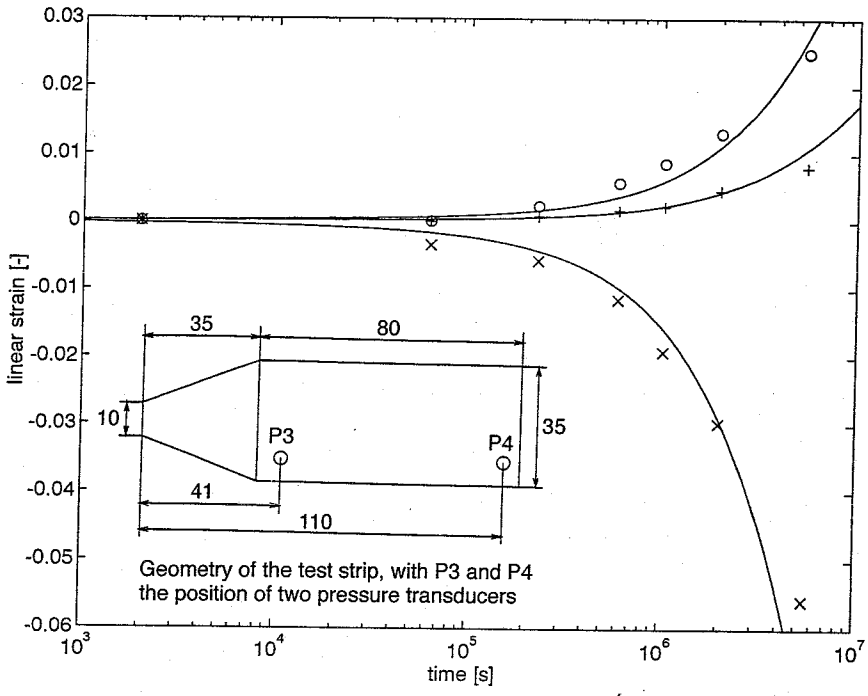

Figure 1-1. Measured (symbols) and predicted (lines) strain due to recovery of the length (×, –), and width at 75 (○, –) and 110 (+, –) mm from the gate. Storage temperature 343 K (Caspers, 1995).

on the combined action of a multitude of parameters, e.g., the density distribution and the frozen-in thermal (and pressure-induced) stresses, which yield short-time warpage, and the frozen-in flow-induced stresses, which represent the molecular orientation and determine the long term stability. The only manipulation that has been applied to the above calculations is that the storage temperature was taken as 4 °C higher (74 °C) than in the experiments (70 °C). The calculated results proved to be extremely dependent on this temperature, shifting the time axis by one decade for a change of only 4 °C.

Figure 1-2 shows the predicted and measured pressure profiles with time, at three different locations on the strip. As usual, the pressure at the gate is taken as the initial condition. The predictions further downstream differ markedly from the experimentally determined values. Simulation with the code revealed that this is due to inaccuracy in the data for the density, which controls the whole process in the post-filling stage where the discrepancy occurs, and not so much to problems with the rheological constitutive equation, wrong values for the thermal boundary conditions, or the influence of mold elasticity.

1.2.4 Density and Stress Distributions

Changes in density upon cooling directly affect the short term dimensions of the molded product and give rise to shrinkage. Apart from long term effects, like physical ageing (the slow but continuous tendency of a material to increase its density by better segmental packing), these changes in density can cause anisotropic shrinkage, given

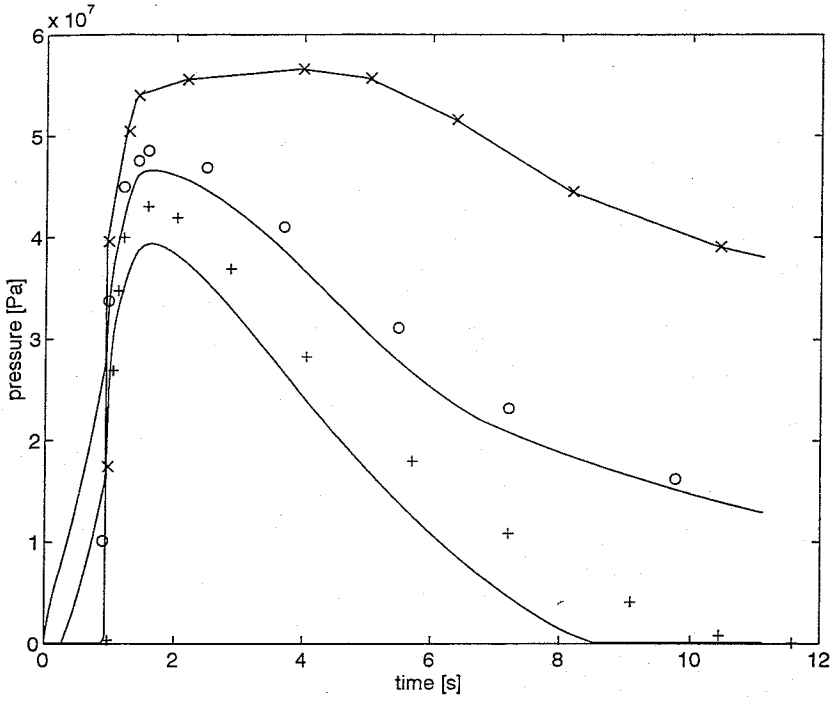

Figure 1-2. Measured (symbols) and predicted (lines) pressure distribution as a function of time, at the gate (×), at P3 (○), and at P4 (+); for their position see Fig. 1-1 (Caspers, 1995).

the 3D density profiles that result from the molding process. In Figs. 1-3 and 1-4, the density distributions throughout the product are given for several processing conditions. The comparison between experimental values and predictions is clearly only qualitative. More attention should be paid to the experimental determination of the parameters in the constitutive equation for the density. This is not straightforward, task, given the severe conditions, with respect to high pressures combined with extreme temperature gradients and fast cooling rates, that occur in injection molding [see, e.g., Piccarolo (1992), Piccarolo et al. (1992), and Brucato et al. (1993)].

The second influence on short-term changes in the dimensions of a product is caused by the occurrence of thermal stresses. They also cause warpage of the product in the case of asymmetric cooling. The development of temperature (and pressure) induced enthalpic stresses during molding is illustrated in Fig. 1-5. Typically for injection molding, as compared to pressureless shaping processes (e.g., during the cooling of metals and glasses), where similar frozen-in stresses develop due to inhomogeneous cooling, is the occurrence of tensile stresses on the outside of the product. These stresses were first computed (see Fig. 1-5) using linearized forms of the different viscoelastic constitutive equations (which is allowed, given the small deformations in this stress build up) and subsequently experimentally determined (see Fig. 1-6). The last is difficult, since by whatever technique is used to determine the thermal stresses (e.g., birefringence, or, more generally applicable, layer removal), it is

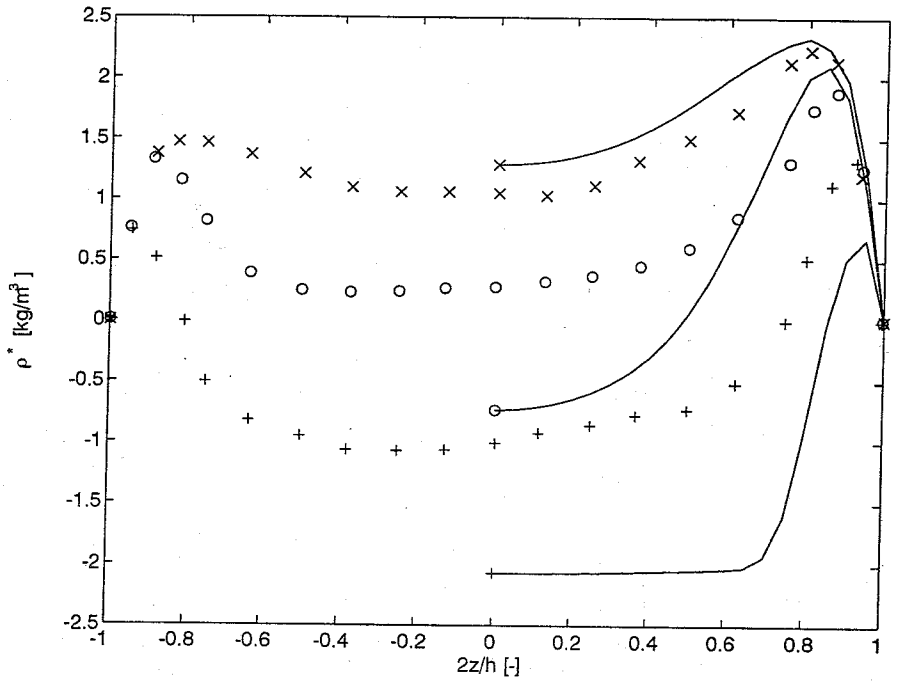

Figure 1-3. Measured (symbols) and predicted (lines) reduced density distributions across the normalized thickness at 8 (×), 28 (○), and 107 (+) mm from the gate (Caspers, 1995).

always extremely difficult to measure accurately close to the walls. In Fig. 1-6 the comparison is made and found to be satisfactory.

Finally, the most difficult to determine stresses are the frozen-in flow-induced stresses, since they depend directly on the quality of the constitutive equation used, combined with an accurate temperature history prediction. Moreover, uncertainties arise given the still unsolved problems that can occur while passing the glass transition region [see, e.g., Wimberger Friedl (1991)]. They give rise to the anisotropic shrinkage found in the long term, especially if the product is stored at relatively high temperatures (see Fig. 1-1). The development of these orientational entropic stresses during the process is depicted in Fig. 1-7, while a quantitative comparison is made in Fig. 1-8. The quality of the prediction is strikingly good, given the problems mentioned above.

The flow-induced stresses can be calculated to a good approximation in a decoupled way, and thus eventually in a post-processing operation, with the kinematics of the process and the temperature history used as input data for the calculation of the stresses, using a viscoelastic constitutive equation (Baaijens and Douven, 1990; Baaijens, 1991; Douven et al., 1995). The kinematics can, in their turn, be calculated with a history-independent, generalized Newtonian rheological constitutive equation. This possibility, which is based on the overruling effect of the boundary and the initial conditions on the kinematics of the flow, which are given in terms of prescribed velocities rather than prescribed stresses, speeds up the calculations of these stresses considerably (with a reduction of the computation

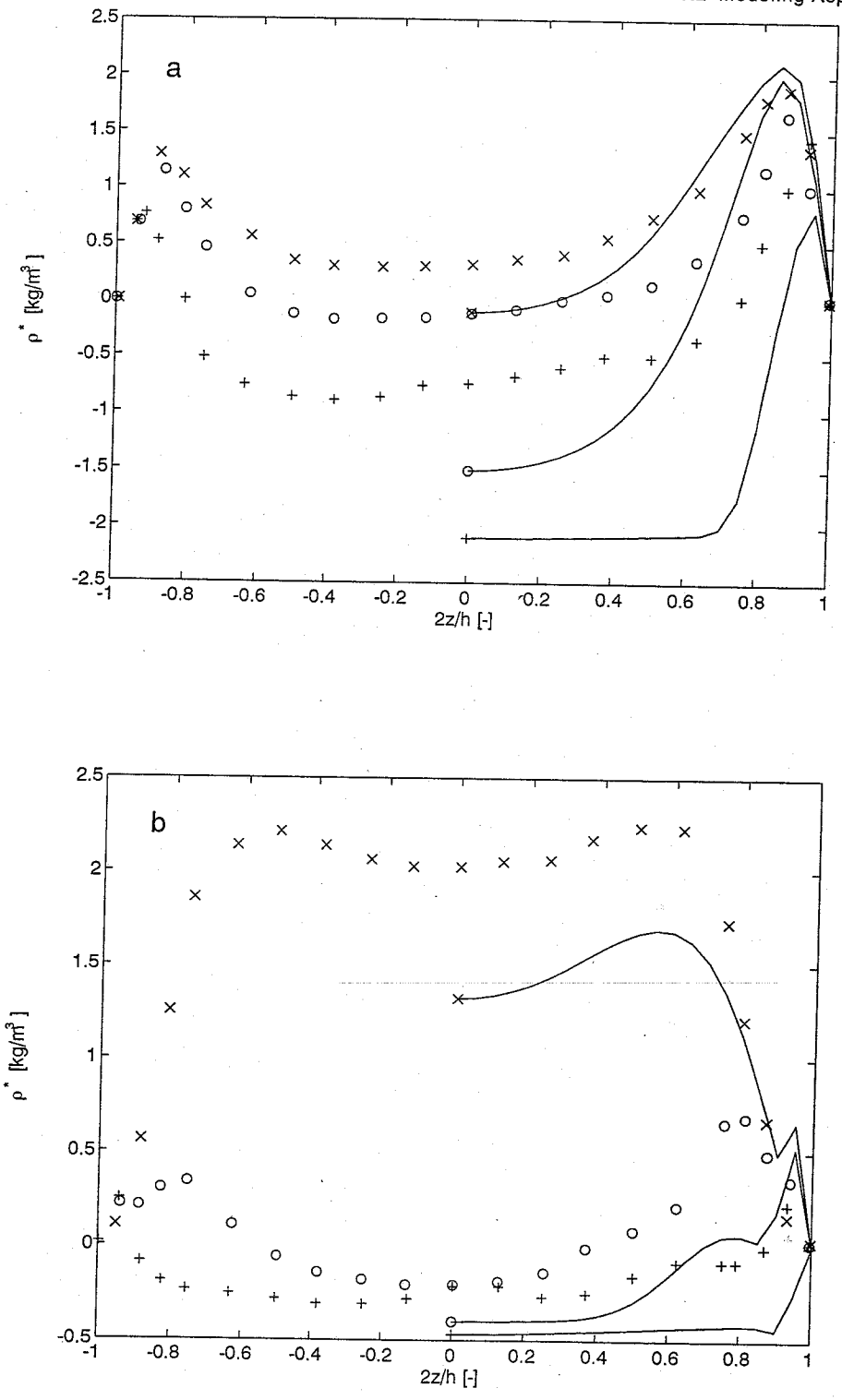

Figure 1-4. As Fig. 1-3, for two different holding pressure profiles (a) decreasing from 80MPa to 20MPa for a holding time of 10s, and (b) increasing from 20 to 80 MPa (Caspers, 1995).

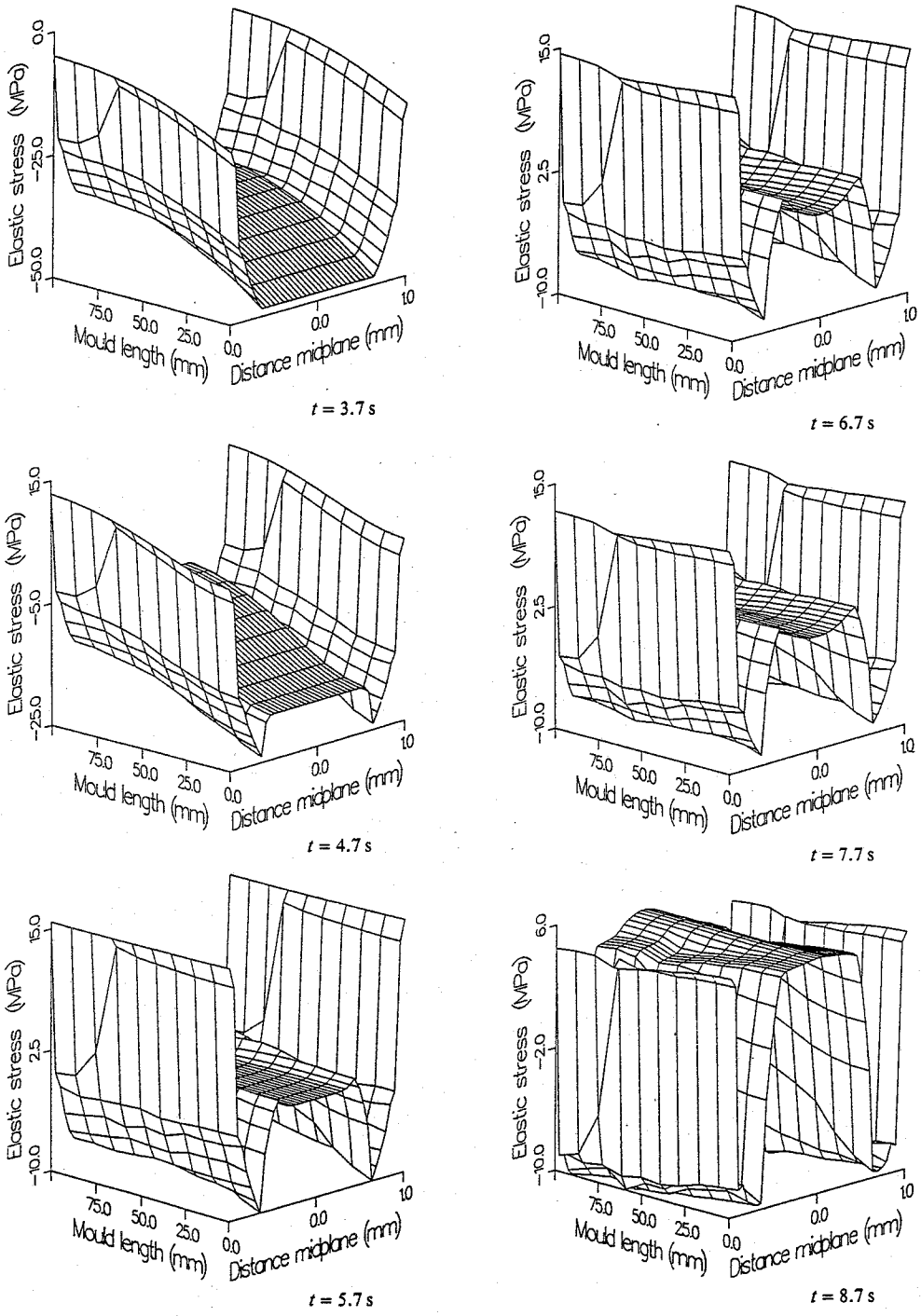

Figure 1-5. Development with time, during injection, holding, and cooling of the temperature and pressure induced stress profiles (σ_{11}) over the thickness and length of the injected strip (Baaijens, 1991).

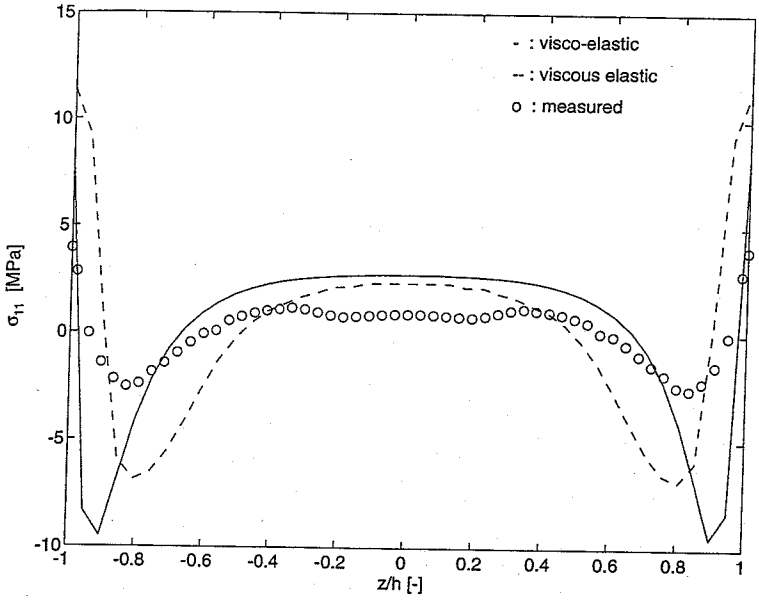

Figure 1-6. Measured (symbols) and predicted [viscoelastic (––), viscous-elastic (–)] residual stress profiles over the thickness of the strip (Zoetelief et al., 1996).

time of 90 %). Similar decoupled calculation methods are applied for the determination of fiber orientation in these kind of flows (Cintra and Tucker, 1994).

1.2.5 Choice of the Constitutive Equation

A major problem encountered in the calculation of flow-induced stresses is the proper choice of the viscoelastic, history dependent, rheological constitutive equation. In the above results, the compressible Leonov model was used. If we fit the rheological data with a KBKZ type of integral model, more specifically with a Wagner model, then the predictions of these stresses differ from the experimental by something like 100 %. This can be reduced to a difference of 20 % if a slight change in the nonlinear damping function, which hardly changes the quality of the fit of the rheological data in shear, is incorporated (Baaijens and Douven, 1990; Baaijens, 1991; Douven et al., 1995). Similar arguments were found in the modeling of the film blowing process (Tas, 1994). Here, an amazing number of film properties, e.g., the modulus, yield stress, tensile strength, elongation to break, and tear resistance, could be related to the stress acting on the frost line, see Figs. 1-9 and 1-10.

In calculating the stress at the frost line, not only does the flow inside the die have to be incorporated, but also a correct choice of the constitutive equation proved to be of utmost importance. A Phan-Thien Tanner (PTT) type model gave much better results then the KBKZ type model (see Fig. 1-11). This is not so much to do with the difference between the integral or the differential constitutive equations, although the numerical analysts generally prefer the latter, but rather with the difference in their description of the nonlinear behavior, especially in elongational flows.

These facts have motivated a number of research groups to use more complex flows to determine the parameters in constitutive equations, via the use of field information rather than boundary information [see, e.g.,

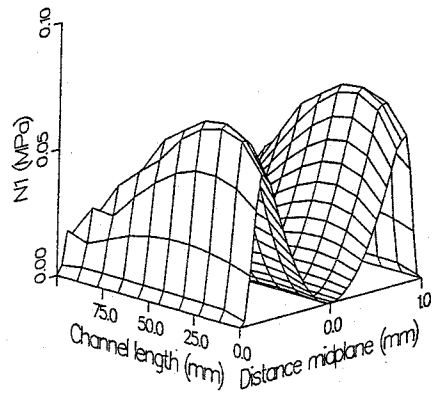

end of filling stage, $t = 0.67$ s

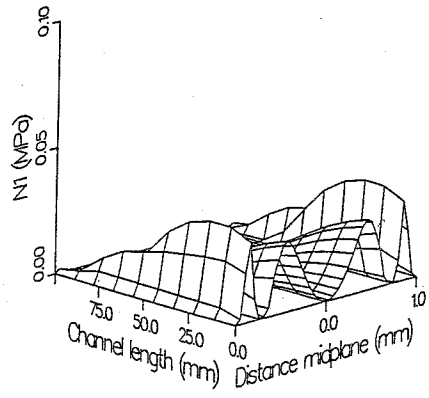

$t = 3.21$ s

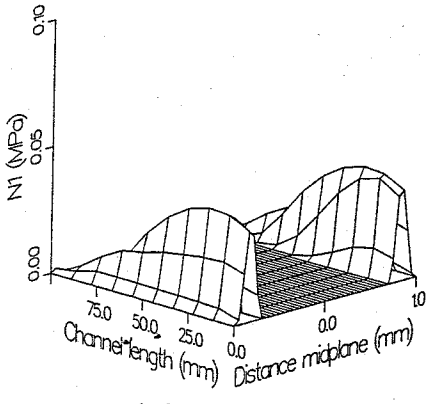

end of compression stage

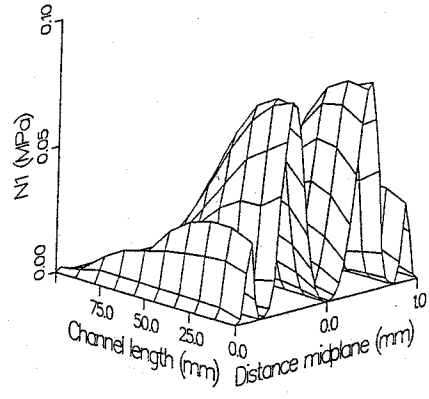

$t = 4.7$ s

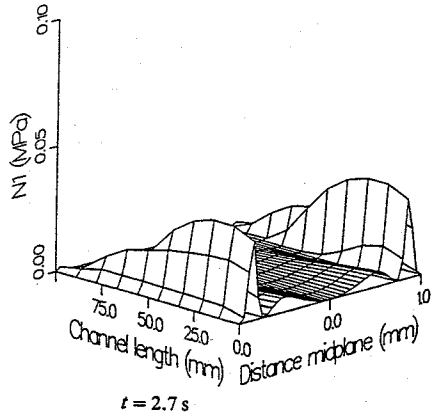

$t = 2.7$ s

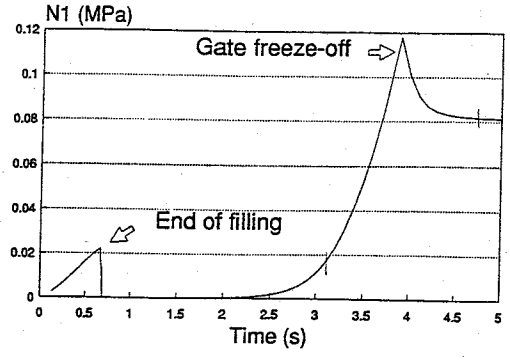

Figure 1-7. Development with time, during injection, holding, and cooling of flow-induced stress profiles (first normal stress difference N_1) over the thickness and length of the injection-molded strip. The bottom right figure gives the N_1 history at $x = 8$ mm, at a distance of 0.35 mm from the midplane, indicating its growth during injection ($\dot{\varepsilon}\uparrow$, $\lambda(T)\downarrow$), the fast decay due to relaxation after the flow stopped, and the steep rise when T_g is approached ($\dot{\varepsilon}\downarrow$, $\lambda(T)\uparrow$) upon further cooling of the product, with $\dot{\varepsilon}$ the deformation rate and $\lambda(T)$, the temperature-dependent relaxation time. For an explanation see Sec. 1.5.2 (Baaijens, 1991).

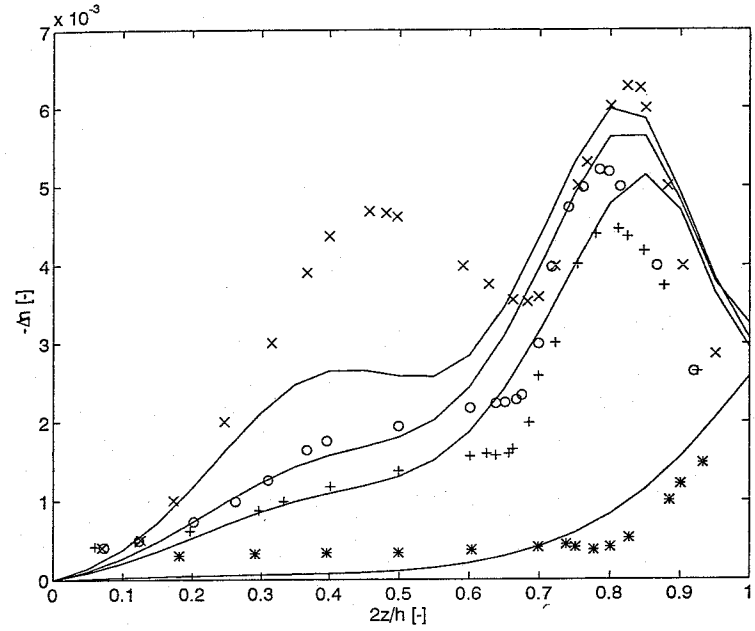

Figure 1-8. Measured (symbols) and predicted (lines) residual birefringence across half the thickness at 25 (×), 41 (○), 60 (+), and 110 (*) mm from the gate (Caspers, 1995).

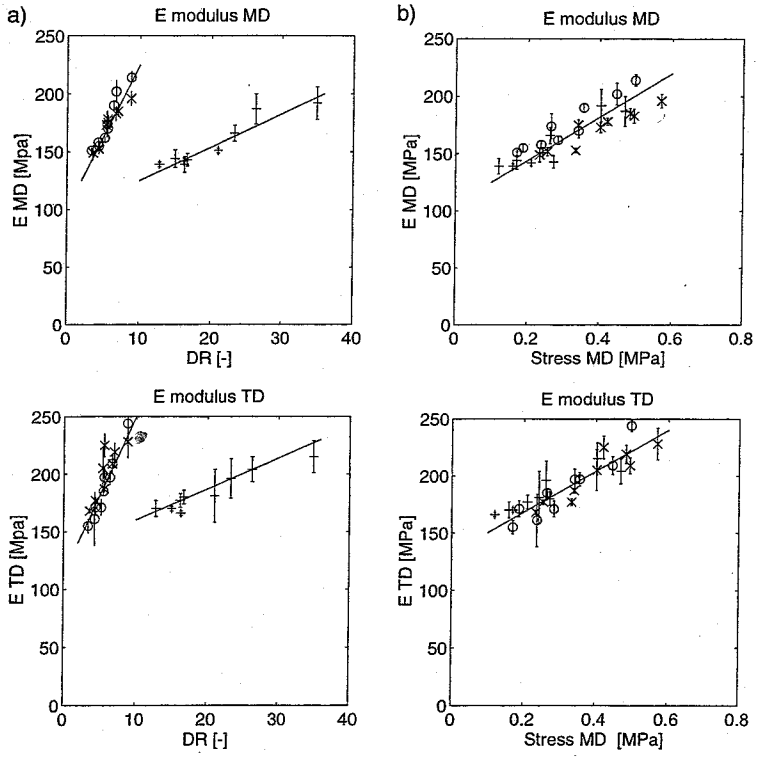

Figure 1-9. Film modulus in machine direction (MD) and transverse direction (TD) versus (a) the macroscopic draw ratio (v_1/v_0) and (b) the stress acting at the frost line, for three types of low density polyethylene (LDPE) of different melt flow index (MFI): L0 (o), L1 (×), (both MFI 1), and L8 (+) (MFI 8) (Tas, 1994).

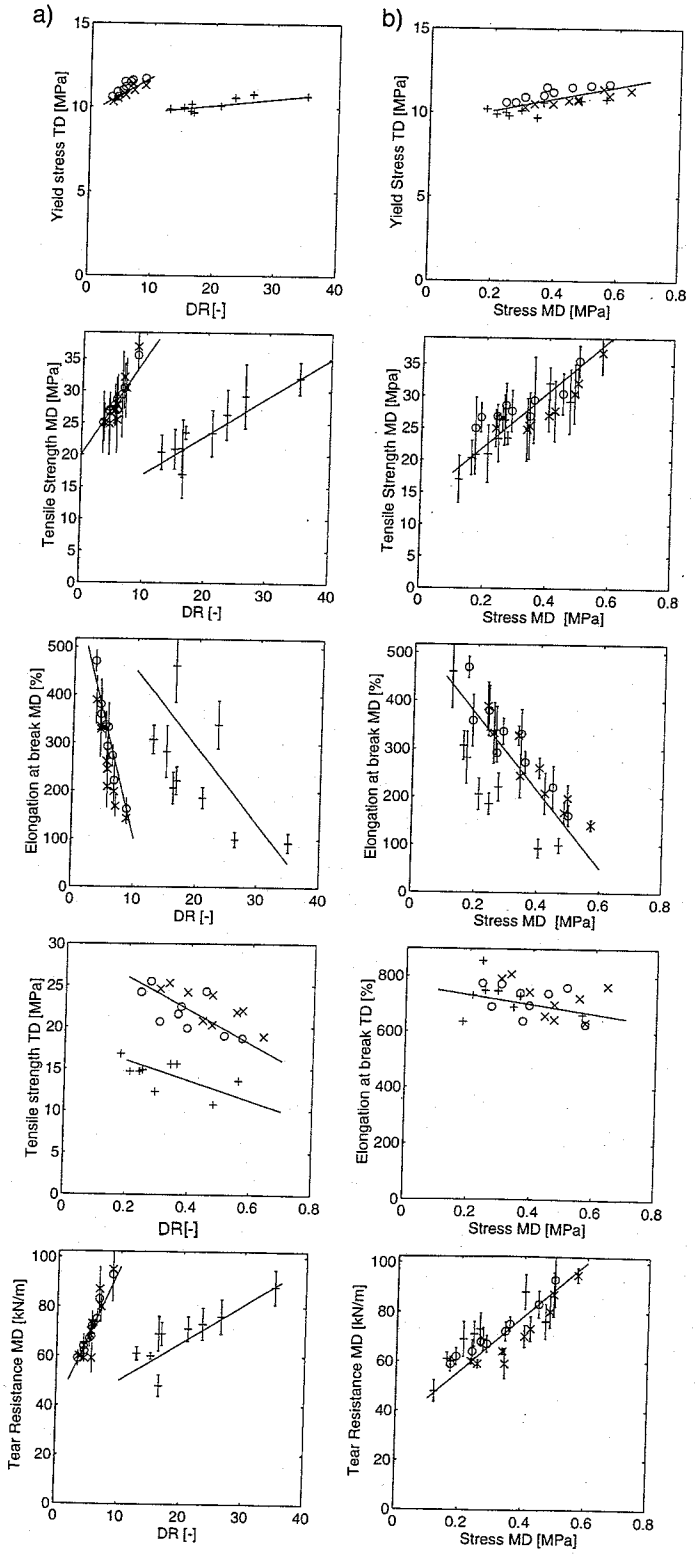

Figure 1-10. As Fig. 1-9, but for the yield stress, the tensile strength in the machine (MD) and the transverse (TD) directions, the elongation to break, and the tear resistance (Tas, 1994).

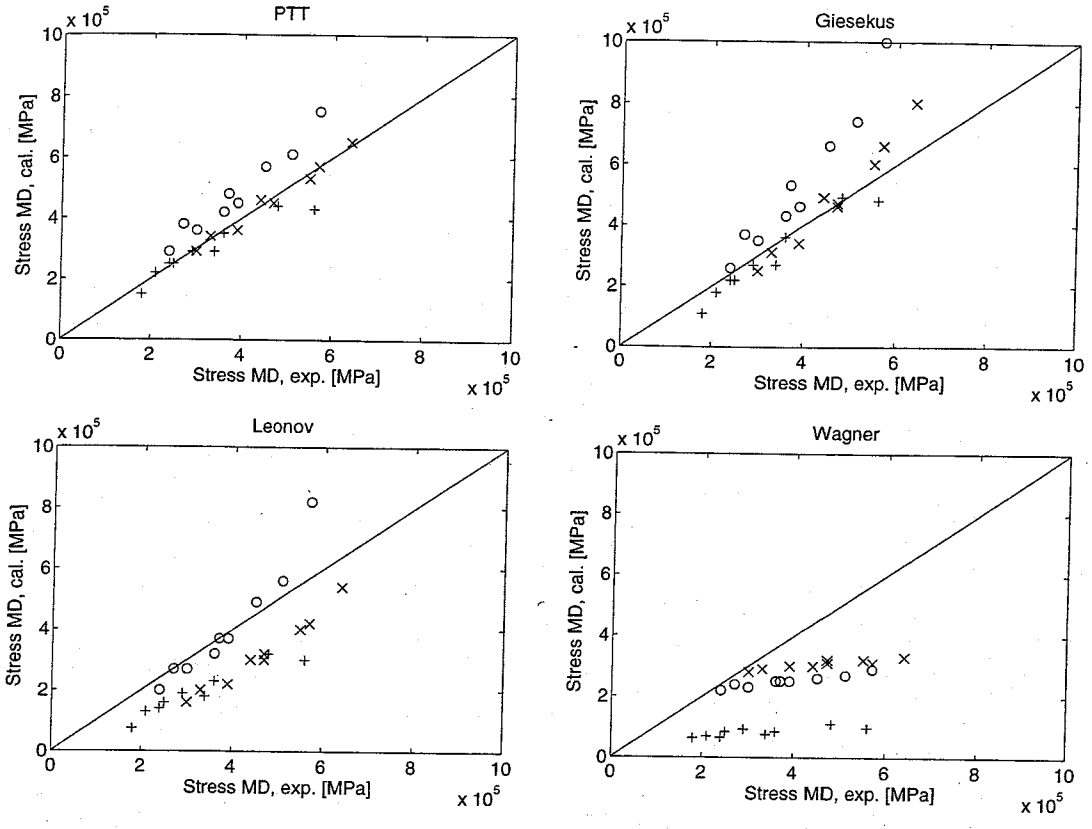

Figure 1-11. Calculated versus measured stress at the frost line, using four different constitutive equations (Tas, 1994).

Brown and McKinley (1994), Baaijens (1994c), and Baaijens et al. (1994, 1995). The most promising method nowadays seems to be the combined LDA (laser Doppler anemometry) and FIB [flow-induced birefringence, measured with the ROA (rheo-optical analyzer)] measurements that determine the kinematics and the stresses [applying the (empirical) stress optical law] in the flow. Typical flows used are the planar 4:1 or higher (up to 32:1) contraction flows, and the flow around a centric or eccentric cylinder placed in a rectangular duct. Typical examples of model predictions compared with experimental results are in Figs. 1-12 to 1-15 using the discontinuous Galerkin method [see, e.g., Fortin and Fortin (1989), Guénette and Fortin (1995), and Baaijens (1994a, b)]. In these types of flows, the Deborah number is defined as $De = VH/\lambda$, with V a characteristic process velocity, H a characteristic geometry dimension and λ the fluid relaxation time. The Deborah number is used as the relevant scaling parameter.

1.2.6 Deformation History

The last examples clearly show that once the geometry becomes somewhat more complex, such that the stresses start to determine the kinematics, the choice of constitutive equation used to determine those kinematics becomes relevant. It should be real-

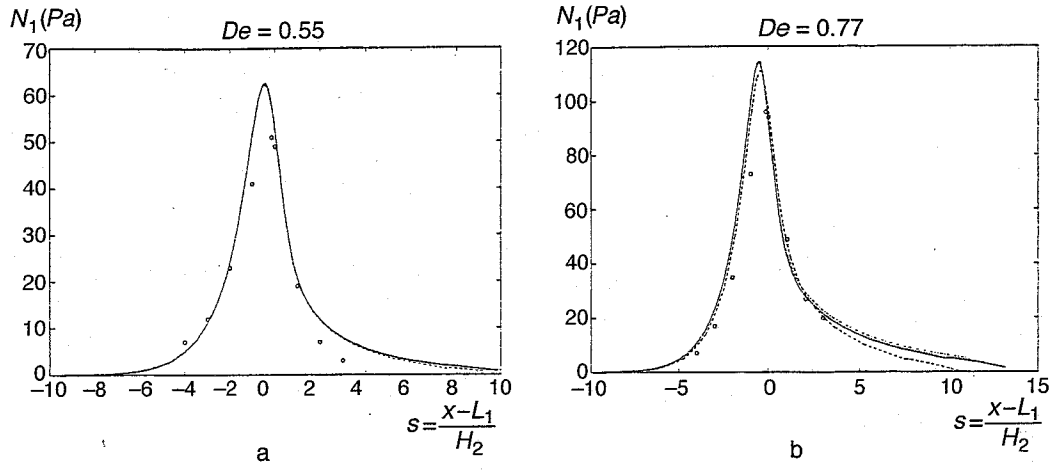

Figure 1-12. Contraction flow (4 : 1) data: comparison of the measured (symbols) and predicted (lines: PTT-a model) normal stress profile at the center line for a polymer solution, for two different values of the Deborah number (*De*): (a) 0.55, (b) 0.77 (Baaijens, 1993).

ized that the prediction of the deformation pattern is a rather sensitive criterion for the quality of our modeling, since deformation patterns consist of the integral with time of the velocity profile. Classical rheological techniques without exception use the velocity profile, differentiated in the direction of the largest gradients, and subsequently integrated in the direction of the smallest gradients, if any, by measuring the stresses via torques or pressure drops. As already stated, the deformation history of the material elements is, moreover, of utmost relevance for predicting product properties that depend on the total temperature-deformation-time history. Thus, computationally, special particle-tracking routines have been developed to solve the equation of conservation of identity equal to zero, $\dot{\xi} = 0$, with the dot the material derivative and ξ being typically the place and time of entering the mold if we deal with injection molding. This pure convection equation suffers from numerical diffusion and dispersion. That is why different strategies have been developed to solve it, e.g., the streamline upwind methods (SUPG) (Brook and Hughes, 1982), the time discontinuous Galerkin least squares methods, and the discontinuous Galerkin methods (Johnson, 1987). The relevance of solving this equation properly originates from the consideration that all convection-dominated problems show the same numerical difficulties, i.e., for example, high Reynolds number flows in hydrodynamics, high Peclet number flows in non-isothermal situations, high Deborah number flows (if viscoelasticity dominates), and high Dahmkoller number flows in reactive molding and extrusion.

If the deformation history has to be predicted with sufficient accuracy in injection molding, or if MMIM (multi-material injection molding), or GAIM (gas-assisted injection molding) have to be analyzed, or if RIM (reaction injection molding) is the topic of research, in all cases it proves to be wise to start the research with simplified geometries. At CPC Eindhoven, the plunger-driven flow was chosen as a representative geometry, given its characteristic of well-defined initial conditions, while maintain-

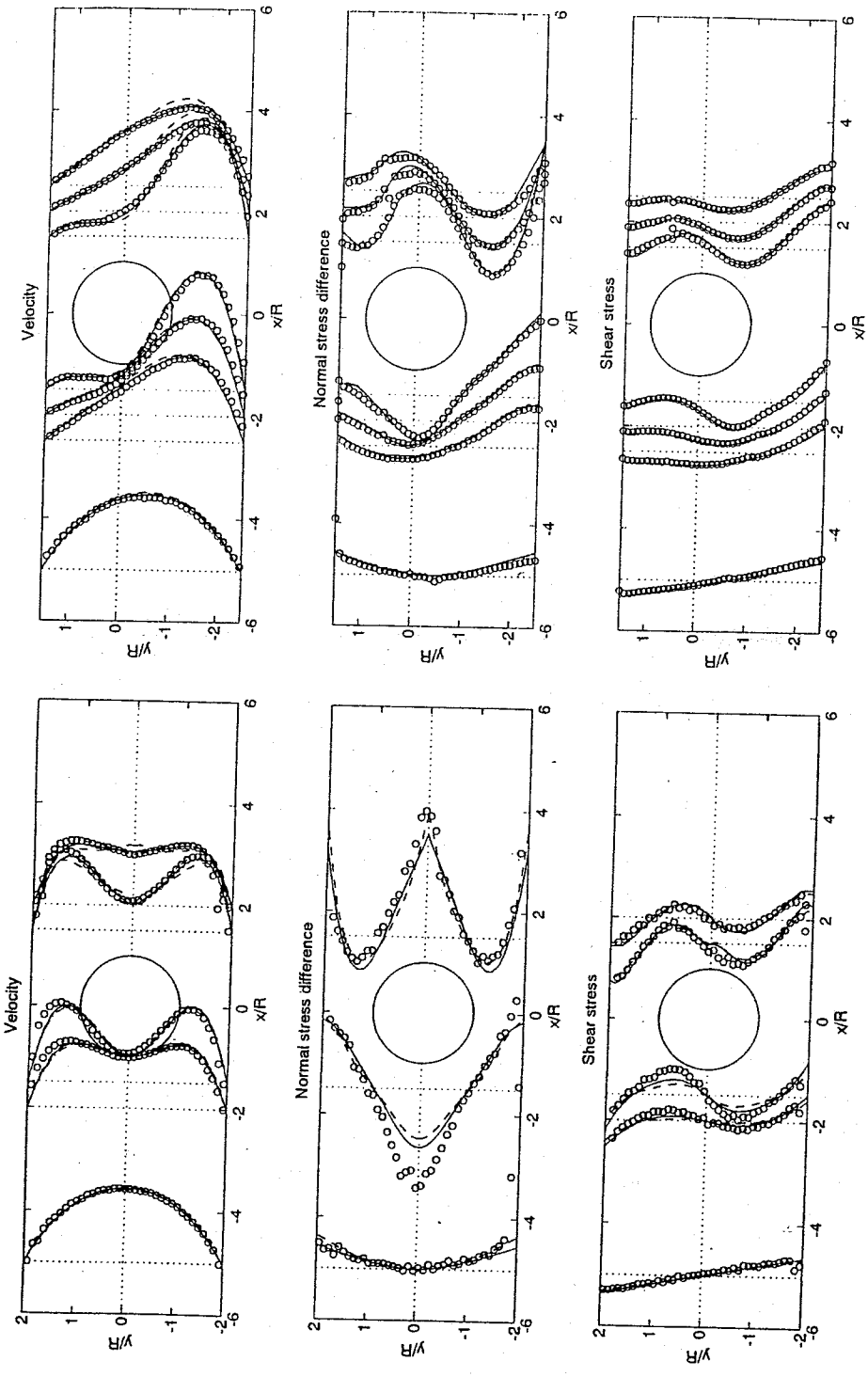

Figure 1-13. Measured (symbols) and predicted (lines: 4-mode PTT-a model with $\xi = \varepsilon = 0.1$) velocity (top), first normal stress (middle), and shear stress (bottom) profiles for the flow of a polymer solution (5 % PIB/C14) around a (a) centric and (b) eccentric cylinder, $De = 1.87$ (Baaijens, 1994c).

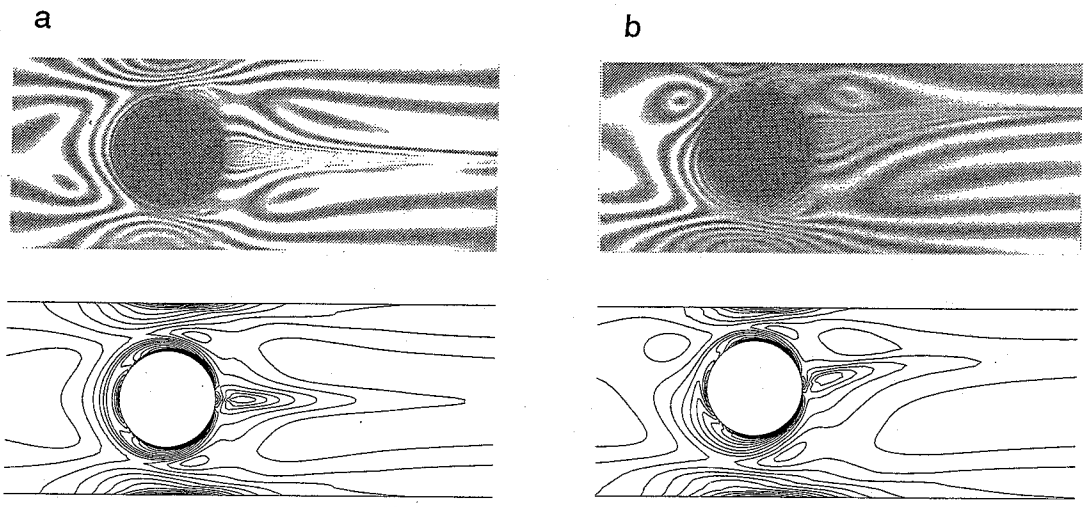

Figure 1-14. Measured (top) and predicted (bottom) birefringence patterns for the flow of an LDPE melt at 190 °C around (a) a centric and (b) an eccentric cylinder, PTT-a (ξ=0.1 ε=0.1), De=4.4 (Baaijens et al., 1995).

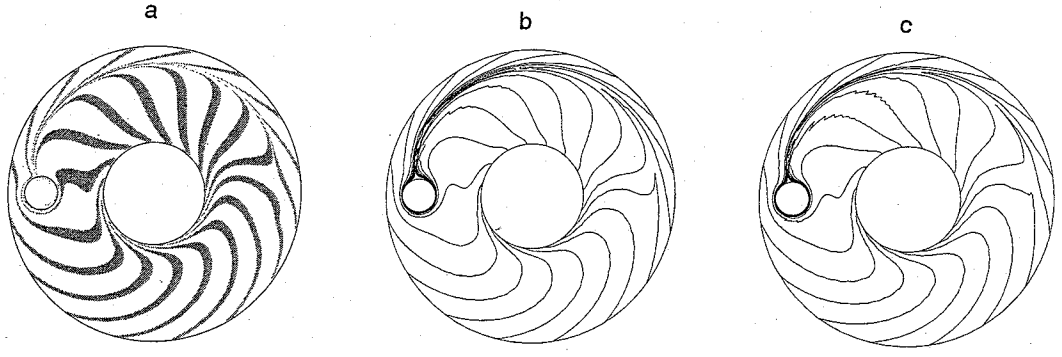

Figure 1-15. (a) Measured deformation pattern of a start-up flow around a cylinder for a PS melt at 175 °C, De=24, predicted using a (b) Carreau Yasuda or a (c) PTT-a model (with ξ=0.1 and ε=0.35) (Selen, 1995).

ing some difficulties encountered in molding processes via the presence of its fountain flow at the top and reversed fountain flow at the bottom plunger (Vos et al., 1991; Spoelstra, 1992; Corbey, 1992; Peters et al., 1994; Zoetelief, 1995). Some results comparing experimental and computed deformation patterns are given in Figs. 1-16 to 1-21.

Finally, an example is given of a splitting flow, as currently occurs in injection molding and where the standard 2.5 D programs show local difficulties. Since the pressure equation is not solved in the direction perpendicular to the streamlines (see Sec. 1.2.2), the flow-splitting cannot be described. Mostly, the properties of the inflowing material are simply copied to both exits. This is physically wrong, since the wrong materials' elements flow in the wrong places. As a consequence, all history dependent parameters, and even the con-

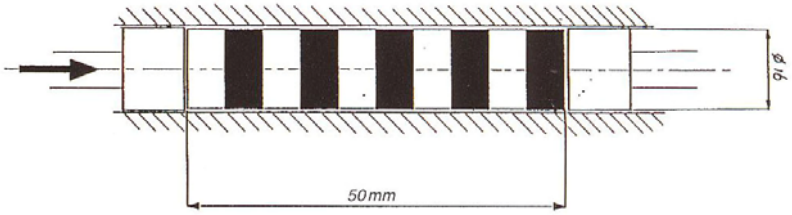

a Experimental

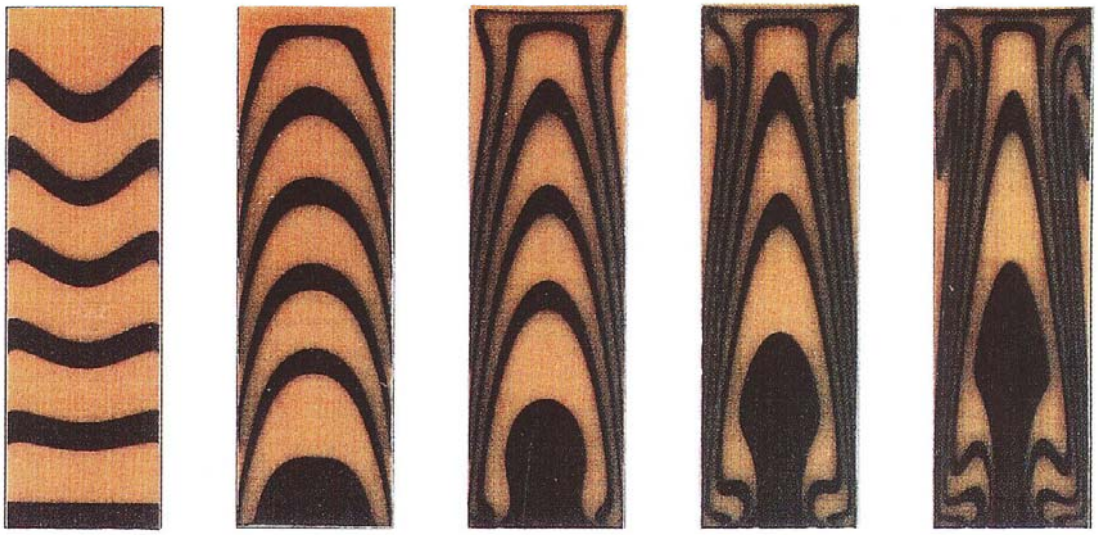

0 *mm* 10 *mm* 20 *mm* 30 *mm* 40 *mm*

b Calculated

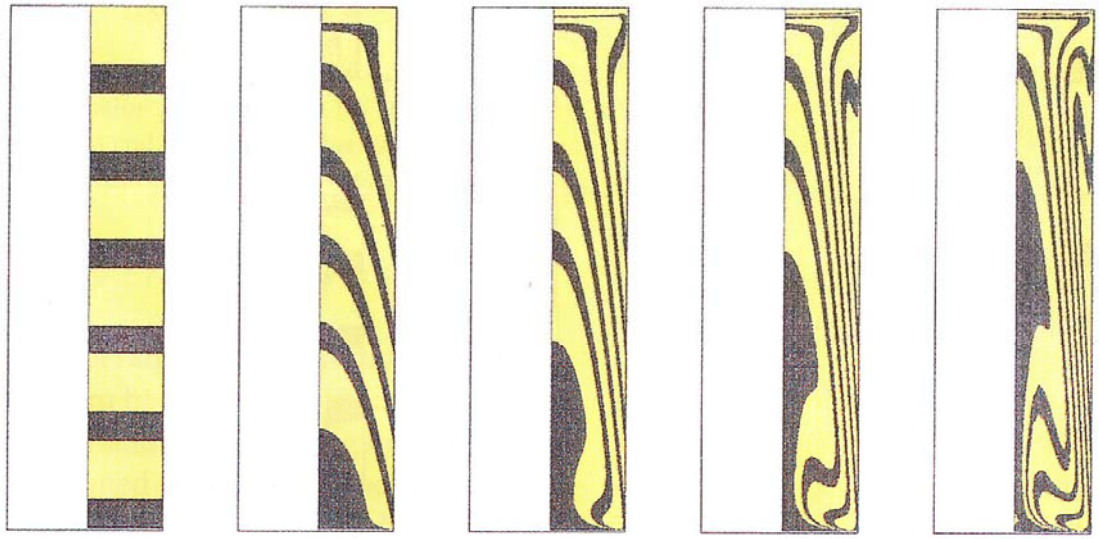

0 *mm* 10 *mm* 20 *mm* 30 *mm* 40 *mm*

Figure 1-16. Measured (top) and predicted (bottom; only the results in half of the geometry are drawn) deformation patterns at the midplane of the cylinder for a polystyrene (PS) melt in the two-plunger flow geometry at 473 K. The parameter is the total axial plunger displacement (Zoetelief, 1995).

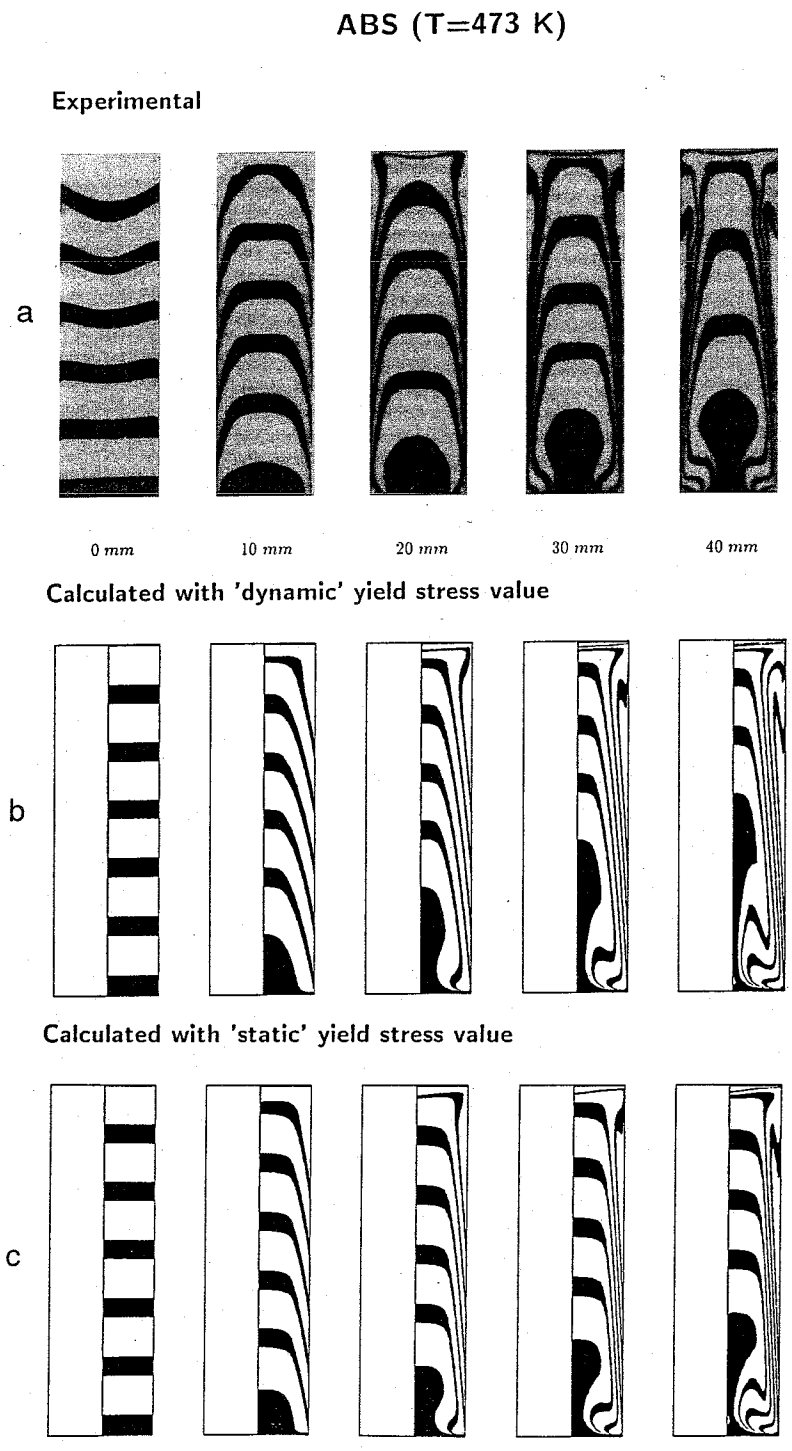

Figure 1-17. As in Fig. 1-16, but for acrylonitrile–butadiene–styrene copolymer (ABS) with (a) experimental, (b) calculations with a "dynamic" and (c) a "static" value for the yield stress (Zoetelief, 1995).

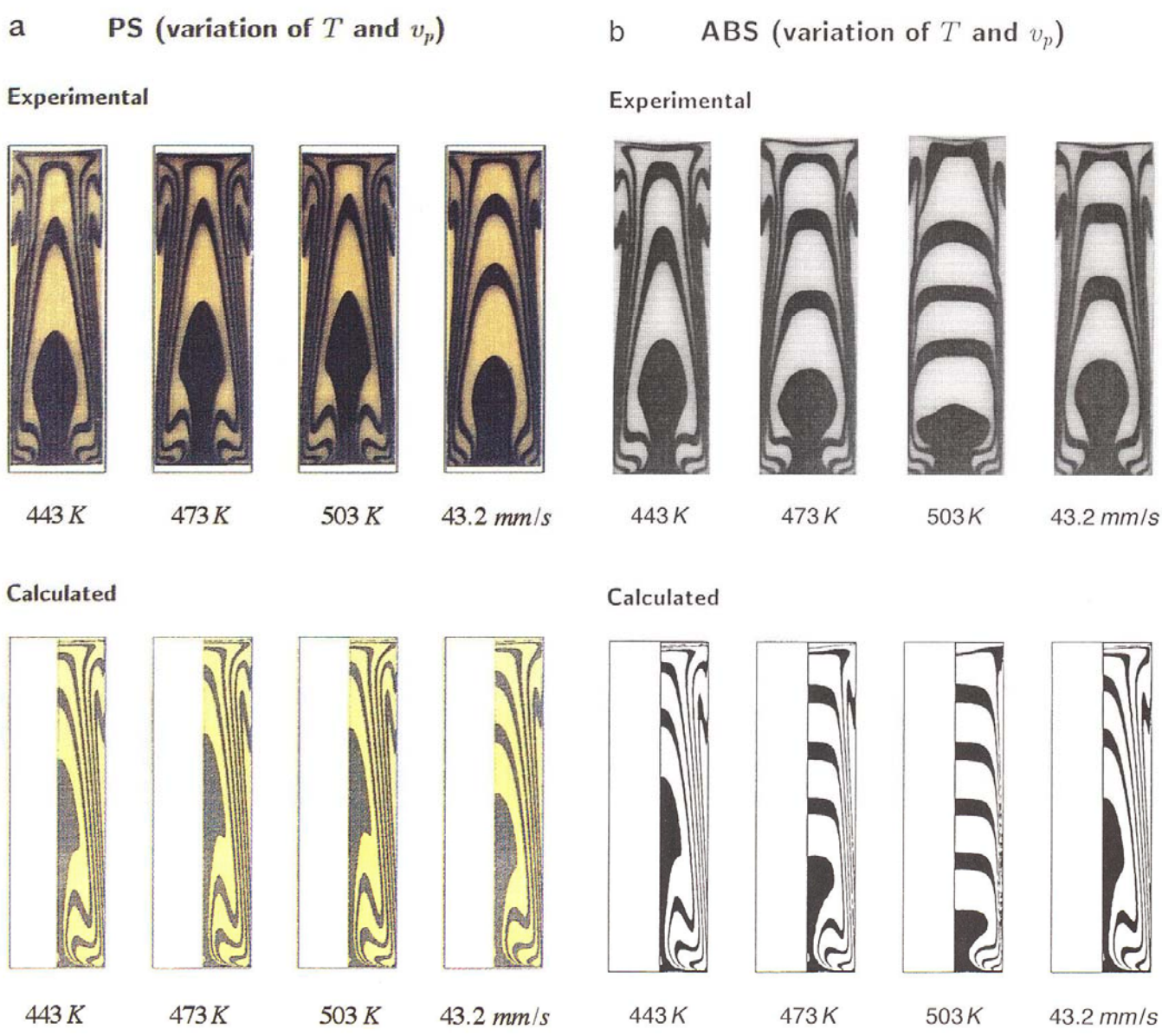

Figure 1-18. Influence of temperature (at piston speed of 1 mm/s) and piston velocity (at a temperature of 473 K) on the deformation pattern for (a) PS and (b) ABS; the remarkable difference in behavior of the two polymers (both measured and predicted) is due to the differences in the temperature dependence of the Newtonian plateau, i.e., the shear thinning transition, versus that of the yield stress (Zoetelief, 1995).

vected temperature, are wrongly predicted. This problem becomes specifically obvious if particle tracking is investigated. A solution is obtained by adapting local analyses (see Fig. 1-22), or alternatively, by using the same particle tracking technique to follow flow fronts. This last, flexible method is easily extendable to full 3 D molding analyses and basically replaces the transient filling problem by a quasi-stationary one. This is realized by taking the through flow of air into account. The air in the mold is quasi-stationary flowing and is, at time $t = t_1$, at the entrance replaced by a polymer melt. The method tracks the air–polymer interface. The polymer is assumed to stick at the walls while, at the interface between the mold and the air, a slip condition is adopted in order to allow for a replacement of air by polymer melt and to prevent the presence

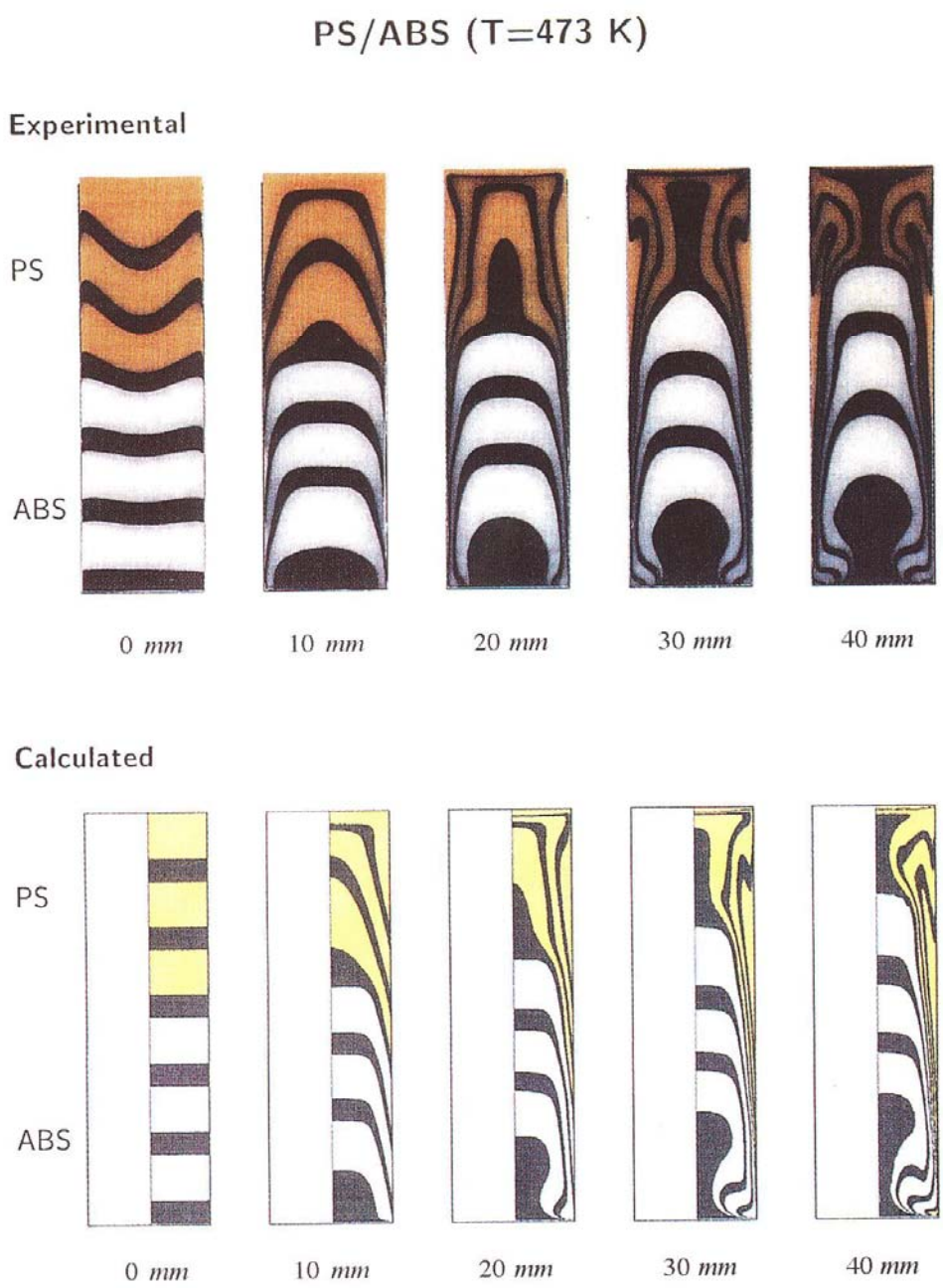

Figure 1-19. As in Fig. 1-16, with PS layers placed on top of the ABS (Zoetelief, 1995).

of (extremely thin) air layers at these boundaries (Reijnierse, 1995). This method is also capable of analyzing the GAIM (gas-assisted injection molding) process by tracking the second (polymer–gas) interface, injected at $t = t_2$ as well (Haagh, 1996) (see Fig. 1-23).

Finally, the inverse problem is mentioned. If, in a specific product, another material should be incorporated locally via co-injection techniques, the inverse problem can illustrate where and when this material should be injected into the mold (see Fig. 1-24).

1.2.7 Discussion

Using the injection molding process (and partly the film blowing process) as an example, it has been illustrated that in the last decade progress has been made in predicting polymer product properties that result from the complex temperature and deformation history experienced during processing.

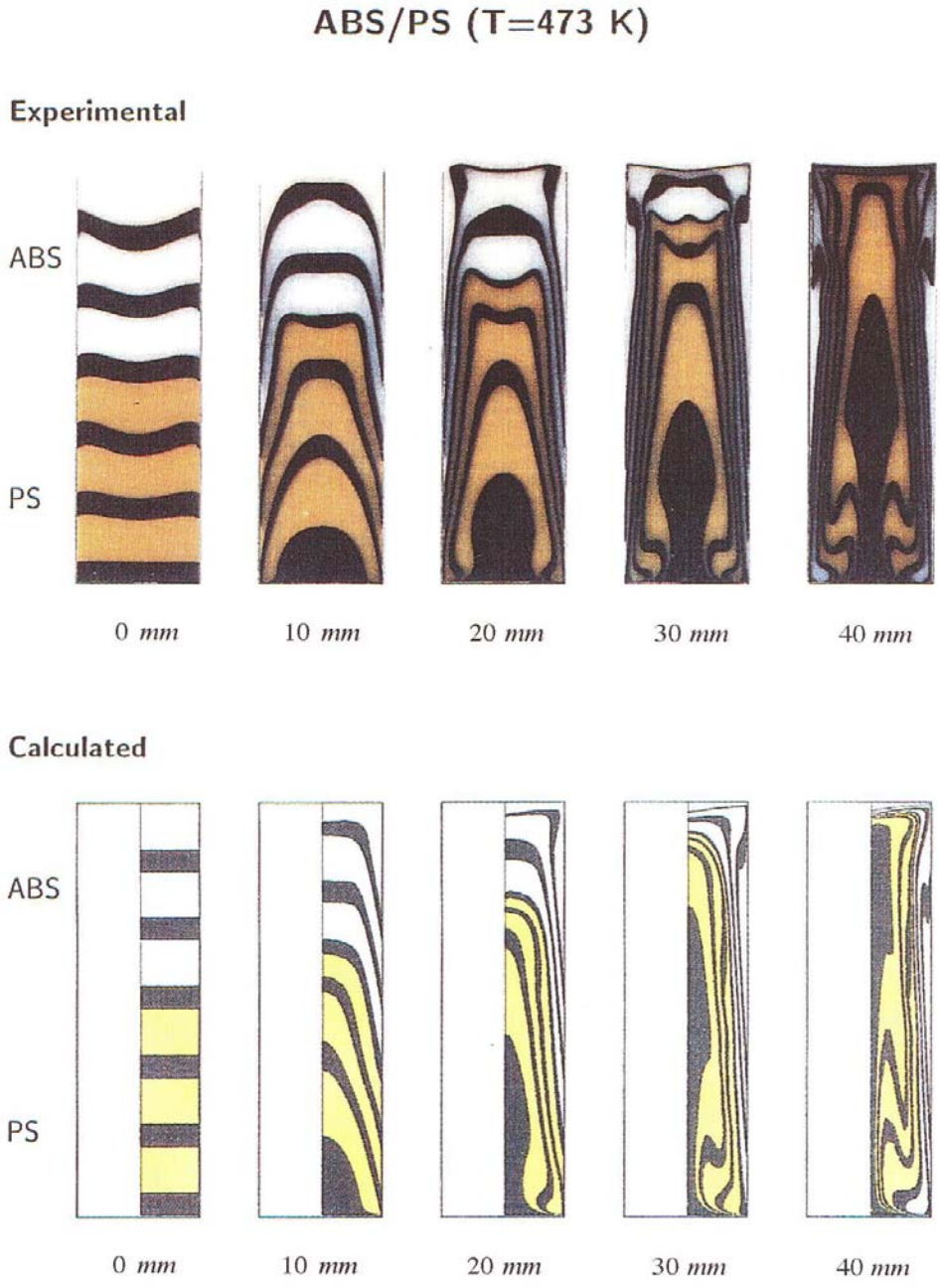

Figure 1-20. As in Fig. 1-16, with ABS layers on top of the PS (Zoetelief, 1995).

Today attention is focused on the solution of the full 3 D problem, using higher order (spectral) elements. The reason is that in most applications where a careful, detailed analysis is a prerequisite for faster product development, as in components for the electronic industry, the 2.5 D approach is no longer valid, since generally not one "thin" direction can be recognized. Interestingly, the assumptions necessary to be able to model transient, nonisothermal, viscoelastic flows in complex geometries like those that occur in injection molding, put less constraints on the validity of the predictions than the uncertainties in the (material) input data. Consequently, a lot of effort is nowadays devoted to accurately measuring the constitutive behavior of polymers. The advantage of this "back-to-basis" approach is evident, since it is more straightforward to relate the molecular structure of polymers to, e.g., their rheology than all the way to the product's properties. In the next section the heterogeneity of polymer systems is reviewed.

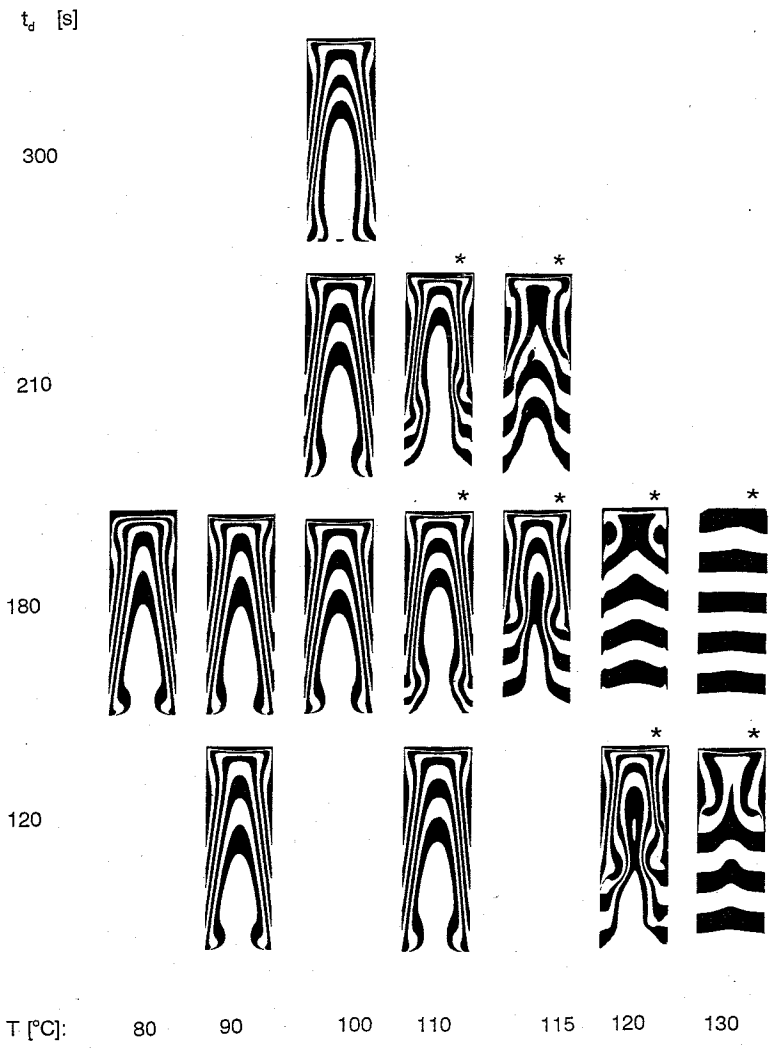

Figure 1-21. As in Fig. 1-16, but for a reactive, highly filled epoxy with different delay times, t_d, before movement of the plunger starts, and different wall temperatures; the stars * indicate the occurrence of wall slip due to progressive curing (Spoelstra, 1992).

1.3 Structure Development During Flow

1.3.1 Introduction

Blending offers a versatile technique to create new materials with specific, well-tuned properties. Many different techniques are applied to combine the properties of the individual constituents in the final polymer mixture, from RMP (reactor modified polymers), via REX (reactive) extrusion blending], and TIPS, DIPS, or CIPS processes (thermally, diffusion, and chemically induced phase separation, respectively), to MMIM (multi-material injection molding). Without exception the properties of the final product are determined by the resulting morphology, and this is why the structure development during flow is studied. For the most simple case of mixing of two fluids, two dimensionless numbers can be defined that characterize the mixing behavior: the capillary number *Ca*, which represents the

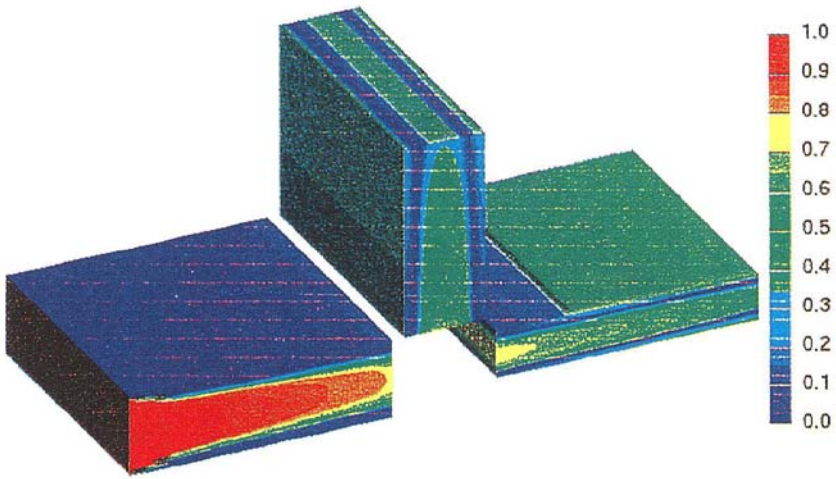

a. (wrong) injection time label

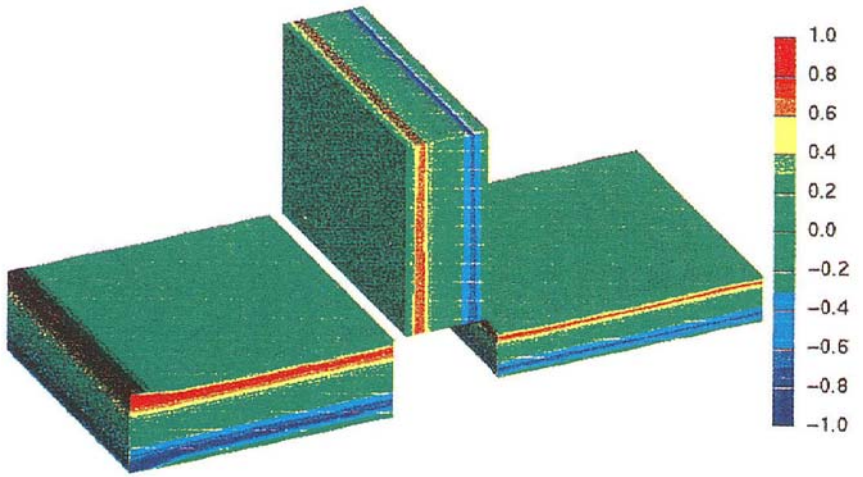

b. (wrong) gapwise injection position label

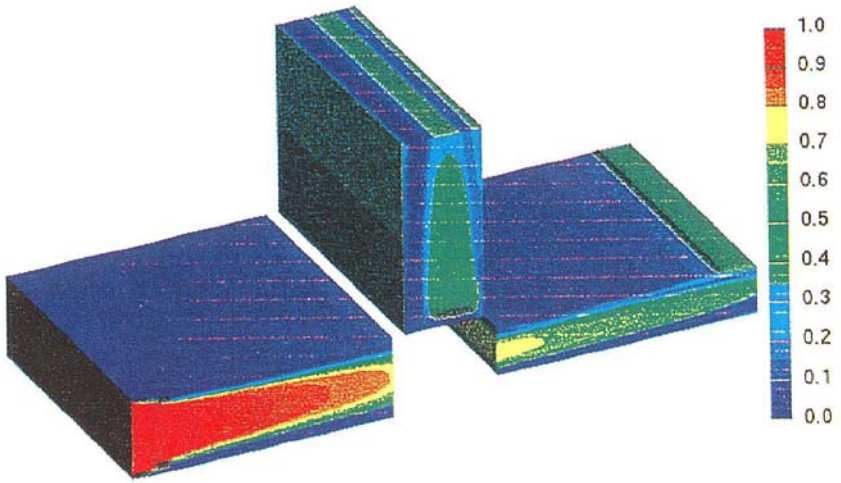

c. (correct) injection time label

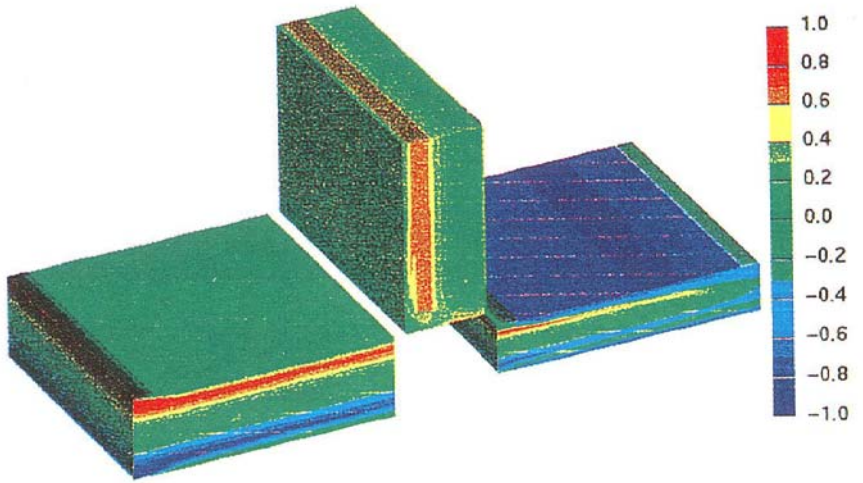

d. (correct) gapwise injection position label

Figure 1-22. Correctly predicted (c) and erroneous (a) injection time and wrong (b) and correct (d) gapwise injection position label distributions after a flow splitting in injection molding (Zoetelief, 1995).

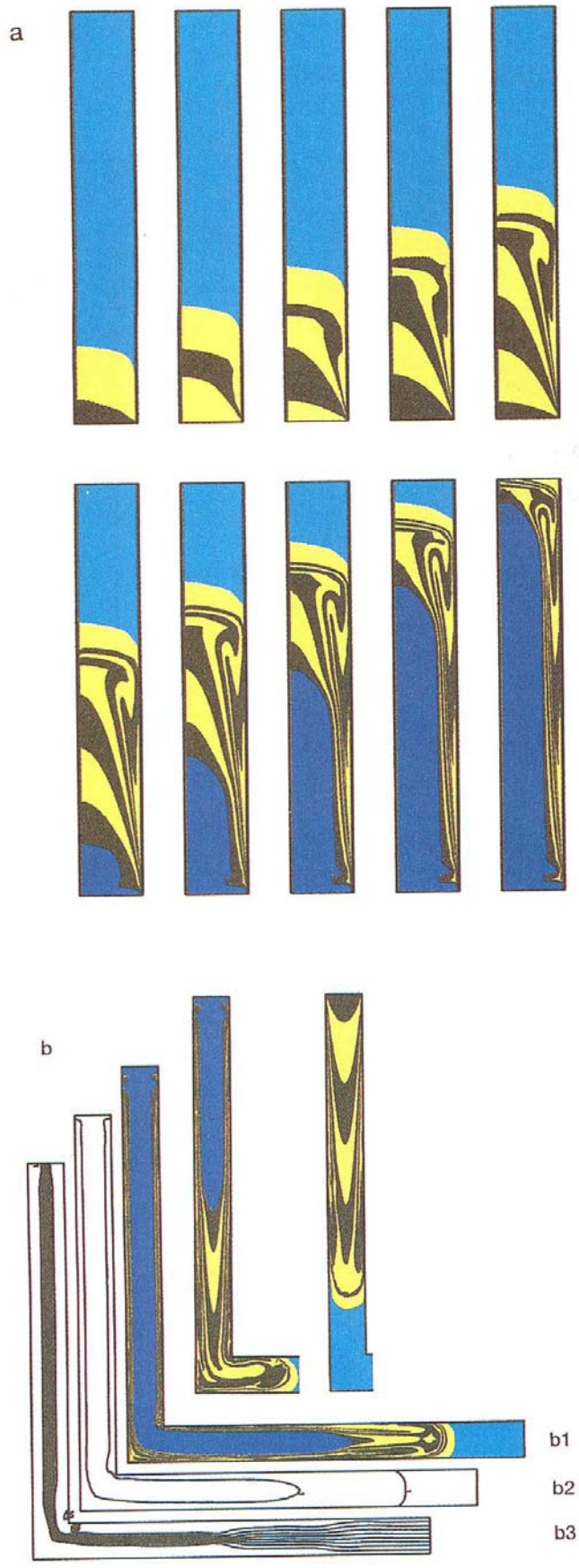

Figure 1-23. Simulation of the transient GAIM process at different stages of injection in (a) a cylindrical channel and (b) a planar flow around a corner. Injection time (material) labels and the air (light blue)–polymer and polymer–gas (dark blue) interfaces are depicted, while in the flow around the corner (b1) these interfaces are drawn explicitly (b2), combined with the resulting velocity field throughout the different phases (b3) (Haagh, 1996).

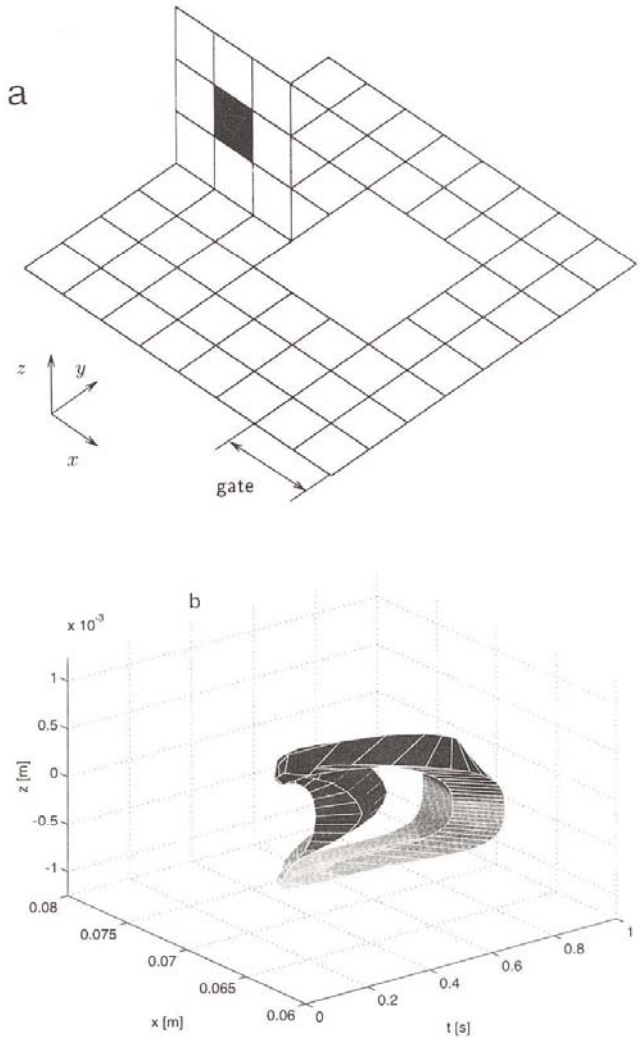

Figure 1-24. Solution of the inverse problem. Figure 1-24 b illustrates where and when a second material has to be injected in the linegate in order to fill a specific area in the final product (see Fig. 1-24 a) (Zoetelief, 1995).

ratio of the shear stress applied ($\tau = \eta_c \dot{\gamma}$) to the capillary pressure (σ/R), and the viscosity ratio p

$$Ca = \frac{\eta_c \dot{\gamma} R}{\sigma} \tag{1-1}$$

$$p = \frac{\eta_c}{\eta_d} \tag{1-2}$$

with η_c and η_d the viscosities of the continuous and the dispersed phase, respectively, $\dot{\gamma}$ the shear rate, R the local dispersed drop radius, and σ the interfacial tension.

In general, at in the beginning of the mixing process, the drop radius is large and the effect of interfacial tension is by far overruled by the shear stress applied. The drops deform affinely with the matrix, provided that the viscosity ratio is not too large if only simple shear is available [see Janssen (1993), Meijer and Janssen (1994), and Chap. 3 of this Volume for further details]. As a consequence, only simple mixing should be analyzed in these regions of the flow, and the focus should be on obtaining exponential rather than linear stretching of the dispersed phase (Sec. 1.3.2). If the capillary number approaches the value of one, by a continuous decrease in the radius of the deformed long slender threads which are formed, Rayleigh distortions grow and the threads disintegrate into lines of drops (Sec. 1.3.3). In a real mixing process, a quasi-stationary situation will result where drop break up and drop coalescence equilibrate, and simple models have been derived for liquid–solid and liquid–liquid dispersions in elementary geometries (Sec. 1.3.4). Of course blending is only one of the techniques that can be used; other processes do exist (Sec. 1.3.5). Finally, even in the seemingly most obvious case of a one-component fluid, structure development during flow can occur if the liquid–solid transition is met, e.g., in crystallizable polymers (Sec. 1.3.6).

1.3.2 Chaotic Distributive Mixing

Based on the elegant approach developed by Ottino and co-workers [see, e.g., Ottino (1989, 1990, 1991)] to study the basics of mixing in simplified geometries, the importance of applying the bakers transformation, even in continuous flows, has become evident. This transformation consists of three elementary steps: stretching, folding, and returning to the original position, and generates exponential rather than linear mixing if repeated in (typically) time or spatially periodic flows. No better procedure exists and, without counteracting forces like the interfacial stresses, nanodimensions are easily reached within a, e.g., 20-fold, repetition of this procedure. All well-designed static mixers (e.g., the Sulzer, Ross, Multiflux, and Kenics mixers) apply the bakers transformation and they can, consequently, be considered as the most efficient mixers, at least for pure distributive mixing. In our laboratory, apart from the rectangular cavity, the periodic curved cavity flow is analyzed as an intermediate step towards more realistic geometries as found in single and twin screw extruders. At the moment, the cavity is only slightly curved and the attention is focused on particle tracking with the conservation of mass of the dispersed blob, the influence of its initial position, and the protocol followed in the movements of the two opposed walls.

In these studies of (almost) 2D isothermal prototype mixing flows, the left and right wall are kept stationary, while the upper and lower walls are sequentially moved in a clockwise direction at a moderately low speed over a fixed distance. A period is defined as one loop in the protocol: if both the upper wall and the lower wall have been sequentially moved once. Periodic points are points that return to their initial position after one (order one) or more (order two, etc.) periods. "Hyperbolic" points favor

mixing, since in their neighborhood efficient stretching occurs due to the presence of hyperbolic streamlines, while the accompanying "elliptical" points form islands and are thus to be avoided. Of course, "parabolic" periodic points also exist, e.g., when an extra obstacle is added to the flow. Periodic points are the key to understanding exponential, chaotic mixing. In both experiments and simulations, a tracer blob is positioned around one of these periodic points and its deformation with time is followed. More details of the experimental set-up and results can be found in Chap. 3 of this Volume. Interestingly, analytical solutions are available for these kinds of flows (even if an extra rotor is added in the midplane), based on a large number (typically 30) of intermediate steps to accelerate convergence of the series expansions. In the final result, only three terms of the expansions have to be taken into account to obtain accurate results (Meleshko et al., 1991; Meleshko and Peters, 1996). Figure 1-25 shows a typical line stretch obtained in this periodic flow, if the original blob is located at a hyperbolic point of order one. Fig. 1-26 illustrates the effects of different initial blob positions and wall movement protocols.

Important in following the blob deformation is the necessity to nonuniformly distribute the points on the circumference of the original blob that are to be traced with time. The reason for this is obvious: during folding and stretching, two neighboring points can, ultimately, be separated infinitely far from each other. This is the definition of (deterministic) chaos. An iterative procedure is adopted which adds extra initial points between two points that tend to separate too far. The necessity of this is illustrated in Fig. 1-27.

Also periodic points of higher order than one prove to be relevant for efficient mixing. This is illustrated in Figs. 1-28 and 1-29, where all periodic points are shown, combined with the different line stretching of blobs placed at these points.

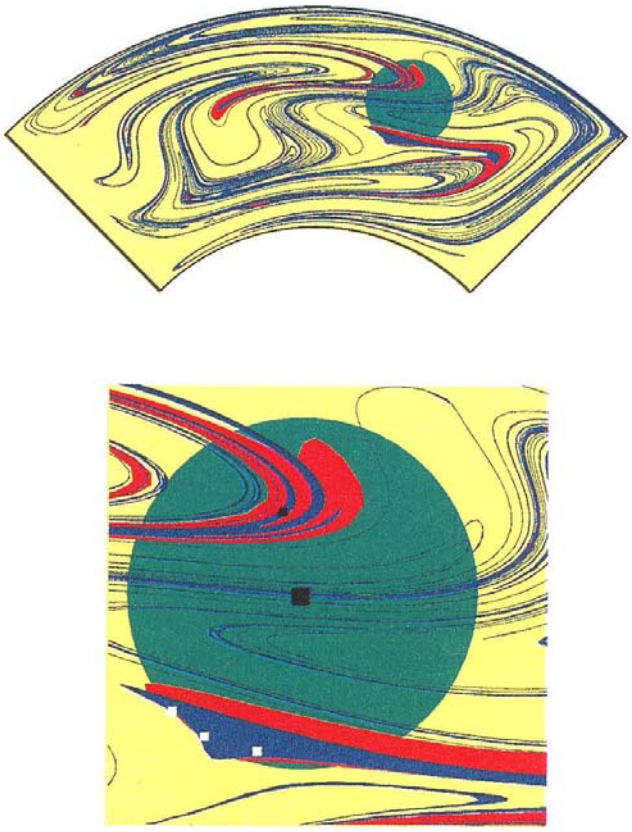

Figure 1-25. Results of modeling the periodic flow in a curved cavity. The initial position of the blob, around a hyperbolic point of order one (■), is indicated in green. The resulting deformed drop is given by the threads (red, partly covered by the blue line) after six and (blue) 12 periods. The bottom figure gives an enlargement showing not only the extremely good resolution obtained from these analytical solutions, but also some higher order periodic points (order 6), indicated with small squares, of the hyperbolic (filled squares) and elliptic (open squares) type (Krasnopolskaya et al., 1996, 1997).

Different measures for mixing can be defined: the statistical square density, the intensity of segregation, and the entropy (Krasnopolskaya et al., 1996, 1997). They yield different results when applied to the periodic flow in the curved cavity. More importantly, they implicitly demonstrate the problems of scale-up in mixing operations, since the absolute grid size chosen for the evaluation of the mixing quality clearly determines the outcome (see Fig. 1-30).

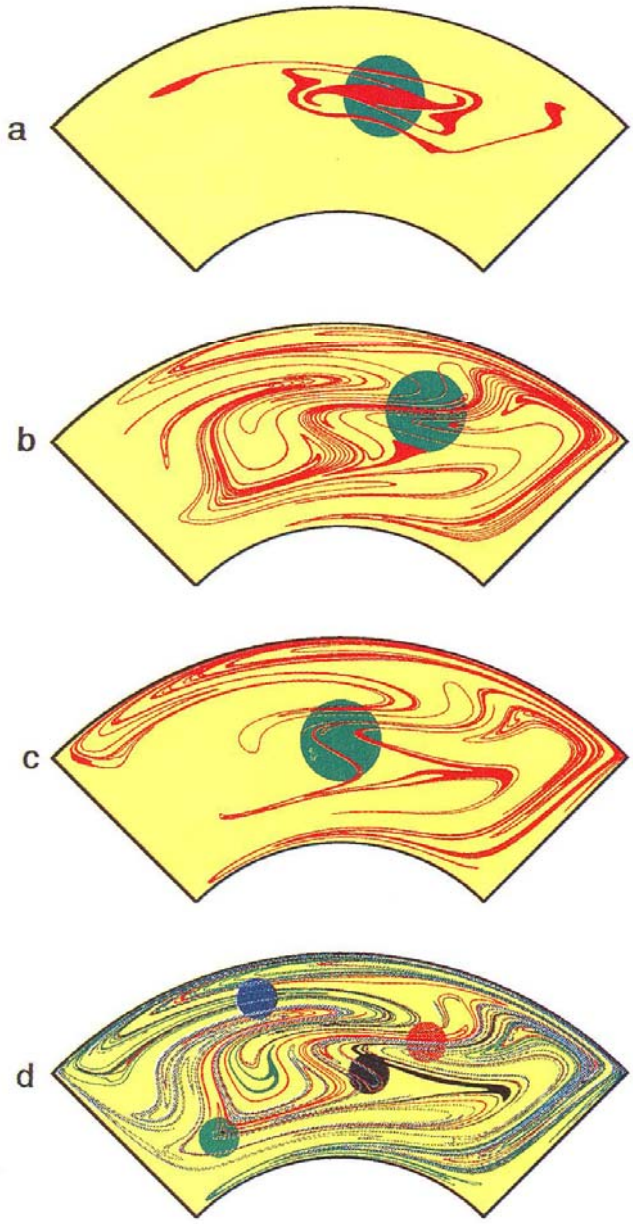

Figure 1-26. Influence of different wall motion protocols and initial blob positions on the final stretching. In Fig. 1-26 a a different protocol (half of the wall displacement of Fig. 1-25) and a different initial position (around an elliptical point of order one) were used (results are shown after 20 periods, yielding the same total wall displacement, and consequently the same "money for mixing", as in Fig. 1-25). Figures 1-26 b (original blob in a hyperbolic point of order one), 1-26 c (central), and 1-26 d (four blobs with the same total size as the big blob, arbitrarily placed) illustrate the influence of the blob position (all results after 10 periods) (Krasnopolskaya et al., 1996, 1997).

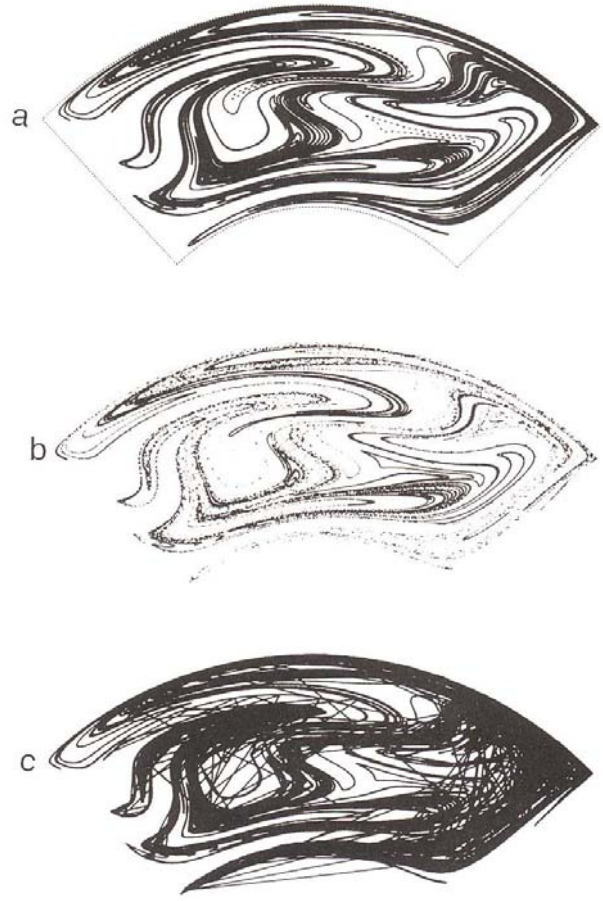

Figure 1-27. Influence of the distribution of the tracer points on the original blob circumference. (a) Non-uniform distribution of 50 000 points, (b) nonconnected, and (c) connected originally uniformly distributed, after 12 periods (Krasnopolskaya et al., 1996, 1997).

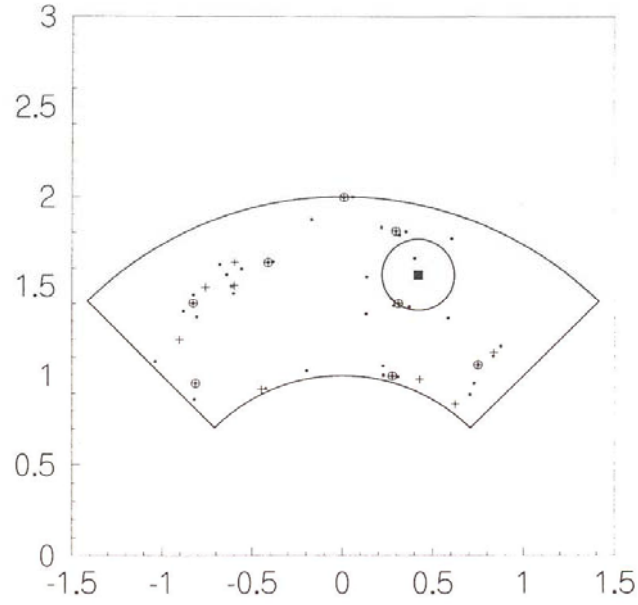

Figure 1-28. Higher order periodic points in the curved cavity flow. Order 1 (■), order 2 (○), order 4 (+), and order 6 (·) (Krasnopolskaya et al., 1996, 1997).

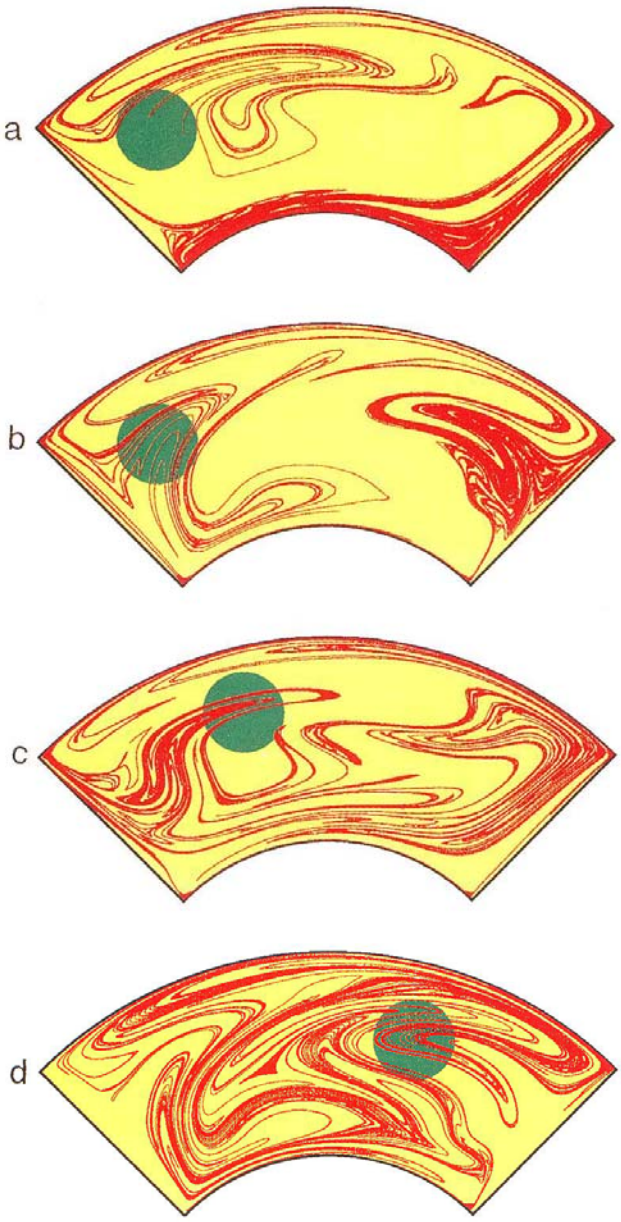

Figure 1-29. Resulting dimensionless line stretch S after n periods of identical protocols of blobs with initial size $\phi = 5$ mm positioned close to a hyperbolic H(o) or elliptical E(o) periodic point of order (o). Figure 1-29 a: $n = 9$, E(2) surrounded by H(6), $S = 1800$. Figure 1-29 b: $n = 9.5$, E(2), $S = 1800$. Figure 1-29 c: $n = 10$, H(2), $S = 1700$. Figure 1-29 d: $n = 12.5$, H(1), $S = 5600$ (Krasnopolskaya et al., 1996, 1997).

Since the prerequisites for efficient mixing are now well understood, at least in elementary geometries, attempts are nowadays made to analyze real 3D mixers (including those that are frequently used in the process industry, e.g., stirred tanks, etc.) via flow simulations using these basic concepts. Thus periodicity is sought exclusively and attempts are made to identify periodic points. This is not a straightforward task. A further extension of this knowledge is sought in the coupling of the overall flow behavior to the local microprocesses that occur, for example, during emulsifying (Tjahjadi and Ottino, 1991; Tjahjadi et al., 1992, 1994; Janssen, 1993; Janssen et al., 1993; Meijer and Janssen, 1994; Janssen and Meijer, 1995).

1.3.3 Dispersive Mixing

As stated above, exponential mixing continuously decreases the length scale of the dispersed phase in the direction perpendicular to the flow, and once the radius of the threads formed are of the order of 1 μm, typical for polymer blends, the interfacial tension becomes dominant and Rayleigh distortions grow with (as a driving force) the decrease in the surface-to-volume ratio. Threads disintegrate into lines of drops. This process was studied in the mid 1930s by Tomotika (1935, 1936), both in a quiescent surrounding and during flow. The latter proves to stabilize the threads, thus retarding disintegration and yielding smaller drops. His analyses were later extended by, e.g., Stone et al. (1986), Stone and Leal (1989 a, b, 1990, 1994), Tjahjadi and Ottino (1991), Tjahjadi et al. (1992, 1994), Janssen (1993), and Janssen and Meijer (1995), clearly showing that the effects of both the viscosity ratio p and the absolute values of the viscosities of both phases are completely different from the conclusions based on quasi-equilibrium experiments such as the classical experiments performed by Taylor (1932, 1934) and Grace (1982). Details can be found in Chap. 3 of this Volume. Here only an illustration is given that break-up processes take time (see Fig. 1-31).

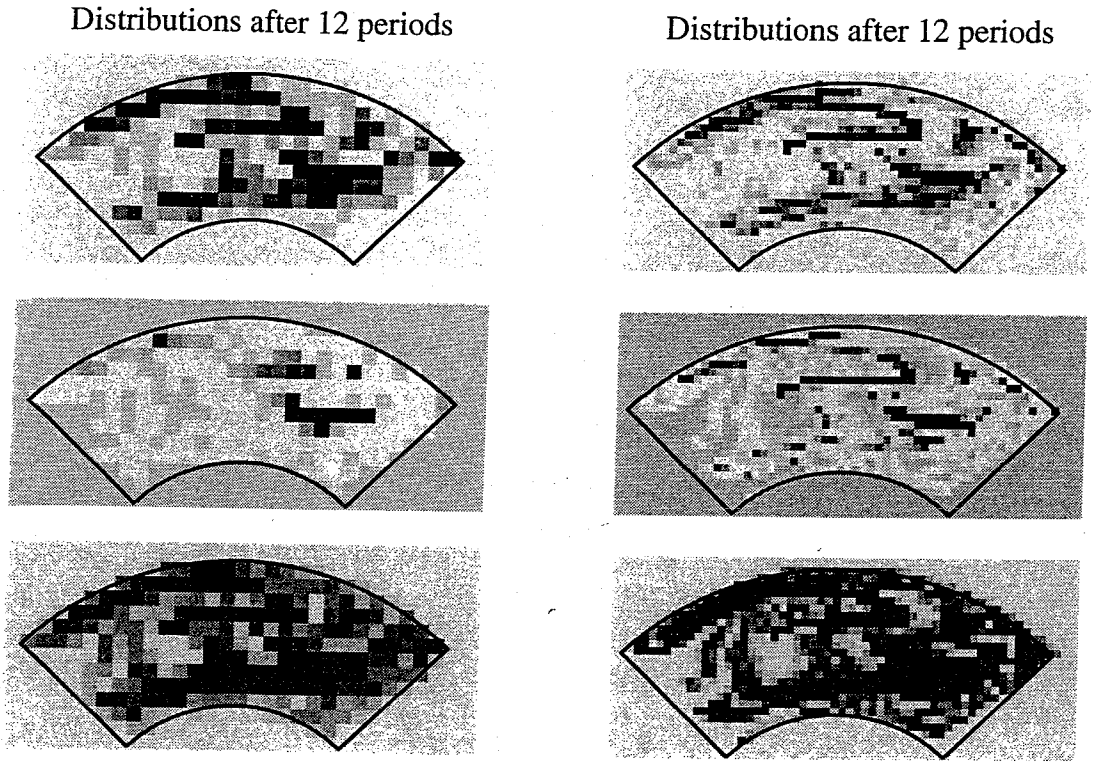

Figure 1-30. Distribution of different mixing measures after 12 periods of mixing: square density (top), intensity of segregation (middle), and entropy (bottom) for two grid sizes. The large grid size (left column) is representative for a typical small scale laboratory mixer, while comparably the small grid size (right column) represents a larger production mixer. During scale up in the practice of mixing, the absolute sizes of the mixed domains should stay constant and longer mixing is necessary in the larger mixers (Krasnopolskaya et al., 1996, 1997).

1.3.4 Two-Zone Models

In a real process, apart from dispersive mixing, the coalescence of drops also occurs, so coarsening the morphology again. Coalescence takes place in the quiescent zones of the mixer, and a successful process depends on the collision frequency (determined by the volume fraction of the dispersed phase and the shear rate) and the thinning rate of the continuous matrix phase in between the drops (which strongly depends on the mobility of the interfaces, which in its turn is influenced by the presence of compatibilizers). Successful models have been proposed to predict and measure these thinning rates (see, e.g., Dell'Aversana et al., 1996), even for partially mobile interfaces where the viscosity of the dispersed phase plays a dominant role (Chesters 1975, 1988, 1991; Chesters and Hofman, 1982; Abid, 1993; Abid and Chesters, 1994). Based on the original work of Manas-Zloczower et al. (1982, 1984), who derived a simplified two-zone model for the dispersive mixing of carbon black (see Fig. 1-32), Janssen and Meijer (1995) succeeded in deriving an analogous model for liquid–liquid mixing. In these types of dynamical models, two typical zones are put in series: a strong zone, representing (typically) the passage of a narrow kneading

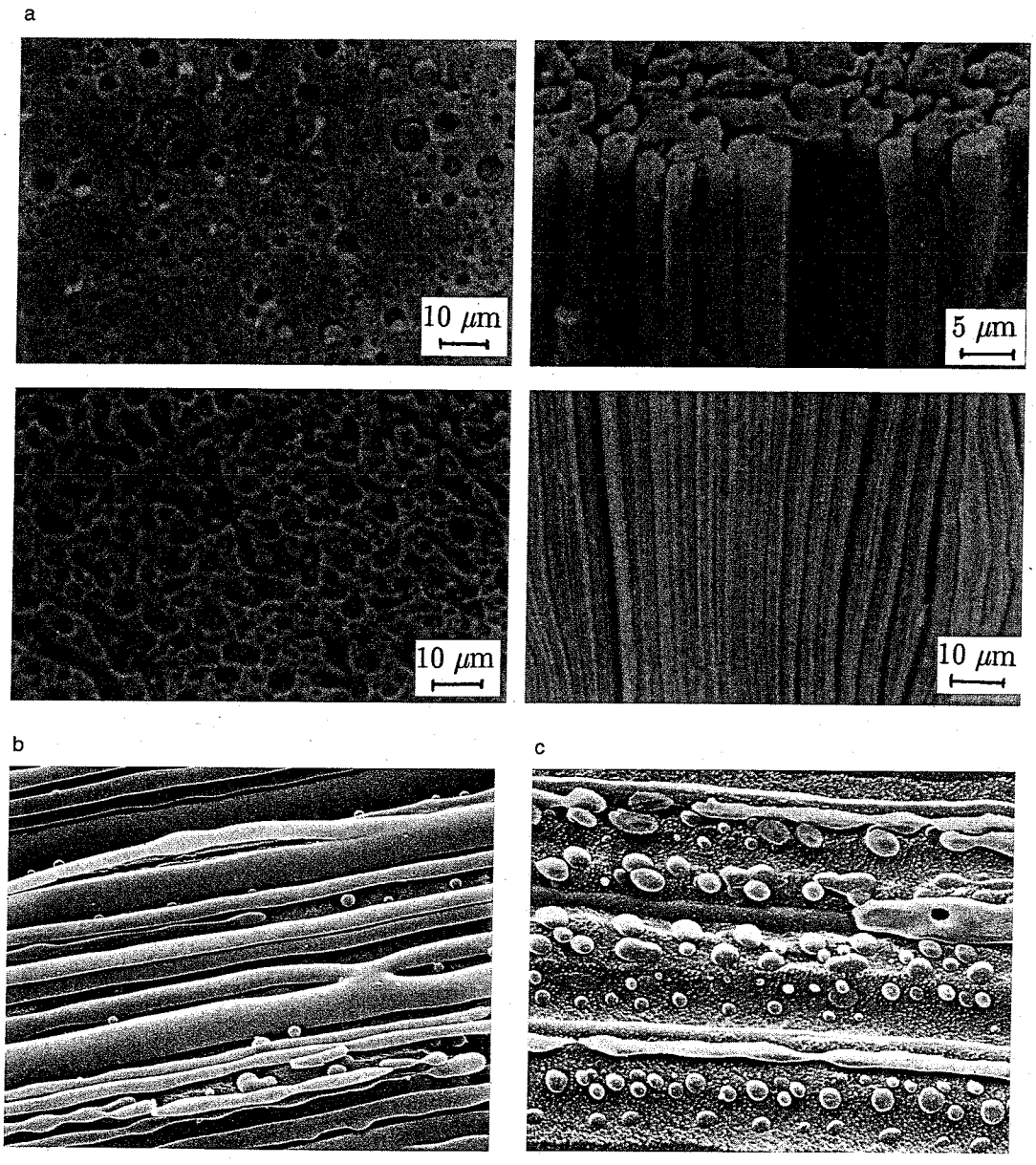

Figure 1-31. (a) Different morphologies as obtained in blends of the incompatible system HDPE/PS. The difference between (b) the threads and (c) the drops is a small increase in the air gap between the extruder die and the quench bath, giving time for break up (Elemans, 1989).

flight in an extruder or batch mixer, and a weak zone, representing the bulk of the volume of the mixer. The fluid is pumped around from one zone to the other, given the overall mixing time available. Models like these combine all the elementary steps of the mixing process and yield not only a dynamic equilibrium of the distinct processes, the dispersive action of deformation and break-up, and the coarsening action of

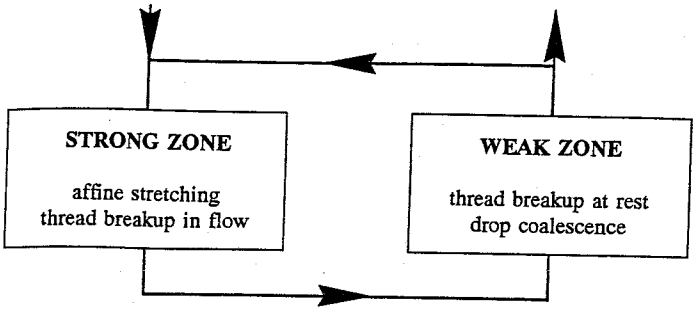

Figure 1-32. Schematic diagram of the two-zone model for mixers (Janssen and Meijer, 1995).

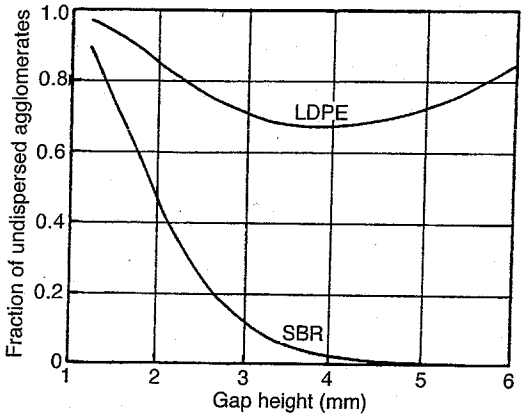

Figure 1-33. Optimum gap size in dispersive mixing of carbon black in styrene–butadiene rubber (SBR) and low density polyethylene (LDPE). The explanation of the differences between the matrix materials is found in the differences in the viscosity. The high viscosity of the rubber causes almost all agglomerates to break, even if the gap height is large (and thus the shear rate is relatively low) (Manas-Zloczower, 1994).

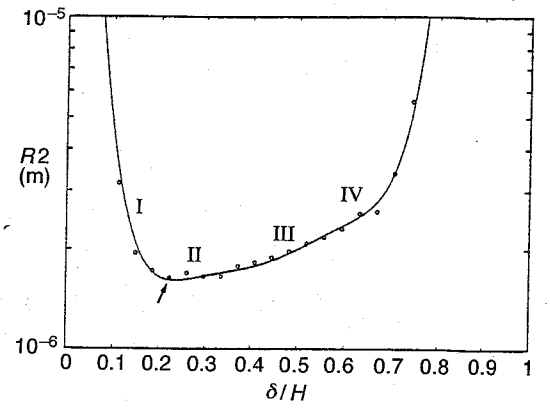

Figure 1-34. Optimum gap size in fluid–fluid mixing (Janssen and Meijer, 1995).

coalescence, but also provide tools to optimize the mixing geometry. A basic design parameter of any mixer is the ratio of the gap height to the channel depth δ/H. If this ratio tends to zero, a very strong zone exists, but hardly any material will pass through this zone, yielding zero throughput in the available mixing time. If, on the other hand, this ratio tends to one, no strong zone exists at all. A clear optimum is found (see Figs. 1-33 and 1-34).

Apparently, it took more than a decade to extend the elegant approach of dispersive mixing of carbon black to that of emulsifying flows. The reason for this is that in the dispersive mixing of solids break-up is a simple yes–no criterion, depending on whether the shear stress overrules the cohesive stresses and is, moreover, independent of the absolute size of the agglomerates (Manas-Zloczower et al., 1982, 1984; Manas-Zloczower (1994) gives a detailed treatment of the prediction of these cohesive forces via a fractal analysis) and no coalescence takes place, where with fluid–fluid mixing the distinct local time scales play a decisive role, while the capillary pressure clearly depends on the local drop (and thread) radius; moreover, severe coarsening can occur. Nevertheless, these basic approaches clearly demonstrate the quality of today's predictive power in mixing.

1.3.5 Phase Separation

In membrane formation, gel applications, and recently also in reactive molding or reactive extrusion, structures are formed via phase separation. Phase diagrams based on thermodynamics are the key to understanding these processes. The attention in modeling is now focused on understanding the kinematics of the process, since mostly non-equilibrium morphologies are vitrified. A schematic representation of different membrane morphologies is given in Fig. 1-35 [after Mulder (1991)], while some separation processes (L–L, G–G, or L–G), including their driving forces, are depicted in Table 1-1.

Table 1-1. Separation processes of liquid–liquid, gas–gas, or liquid–gas separation and their driving forces.

Process	Separation	Driving force[a]
Microfiltration	L-L	Δp
Ultrafiltration	L-L	Δp
Reverse osmosis	L-L	Δp
Gas separation	G-G	Δp
Prevaporation	L-G	Δp
Thermo-osmosis	L-L	$\Delta T/\Delta p$
Membrane-distillation	L-L	$\Delta T/\Delta p$
Dialysis	L-L	Δc
Electrodialysis	L-L	ΔE

[a] Δp = pressure, Δc = concentration, ΔE = electric field, and ΔT = temperature.

Membranes can be symmetric or asymmetric with different pore sizes (typically 0.2–5 μm) or dense. In asymmetric membranes the skin takes care of the selectivity, while the supporting porous underlayer provides a high yield. Microfiltration, ultrafiltration, and reverse osmosis are all pressure-driven processes where liquids are separated (Mulder, 1991; Kesting, 1985a, b). Microfiltration is used when relatively large particles (>100 nm) have to be separated; these membranes usually have an open structure, and only low pressure drops are required. When macromolecules need to be separated from a solution, denser membranes are used, accompanied by a larger pressure drop requirement. The process is now called ultrafiltration. For even smaller molecules reverse osmosis is used, with a very dense membrane and high pressure drops [10–100 bar (10^6–10^7 N m^{-2})]. When gas molecules need to be separated, the mechanism used is not sieving. Instead a so-called solution–diffusion mechanism takes place (Graham, 1866). The solubility is determined by the membrane material and

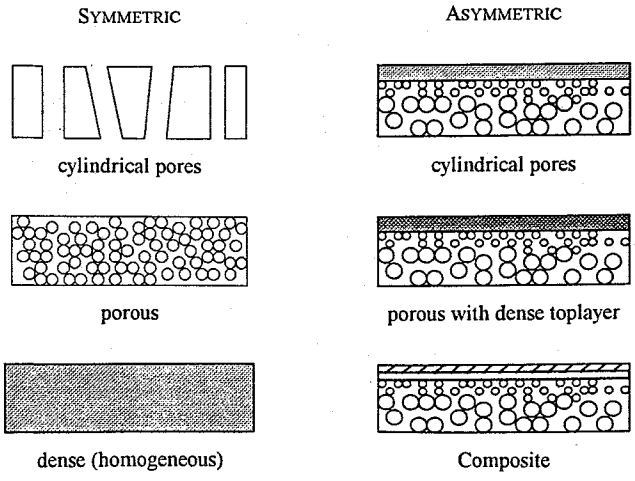

Figure 1-35. Schematic representation of different membrane morphologies (Berghmans, 1995).

the molecule to be dissolved. At the permeate side of the membrane, the chemical potential of the molecules is lower, causing diffusional mass transport as long as a gradient exists. The permeability of a membrane is the product of the solubility S and the diffusion constant D (von Wobreski, 1879)

$$P = D \times S \tag{1-3}$$

Since both the solubility and the diffusion constant are material parameters, the permeability of a membrane is a fundamental property, independent of the thickness of the membrane (Koros and Fleming, 1993). The flux J can be expressed as the permeability P multiplied by the pressure gradient $\Delta p/d$, with d the thickness of the membrane

$$J = P \times \frac{\Delta p}{d} \tag{1-4}$$

The ideal separation of these membranes can be expressed with the separation parameter, or the selectivity, α_{AB}, for a pair of components A and B, and is defined as

$$\alpha_{AB} = \frac{P_A}{P_B} \tag{1-5}$$

In principle this selectivity is a fundamental property, so it has a fixed value. In practice, the selectivity is usually lower and determined by measuring the flow rate of both gases and taking their ratio. Polymers used for membranes can be rubbery as well as glassy. Typical membrane materials include silicone rubber, polysulfone (PSF) and polyethersulfone (PES), polycarbonate (PC), polyetherimide (PEI), polyarylate (PAR), polyhydroxyether (PH), polyphenylene-ether (PPE), and cellulose derivatives such as cellulose acetate (CA), cellulosetriacetate, and ethylcellulose. For gas separation membranes glassy polymers are used, because of their higher selectivity. Their permeabilities are lower than for the more rubbery polymers, but this can be compensated for by reducing the thickness of the skin. Table 1-2 gives an overview of their selectivities and permeabilities towards oxygen and nitrogen, indicating that the selectivity increases when the permeability decreases, while Table 1-3 indicates the selectivity differences for different gases to be separated.

Table 1-2. Ideal selectivities and permeabilities towards oxygen and nitrogen for some typical membrane materials.

Membrane material[a]	P_{O_2} (Barrers[b])	P_{N_2} (Barrers)	α_{O_2/N_2}
PPE	15.5	3.1	5.0
PA	1.7	0.33	5.1
PC	1.5	0.27	5.6
PSF	1.2	0.20	6.0
PEI	0.4	0.05	7.6
PH	0.1	0.015	6.7

[a] For abbreviations, see text; [b] 1 Barrer = 10^{-10} cm^3 (STP)-cm/cm^2-s-cm-Hg, data from Kesting and Fritzsche (1993) and from Smid et al. (1991).

Table 1-3. As Table 1-2, but now towards helium/methane and carbon dioxide/methane.

Membrane material	α_{He/CH_4}	α_{CO_2/CH_4}
PPE	20.8	15.6
PA	35	18.8
PC	51	23.6
PSF	52	23.4
PES	80	28.0
PEI	264	37.4
PH	132	21.2

In order to reach a high yield combined with maximum selectivity, asymmetric membranes are used, made via a phase separation process for which different techniques are available. If a crystallizable polymer is dissolved in a solvent, liquid–solid (L–S) phase separation can occur. Otherwise, liquid–liquid (L–L) phase separation can generally take place, where the solution

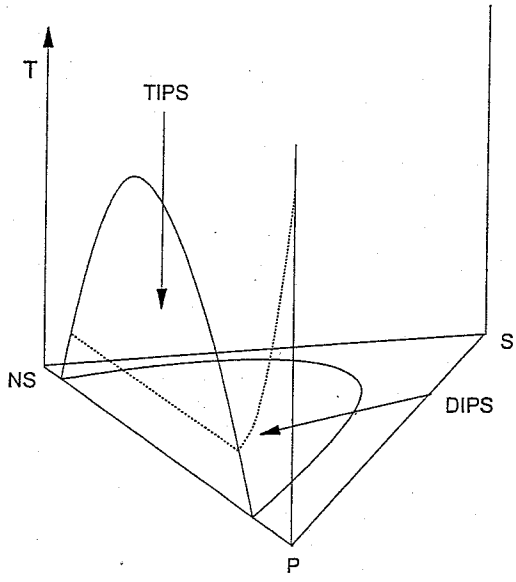

Figure 1-36. Schematic representation of the TIPS and DIPS processes (T, temperature; P, polymer; S, solvent; NS, nonsolvent (Berghmans, 1995).

separates into two liquids. These phase separations can be induced by either changing the temperature (TIPS) or changing the concentration (DIPS) (see Fig. 1-36).

In order to freeze in the morphology induced by phase separation, solidification of the polymer has to be realized. This is usually obtained by passing the glass transition temperature of the polymer, although crystallization itself can also be used (L–L followed by L–S). The use of TIPS in making membranes is only recent and mostly DIPS, as originally introduced by Loeb and Sourirajan (1962), is applied. In this process, no temperature change is required to induce phase separation. Instead, a change in concentration is induced by exchanging solvent for nonsolvent. Of course the solvent and the nonsolvent have to be mutually soluble. The formation of the structure with both processes is schematically shown in Fig. 1-37.

Vitrification, either by crystallization or by passing the glass transition temperature

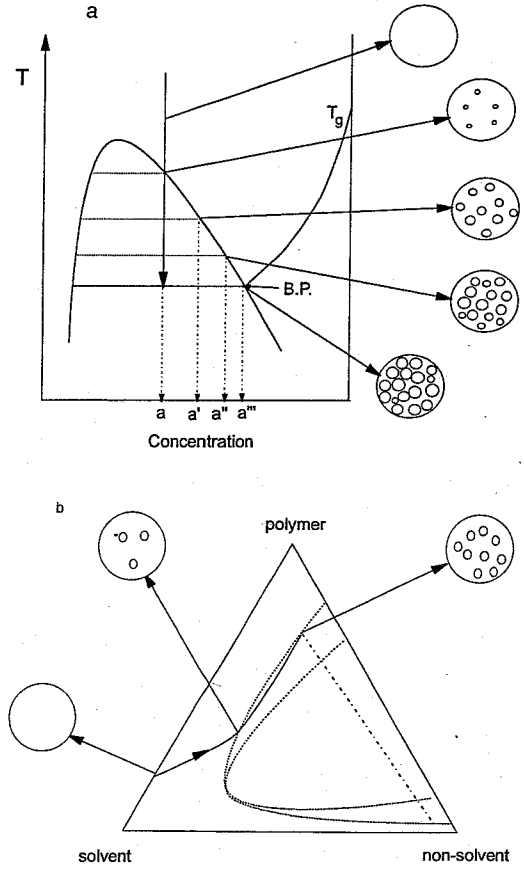

Figure 1-37. (a) TIPS: mechanism of phase separation by lowering the temperature (B.P. is the Berghmans point); (b): DIPS: phase separation by changing the composition, exchanging solvent for nonsolvent (Berghmans, 1995).

is depicted in the ternary phase diagrams of Fig. 1-38.

As an example we will use the continuous spinning of hollow porous asymmetric fibers of poly(phenylene-ether) (PPE), used for oxygen/nitrogen gas separation. Although PPE is known as an amorphous polymer, it can crystallize from solution. Interestingly, the crystallization line and the liquid–liquid demixing line almost coincide, see Fig. 1-39, which shows the phase behavior of PPE using cyclohexanol as a solvent. In this case L–S and L–L demixing mutually interfere.

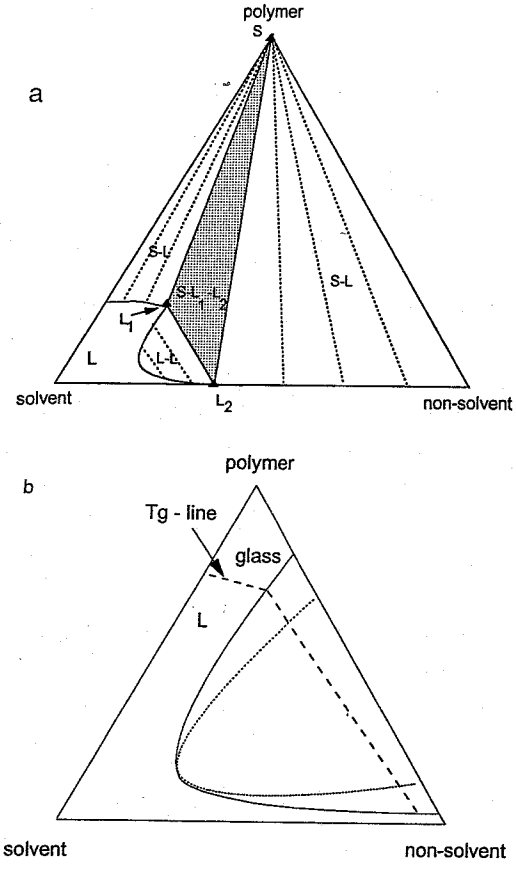

Figure 1-38. Ternary phase diagrams where interferences with liquid–liquid demixing are possible: (a) crystallization and (b) glass transition (Berghmans, 1995).

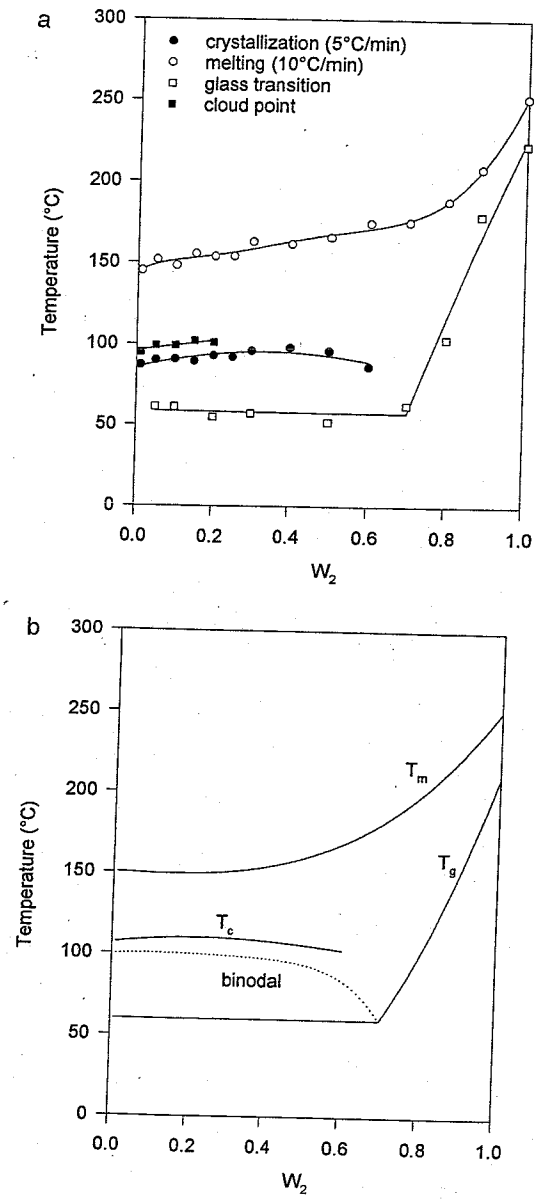

Figure 1-39. Temperature–concentration diagram of PPE in cyclohexanol, (a) as measured and (b) schematically. W_2 is the weight fraction of PPE (Berghmans, 1995).

This is indirectly made use of in spinning asymmetric hollow fiber membranes. Initially, a homogeneous polymer solution is prepared of PPE–TCE (trichloroethylene), to which some nonsolvent (EtOH, 2-ethyl-1-hexanol) is added in order to start at a position closer to the binodal demixing line. This situation is enhanced by the evaporation of some solvent in the air gap, yielding gradients over the thickness of the fiber that are even more enlarged by the introduction of temperature gradients due to slight cooling in the same air gap (mostly TIPS, consequently). In the coagulation bath, the solvent is replaced by nonsolvent (MeOH, methanol), i.e., the DIPS process, combined with efficient cooling, yielding fast vitrification, and eventually a closed, thin skin. From the inside, the hollow fiber

is fed with a solvent/nonsolvent mixture to allow only DIPS here, resulting in an open, porous structure. The process was successfully developed by KRITNO and Aquilo [see Smid et al. (1991)]. Theoretical approaches have been developed for TIPS and DIPS processes [see Cheng (1993), Cheng et al. (1994), and Berghmans (1995)]. In Berghmanns's thesis, some nice illustrations can be found using the more accessible system poly(ethersulfone)/*n*-methyl-pyrolidine (PES/NMP) with water as a nonsolvent, illustrating funny shaped interiors of the fibers (see Fig. 1-40), and more seriously, a closer study of unwanted macrovoid formation, which grows from instabilities on the surface and possesses a kind of fractal structure (see Fig. 1-41).

In this section, it was illustrated how specific structures can be obtained in the processing of polymers if phase separation and early vitrification are used as a way to create the desired morphologies. In Sec. 1-4 of this introductory chapter, and in Chap. 10 of this Volume, the focus will be on the chemically induced phase separation process, CIPS, where phase separation is chemically induced by polymerizing the (reactive) solvent after molding. Upon polymerization, the solvent converts into a nonsolvent, thus introducing phase separation, and in most cases, phase inversion. Finally, the solvent

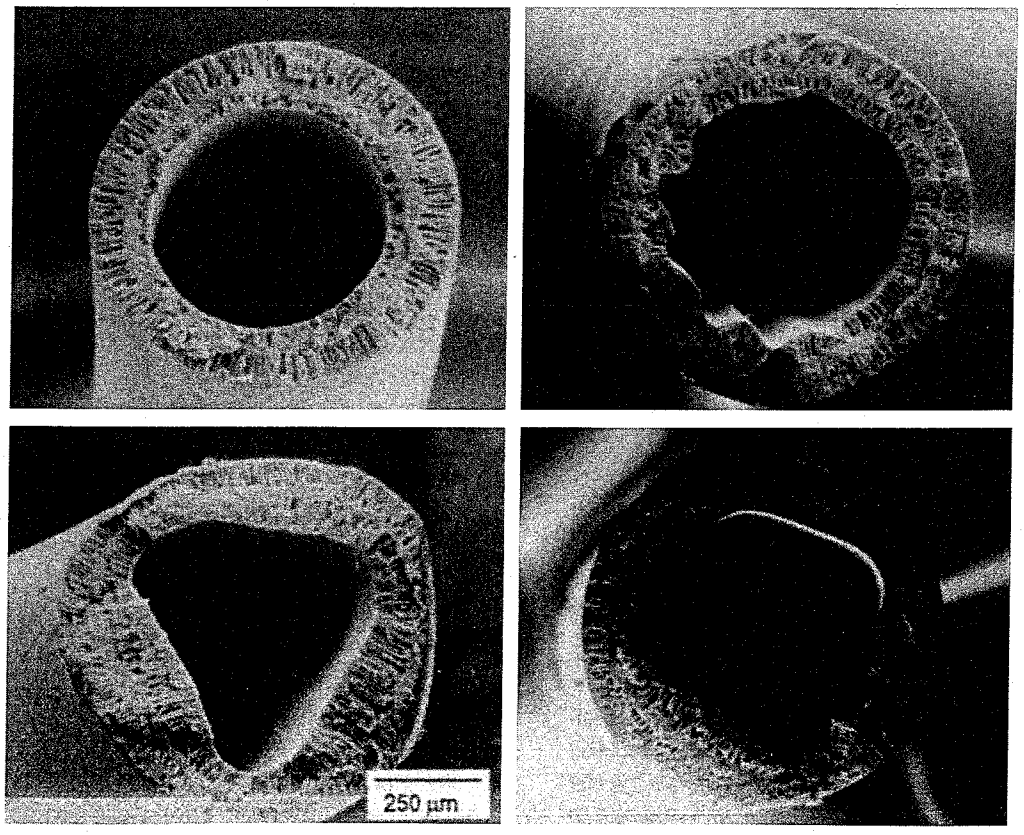

Figure 1-40. Different cross sections of PES fibers made using different compositions of the internal bore liquid causing DIPS on the inside (Berghmans, 1995).

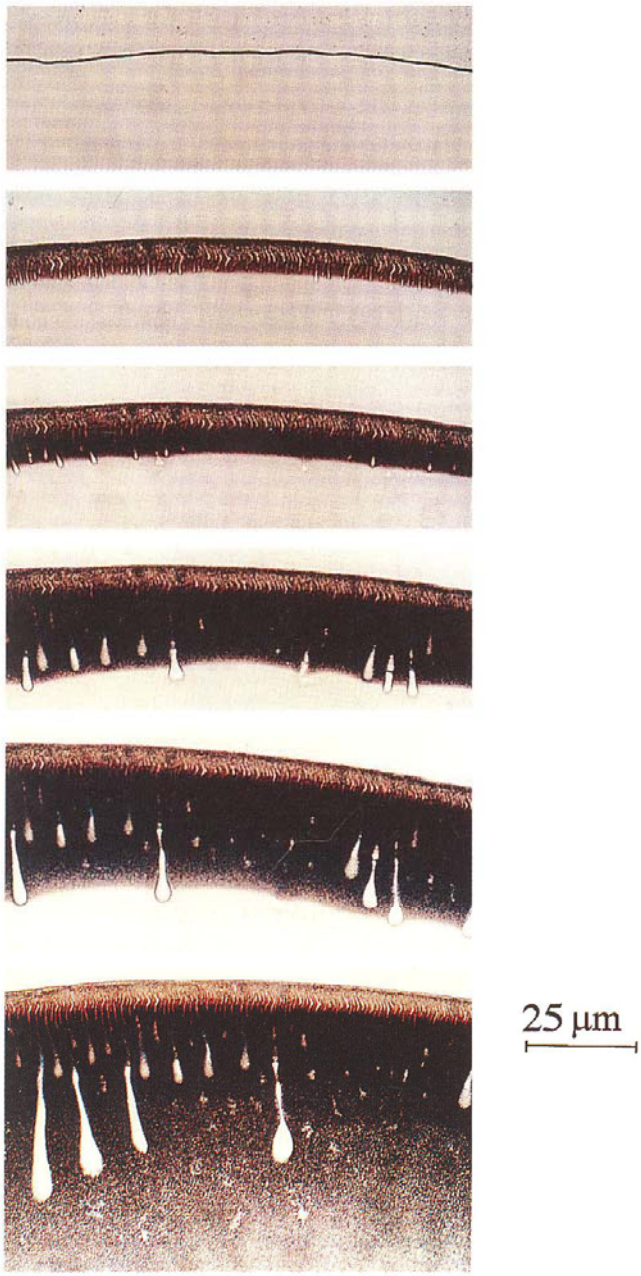

Figure 1-41. Visualization of the formation of macrovoids in PES placed in between two glass plates, and at different times after being surrounded by nonsolvent (Berghmans, 1995).

becomes, as a second, dispersed phase, an integral and often even structural component of the final product. This method proves to have great potential for creating unique materials, on the one hand by precise control of the size of the dispersed phase (from 1 μm down to 20 nm) via the prevention of coalescence, and on the other hand by turning the final properties of this phase from completely rubbery to glassy by starting with aliphatic or aromatic epoxies as the reactive solvent.

1.3.6 Crystallization

As already mentioned in the introduction to this section (Sec. 1.3.1), even in one-phase systems morphology development during flow can be important for the final properties, provided that we deal with crystallizable polymers. Two chapters (Chaps. 4 and 5, respectively) of this Volume, are devoted to the modeling of shear-induced crystallization, so in this introductory chapter only some examples will be given.

As in the determination of proper constitutive equations for the time- and temperature-dependent nonequilibrium density and the history dependent viscoelastic stresses, also in crystallization the problem is not so much a mathematical one, but much more an experimental one. In differential scanning calorimetry (DSC), the crystallization kinetics can in principle be measured. However, upon shear, drastic changes of orders of magnitude can occur, caused by shear-induced nucleation. Important in this respect is the fact that the high end tail of the molecular weight distribution will be oriented in flow the easiest. It is this tail that can hardly be measured using conventional characterization equipment, e.g., gel permeation chromatography (GPC). These flow-induced nuclei not only accelerate the crystallization process tremendously, but also cause anisotropy by directing the crystal growth direction. As a particular example, it was shown by Bevis and co-workers at Brunel University (Allan and Bevis, 1992; Bevis, 1994) that by using a special injection molding technique, the so-called multi-live-feed system which keeps mildly shearing the melt during solidification (thus only orienting those molecules that have a

long relaxation time; i.e., the high molecular weight tails which are close to the crystallization temperature), a more than 90 % shish-kebab morphology could be realized through the whole thickness of the product. Originally, the technique was developed to eliminate weld lines. Later it was used to control the (eventually multiaxial) orientation over the thickness by shearing in different directions at different stages of the cooling process. Most interesting is that this technique allows, for the first time, the control of whatever happens in the mold, independent from the product design and the position of the filling gates (the sprues), since the influence of the flow during mold filling is clearly overruled by the flow applied during solidification.

As a second example some recent data are presented, as obtained in our laboratory for isothermal crystallization experiments with slightly supercooled polypropylene (PP) melts using a standard Rheometrics device (RDSII) (Vleeshouwers and Meijer, 1996). The following procedure was adopted: PP samples, placed between the standard cone and plate geometry, were molten at a high enough temperature, usually 260 °C, long enough to erase the crystal memory but for insufficient time to obtain excessive degradation. Subsequently the sample and the measuring chamber were brought to a lower temperature, usually 138 °C, and a dynamic test was started. The temperature for (slight) supercooling was chosen as such that it took a long time before any noticeable effect of the proceeding crystallization occurred in both the increasing dynamic modulus and the decreasing loss angle. Secondly, the samples were pre-sheared at the high temperature and the same procedure was repeated; the results are plotted in Fig. 1-42.

The influence of the nucleation-induced crystallization is clear. Using different shear histories, it could be established that the total shear proves to be the determining factor, although a higher shear rate results in a high shear time. Of concern is that different grades of PP, with different molecular weight (distributions), revealed completely different behavior (see Fig. 1-43).

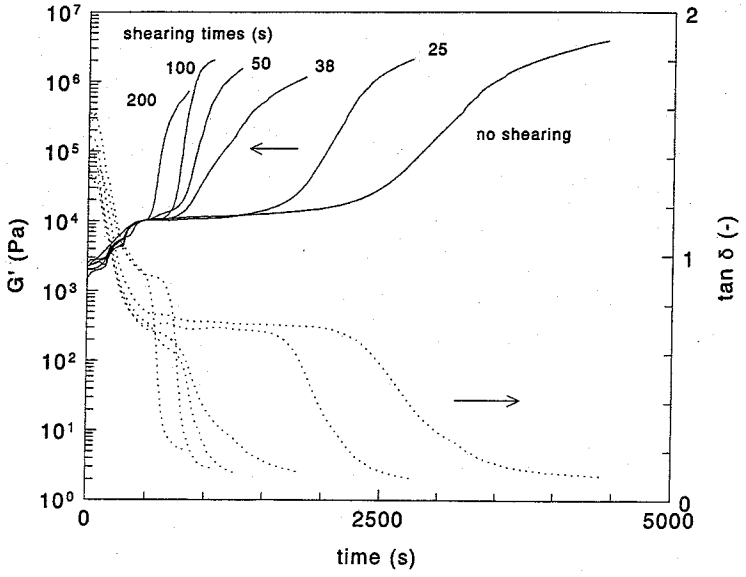

Figure 1-42. Isothermal crystallization experiments in a Rheometrics RDSII for a PP melt with different pre-shear histories, 5 s^{-1} at 260 °C (tan δ is the loss angle and G' the dynamic modulus) (Vleeshouwers and Meijer, 1996).

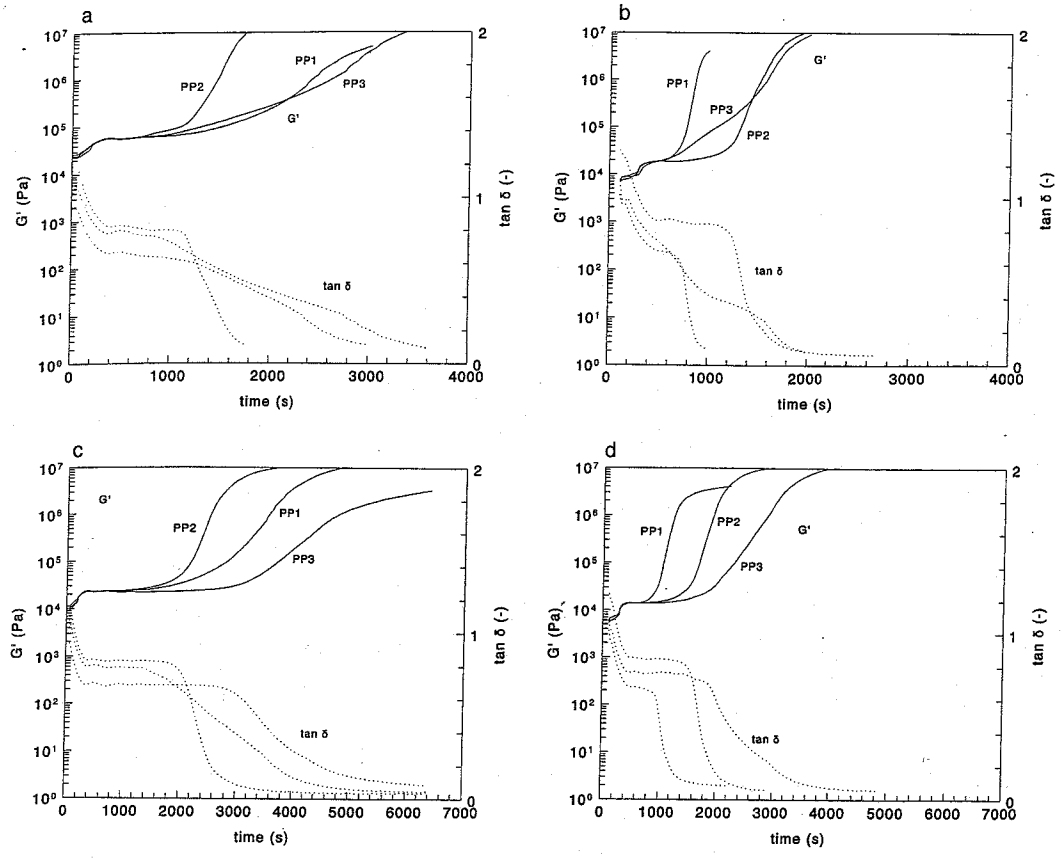

Figure 1-43. As Fig. 1-42, for three different PP grades: a high molecular weight (PP1) a low molecular weight (PP2), and a broad molecular weight distribution (PP3), in between the other two. The conditions were: (a) without shearing before quenching to 138 °C, (b) after pre-shearing at 200 °C and 5 s^{-1} for 100 s, (c) without pre-shearing before quenching to 140 °C, and (d) after pre-shearing under the same conditions as (b) with subsequent quenching to 140 °C (Vleeshouwers and Meijer, 1996).

These aspects are relevant for all polymer processes where crystallization occurs after pronounced shearing, and the different behavior of different grades of, e.g., PP and PE in fiber spinning, film blowing, and injection molding, could possibly be explained based on these properties. Tuning of the molecular weight distribution still proves to be a powerful tool in designing optimum grades for these (bulk) processes, especially now the new metallocene catalyst systems, which enable previously impossible fine-tuning, are increasingly used. More research is apparently needed in this area.

1.3.7 Liquid Crystalline Polymers

Of all polymers, the liquid crystalline polymers show the most pronounced structure development during flow. Lyotropic systems are used in high performance fiber processes (see Chap. 11 of this Volume), while thermotropic systems are generally extruded and, in particular, injection molded. Numerous papers have been published

on the resulting layer structure in molded products. It is far beyond the scope of this introductory chapter to review all these developments. It could even easily be stated that most of the structure development can be considered as an unwanted effect, yielding delamination problems. More restrictive still, however, is the price of liquid crystalline polymers, and after a boom of attention in the late 1980s and early 1990s, industrial interest seems to have stopped completely, apart from some niche markets, in particular the electronics industry, which requires properties such as dimensional stability at high temperatures, solvent resistance, etc., and of course the fiber world. Scientifically interesting results on the structure development of liquid crystalline polymers have been obtained on the theoretical side by Doi (1981), Marrucci and Greco (1993), and Marrucci and Maffetone (1993), and experimentally by the group of Mewis and Moldenaers in Leuven [see, e.g., Moldenaers et al. (1989, 1993), Yanase et al. (1991), Grizaud et al. (1993), and Maffetone et al. (1994)], and in Bristol by Fischer et al. (1996).

Also worthwhile mentioning are the many attempts that have been made in the direction of blending stiff molecules with flexible ones, mainly aimed at lowering the price of the resulting systems and reducing the processing and delamination problems. Interesting morphologies were obtained by uniaxially stretching macroscopic blends in a spinning device [see, e.g., Crevecoeur and Groeninckx (1990a, b, c, 1991), and Crevecoeur (1991)]. The mechanical properties of these systems, however, never exceeded the Halpin-Tsai type rule of mixtures, and the limitation to fiber-shaped products prevented their widespread application.

More interesting in view of the perspective properties is a dispersion of single rigid rod macromolecules in a flexible coil polymer matrix, such that the rods act as a reinforcing component. Although a mixture of rigid rod and flexible coil polymers on a molecular scale is entropically unfavorable (Flory, 1953, 1969) and self alignment of the rods via phase separation will occur, there are ways to prevent macroscopic phase separation between the two types of polymer. Firstly, a chemical bond between the two polymers in terms of block and graft copolymers results in a phase separation limited to nanoscopic dimensions (Dang and Evers, 1991; Dotrong et al., 1992; Arnold et al., 1989, 1990). These types of polymer assure an efficient translation of the stress applied between the reinforcing element and the matrix material. Besides this, other chemical variations lead to molecular composites such as the homogeneous blending of two flexible polymers where one can be transferred at elevated temperatures into a stiff chain configuration [so-called in situ generation of molecular composites (Arnold et al., 1989, 1990)]. Here a phase separation cannot occur and the stiff chain macromolecules are somewhat "trapped" in the flexible matrix. Finally, the use of low molecular weight stiff compounds with Y-shapes and star shapes (multipodes) may increase the compatibility due to the small molecular weight of the multipodes. They might act in the same way as reinforcement on a molecular scale (Braun et al., 1993). Most important is the fact that such a reinforcement is reported to act in all three dimensions. Other investigations on polymers with similar structural elements show synergistic effects in blends with PETP (Hinrichsen and Rötting, 1993). However, the processing of blends of unmodified rigid rod and flexible chain polymers can also lead to polymer composites with stiff reinforcing elements on a nanoscopic scale. For that purpose, processing via dissolving both polymers in a common solvent is required.

The critical concentration above which phase separation will occur even in solution, is limited to about 4–5% polymer (Flory, 1953, 1969). Rapid coagulation of such solutions leads to the composites described above with mechanical properties according to the Halpin–Tsai equation, and with aspect ratios of the reinforcing elements of above 100 (Takayanagi et al., 1980; Helminiak et al., 1983; Kummerlöwe and Kammer, 1990).

The synthesis of stiff chain polymers in solutions of flexible chain polymers, or a shear-induced homogenization of demixed solutions, can shift the value of the critical concentration to about 8% polymer in the solution (Berger et al., 1993). Phase separation may even be completely suppressed if specific interactions between the two polymer types (ionic interactions, acid–base interactions) exist. This has not only been predicted theoretically (Eisenbach et al., 1995; Noolandi and Shi, 1996), but it has also been experimentally explored by Eisenbach et al. (1995) and Harra and Chen (1996). The resulting blends are on a molecular scale but, more important they are transparent and melt-processable. The reported mechanical properties for these composite materials exceed the theoretically predicted values.

1.3.8 Discussion

In this section, it has been demonstrated that structure development during flow is of utmost important for the processing of polymer systems. The main reason is that almost without exception polymers are combined with other polymers, reinforcing agents, stabilizers, antioxidants, etc., to make them really suited for their final task. Apart from the case of reactor-modified polymers, processing plays a decisive role. It is clear that, despite the progress made in recent years, still a lot of research is necessary in this area to really be able to predict the performance of polymeric systems, as obtained via processing, depending on the properties of the constituent phases. In the next section, reactive processing is briefly reviewed.

1.4 Reactive Processing

1.4.1 Introduction

Reactive processing is traditionally exploited in molding processes such as (R)RIM, (S)RIM (reinforced and structural reaction injection molding) and RTM (resin transfer molding), also in BMCs (bulk molding compounds) that are injection or compression molded, and in composite processes like GMC [glassfiber (mats) reinforced compounds]. They are applied in prepregs and in monomer-wetted, continuous roving processes, e.g., pultrusion and filament winding. Finally, hand lay-up processes exist which involve a lot of labour and where, eventually, hot presses or autoclaves are used to cure the product. Another extremely important area is that of coatings and paints. Usually epoxies, unsaturated polyesters, and polyurethanes (PUR) are used, although specialities like caprolactam (anionically polymerized) also find applications. Handbooks that summarize the state-of-the-art of the modeling of these processes are available, see, e.g., Macosko (1989), Isayev (1987), and Tucker (1989). Chapter 9 of this Volume deals with (R)RIM processes, especially of the most important class of materials: the PURs in RIM processes, while Chap. 7 of this Volume treats the fundamentals of network formation. Today reactive extrusion has also gained a lot of attention, mainly because of the versatility of the continuous compounding technique. Since extruders can in principle be defined

as intensively stirred, self-transporting mixers with a small volume (thus expensive) and an improved heat exchange possibility relative to stirred vessels, which is, however, still limited, especially if highly viscous systems are used; hence severe limitations exist in practice with respect to the number of possible reactive systems that can be explored successfully. The requirement of total conversion puts an even more severe constraint on the choice of system to be used. Chapter 6 of this Volume gives a detailed review on reactive extrusion, while Chap. 8 of this Volume focuses on the reaction at interfaces in polymer blends. In this section the CIPS (chemically induced phase separation) process will be briefly introduced, in addition to the TIPS and DIPS processes dealt with the previous section (Sec. 1.3), while more details can be found in Chap. 10 of this Volume.

1.4.2 Thermoplasts in Reactive Solvents

The use of reactive solvents offers an interesting and flexible route to extend to processing characteristics of thermoplastic polymers beyond their existing limits. This holds for both intractable and tractable polymers. The first mainly applies for amorphous, high T_g polymers, where processing is usually limited due to the high temperatures required, which are close to their deterioration temperature, and where the solvent helps to reduce the processing temperature considerably. The second mainly holds for semi-crystalline polymers, and the attention here is focused on obtaining low viscosities in order to be able to apply alternative processing routes, e.g., pouring or casting, for those polymers that are generally easy to process by more conventional techniques such as injection molding or extrusion. In both cases the solvent is polymerized after molding, thus converting it into a nonsolvent, and becomes, after the concurrent phase separation and phase inversion, an integral and often structural part of the final product. Interestingly, specific morphologies, in terms of the size of the dispersed (previous solvent) phase formed or the position and thickness of the in situ formed interlayers if polymerization occurs in the presence of a polar surface, can be obtained which can otherwise be extremely difficult to realize. Moreover, the flexibility of the choice of the reactive solvent creates tuneable mechanical (and if requested, other) properties for these phases, varying from glassy, with a T_g of typically 200 °C, to completely rubbery, with a T_g far blow room temperature. Of course a disadvantage of the technique is that a polymerization step must occur after the shaping process. Compared to more standard reactive processing techniques, however, clear advantages exist with respect to the absence of the need for 100 % conversion, the occurrence of early vitrification (yielding a fast demolding possibility) produced by the reaction-induced phase inversion, and the fact that the continuous thermoplast phase ultimately determines the main product properties, including the possibility of second stage deformability and reprocessability.

In order to meet the ever-increasing demands put on polymeric materials in new applications, polymer chemists continue to synthesize new polymers that can often be regarded as intractable from a processing point of view. This is the case for the group of high temperature polymers developed for structural applications, where a high glass transition temperature is required, and for polymers designed for those applications where a high molecular weight is necessary for mechanical reasons. Basically, the main advantage of polymers over the more traditional materials, which is their easy processability, is often lost and either compromis-

es are accepted, e.g., by introducing flexibility to the polymer backbone, thus lowering the T_g or by blending with more flexible polymers, e.g., in PPE–PS blends (Noryl from General Electric Plastics), or expensive post-machining is used, e.g., in products made from ultrahigh molecular weight polyethylene (UHMWPE) pressed and fused plates; alternatively processing aids like volatile solvents are applied, e.g., in spin coating or solution spinning, for example, of the same UHMWPE used to produce high performance fibers. This last solution is restricted to products with a high surface-to-volume ratio, usually fibers and films, and violates the air quality regulations, thus necessitating the need for complete solvent recovery. Moreover, the final product is only a (often relatively small) part of the main stream in the production process, which almost exclusively consists of closed loop evaporation and condensation operations for the solvent. All these problems make the products of such a process necessarily expensive but, more importantly, they limit the use of these attractive polymers in many possible new applications.

Basically it could be stated that the major part of recent polymer development, as occurs in most of the large research laboratories of the main polymer producers all over the world, and sometimes in the laboratories of important and big enough end-users, can be summarized as being a continuous compromise to the stated necessity of introducing a low enough viscosity as required for easy processing while maintaining the most important mechanical properties of the product: stiffness, strength, and especially, work-to-break (impact strength). The molecular weight (distribution) of the pure polymers is finely tuned and/or blending/compounding with different polymers is practised to obtain principally heterogeneous materials that should possess a stable enough morphology to survive the subsequent shaping step. The easily recognized alternative of using reactive processing techniques, as mentioned in Sec. 1.4.1, seemingly solves the problem, since monomers are generally present during processing and they are converted into polymers only after their final shaping operation. Disadvantages and limitations exist, however. Apart from the introduction of chemistry to the end-user, which does not automatically guarantee the best control during polymerization, there is a need for almost complete conversion, since the product's properties are directly and exclusively determined by the chemistry, and only at the end of the polymerization are the final mechanical properties obtained.

A possible solution to some of the problems mentioned is to make use of reactive solvents. Basically the idea is to sell the solvent with and within the product after having made it harmless by applying a polymerization step. During processing, the solvent either causes a strong reduction in the processing temperature (which is important for the intractable high temperature polymers) or it decreases the viscosity of the polymer such that standard (for intractable high molecular weight polymers) or alternative (for tractable polymers) processing techniques, where a low viscosity is a prerequisite, come within reach. After shaping, the solvent is converted into a nonsolvent induced by the first polymerization steps. Phase separation results, generally accompanied by phase inversion, which happens to occur anyway if the volume fraction of the polymer exceeds about 10%. A dispersed phase results, locking the original solvent inside the thermoplastic matrix material that forms the continuous phase. A schematic impression of this is depicted in Fig. 1-44.

In Chap. 10 of this Volume, several systems which can be regarded as primary

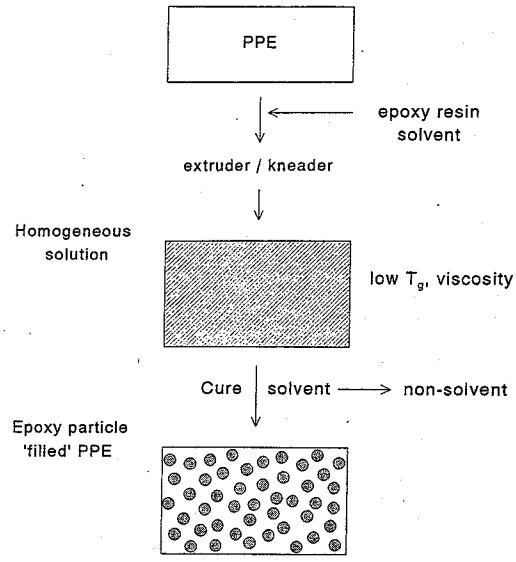

Figure 1-44. Schematic diagram of the procedure for processing polymers using reactive solvents (after Venderbosch, 1995).

examples of this novel processing technique are reviewed: The first, and by far most extensively investigated system, is PPE–epoxy, an example of the processing of an intractable polymer (Venderbosch, 1995; Venderbosch et al., 1994, 1995 a, b; Meijer et al., 1996). The phase diagram and the (chemo)rheology (which are important for polymer processing) are determined and the morphology development, which yields the final product properties, is recorded. Different epoxies, aromatic versus aliphatic, are used to adjust the properties of the dispersed phase. Accordingly, composite applications have been explored, where unique morphologies are obtained since phase separation preferentially occurs at the polar surfaces of the fibers and the "optimal" composite could possibly be fabricated using this technique. Subsequently, the systems polyethylene–styrene (PE–St) and polyethylene–butylmethacrylate (PE–BA) are reviewed as examples of tractable polymers. In these cases, crystallization interferes with the chemically-induced phase separation and the focus will be on the morphology development during reaction. Some of the outlooks on possible applications in other fields, making use of the flexibility of this technique, are mentioned.

1.4.3 In Situ Characterization

Systems like these resemble the techniques used to obtain IPNs (inter-penetrating networks), where one monomer is polymerized in the presence of a polymer network, so forming a second, interpenetrating network. Also, both networks can be formed simultaneously or sequentially. Depending on the chemical or physical nature of the network, crosslinks or entanglements, or combinations of both, the nomenclature is different. The above examples can be classified as semi-IPNs. Not only is the introduction of processability an important issue in these systems, but a controlled phase separation is also of importance for obtaining the desired properties in the final product. As in the in situ polymerizations of block copolymers, e.g., with hard and soft segments, as in polyurethanes, chemically induced phase separation can yield unique morphologies and the monitoring thereof is of great practical use. Therefore complex in situ characterization methods are increasingly being used [see e.g., Goossens et al. (1997) and Chaps. 10 and 9 of this Volume]. Examples of these methods are Raman spectroscopy, which can distinguish between reaction kinetics and the kinetics of phase separation (see Figs. 1-45 and 1-46 for examples), and combined time-resolved wide and small angle scattering patterns (WAXS and SAXS), which can distinguish between the kinetics of phase separation and crystallization (see Fig. 1-46). The last measurements are usually performed using synchrotron X-

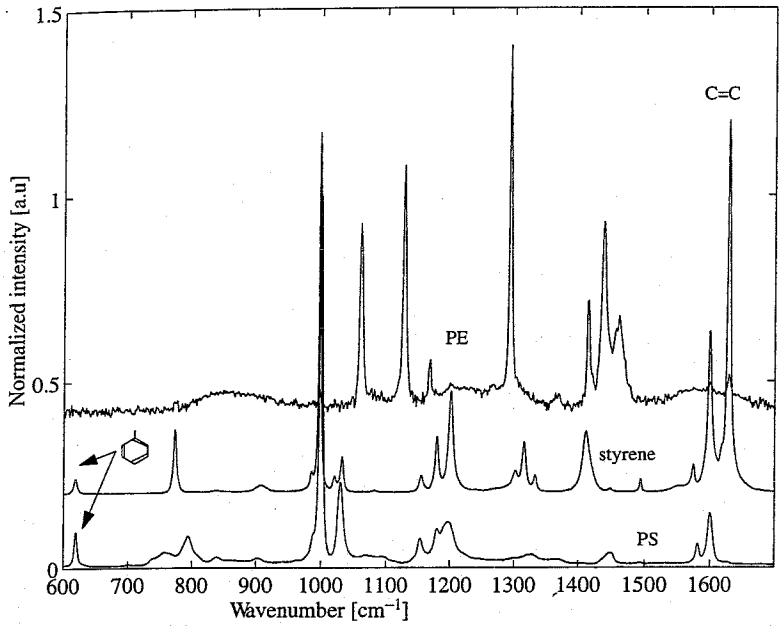

Figure 1-45. Raman spectra of PE, PS, and styrene.

ray sources like those in Daresbury, Hamburg, and Grenoble.

As an example of the possible control of the morphology of the dispersed phase, the system poly(methylmethacrylate)(PMMA)–(aliphatic) epoxy is used. Polymerizing two compositions (50/50 and 70/30) at three temperatures (60, 100, and 140 °C, resp.) yields not only completely different particle sizes of the dispersed phase, but also different trends (see Fig. 1-47) (Jansen et al., 1997).

In this case we are aiming at the smallest possible particle sizes of the rubbery dispersed phase (usually ca. 20 nm) in order to obtain the maximum mechanical properties in terms of toughness (see Sec. 1.5 of this Chapter and Chap. 12 of this Volume). The explanation for the experimental findings concerning the resulting particle size in Fig. 1-47 is based on the understanding that, during polymerization, coalescence of just phase-separated particles should be avoided as much as possible. This can be realized by either slowing down coalescence by keeping the continuous phase highly viscous, thus performing the polymerization close to the (composition-dependent) T_g of the matrix material, or by overcoming coalescence by reaction kinetics. Both aspects can be seen by inspection of the results presented in Fig. 1-47. Given the composition-dependent glass transition temperature of the original solution (Fox equation, see, e.g., Fig. 1-37), plotting the resulting particle sizes against $T_{eff}=(T_{pol}-T_g)$ would result in a single curve showing a maximum. From $T_{eff}=0$, the particle sizes increase due to the pronounced effect of coalescence; after the maximum, the particle sizes decrease due to the temperature dependence of the reaction kinetics. By chemically increasing the reaction kinetics, independent of the polymerization temperature, the whole curve would come down. From this analysis, a time-dependent polymerization temperature can eventually be derived by a stepwise

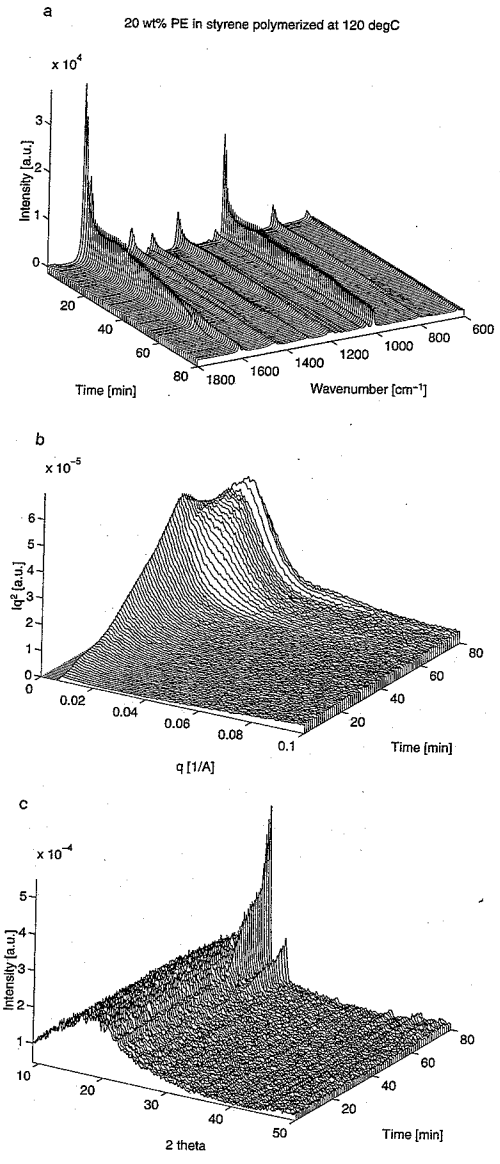

Figure 1-46. (a) Time resolved Raman spectra, and (b) WAXS and (c) SAXS patterns measured during polymerization at 120 °C of 80 % styrene (slow system) in 20 % polyethylene (Goossens et al., 1997).

increase, given the conversion-dependent Fox equation and thus the conversion-dependent T_g (see Figs. 1-48 and 1-49).

Things become even more complicated if both constituents are reactive, such as in the case of MMA–epoxy (Jansen et al., 1997). Depending on the relative reaction kinetics of both monomers, the time- and composition-dependent glass transition temperature will change, and thus different polymerization protocols will result. Generally, in the polymerization of IPNs this is not taken care of and, almost without exception, these materials are polymerized at a relatively high temperature. A lack of control of the phase separation process results unless multi-block polymers are synthesized as in the case of, e.g., polyurethanes.

1.4.4 Discussion

In this section the CIPS process has been introduced, which combines easy processing with unique properties of the resulting polymeric systems via a controlled, chemically induced phase separation process. A disadvantage of the technique described is that chemistry is introduced to the end-user, since, in order to obtain small particle sizes, CIPS should be applied in quiescent surroundings, e.g., in the mold. Raw material manufacturers are currently investigating how the technique using reactive solvents can be successfully exploited in the production of feedstock polymers in the form of (thermoplastic) granules, e.g., via reactive compounding. From a combination of the conclusions from Secs. 1.3 and 1.4 of this introductory Chapter, it will be directly clear that in this case a large number of time-dependent processes interfere, which is complicated by a shear-induced phase inversion process. In fact, HIPS (high impact polystyrene) and ABS (acrylonitrile–butadiene–styrene) polymers are more or less made via these routes in stirred vessels. It is obvious that a lot of research is still necessary in this field in order to be able to make quantitative, or even qualitative, predictions. Apart from the necessity to chemically stabilize the structure obtained, advantag-

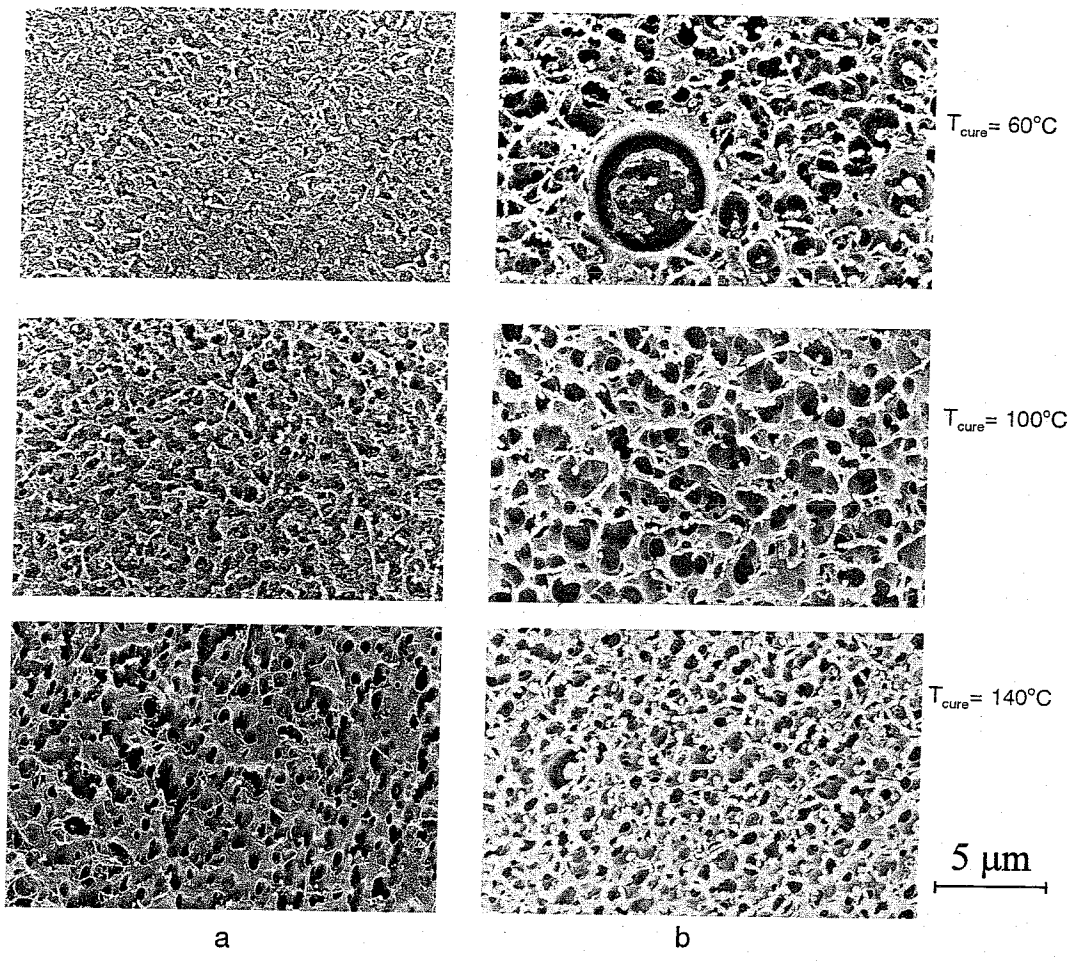

Figure 1-47. Resulting particle size after polymerizing PMMA–epoxy of two compositions: (a) 70/30 and (b) 50/50, at three different temperatures (Jansen, 1996).

es with respect to low viscosities in the subsequent shaping process are naturally lost.

The next section deals with obtaining the ultimate properties of polymers via processing.

1.5 Processing for Ultimate Properties

1.5.1 Introduction

In the preceding sections, it has become clear that the processing of polymers, at least partly, determines the properties of the final product. Particularly in the area of ultimate properties, processing makes all of the difference between mediocrity and excellence. This might be best illustrated by the processing of high performance fibers (HPF) based on flexible polymers, notably the linear polyethylenes. The difference in mechanical properties between a garbage disposal bag and an HPPE ultra strong fiber is only obtained by orienting the macromolecules in a processing operation. In this section we will briefly review some of the elementary steps in these processes. Starting

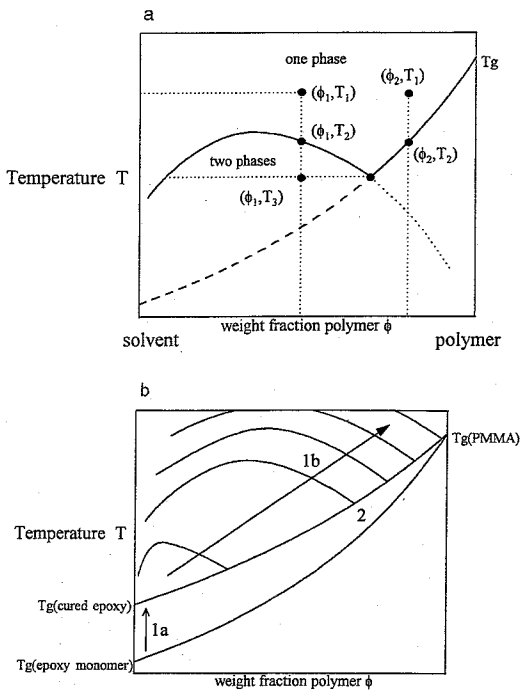

Figure 1-48. (a) Solvent–polymer phase diagram (schematic) and (b) epoxy–PMMA phase diagram showing the glass transition temperature of a one-phase epoxy monomer–PMMA solution, the glass transition temperature of the molecular, dispersed, cured epoxy–PMMA solution (hypothetical), and the coexistence curves between epoxy and PMMA which shift in the direction of the arrow as the epoxy polymerizes (Jansen, 1996).

with mechanical properties such as the modulus and strength (Sec. 1.5.2; see also Chaps. 11 and 16, respectively, of this Volume), we will continue with the toughness (Sec. 1.5.3.; see also Chap. 12 of this Volume) and end with a short discussion (Sec. 1.5.4).

1.5.2 Ultimate Modulus and Strength

The invention of high performance aromatic polyamide fibers, such as Kevlar from Dupont and Twaron from Akzo-Nobel, started a long time ago with the observation that, upon increasing the concentration of

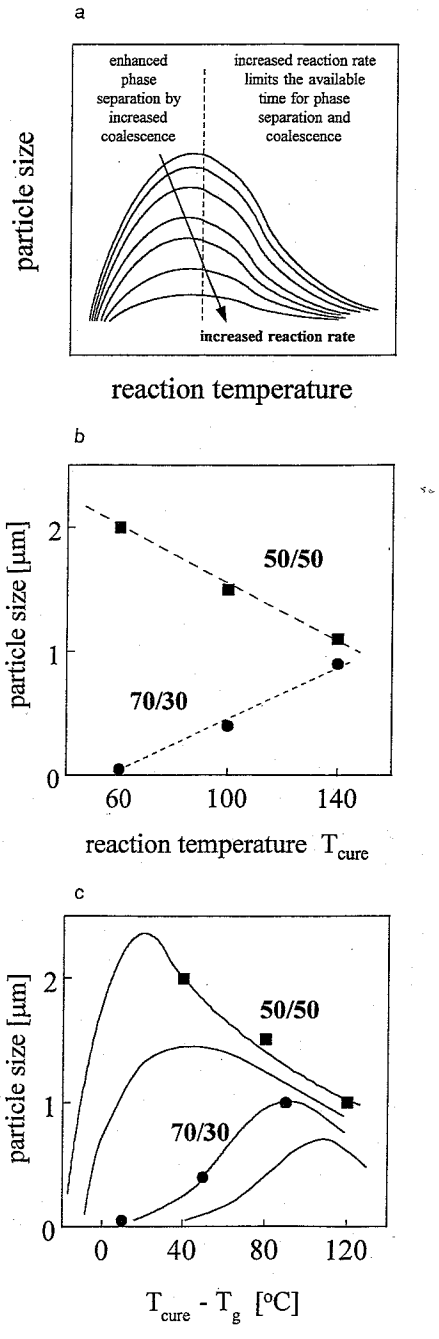

Figure 1-49. Resulting particle size as a function of the (conversion-dependent) effective polymerization temperature for aliphatic epoxy blends with either 70 wt.% PMMA or 50 wt.% PMMA; (a) schematic, (b) as measured (compare with Fig. 1-47), and (c) replotted data of Fig. 1-49 b in terms of Fig. 1-49 a (Jansen, 1996).

relatively stiff aramid molecules in solution, a tremendous drop in viscosity was suddenly observed. This drop in viscosity proved to be related to the occurrence of the so-called nematic state: a kind of self-assembling of the individual molecules into domains: bundles of molecules. This process is a natural one and has been exploited through the ages, e.g., in the transport of tree trunks via natural and cheap mechanisms like flowing rivers. This self-assembly can also be found in disposits and wreckwood in natural vortices as occur, e.g., close to waterfalls, notably Niagara Falls. Also closer to home: floating fishfood in the form of cylinders with a limited aspect ratio tends to form bundles, even in the absence of flow, in the backyard pond. Back to aramids: the drop in viscosity observed, not only served to provide easy processability of rigid rod molecules in solution, but also made it possible to orient complete domains rather than individual molecules, e.g., in extensional flows. This orientation is prerequisite for obtaining the ultimate properties of macromolecules, as already explained in the introduction (Sec. 1.1 of this Chapter). Apart from the problems encountered in the polymerization of rigid rod molecules and the aggressive solvents that have to be used, the spinning of these solutions into fibers is a relatively straightforward task. The strong elongational flow into the die, followed by the complete irrotational flow during the draw-down applied in the (small) air gap between the die exit and the subsequent coagulation bath, is sufficient to orient these domains into the direction of the fiber axis. Given typical polymer concentrations of 15 %, the only mismatch originates from the removal of solvent during coagulation. This pushes the case for high molecular weight polymers, given their more modest off-axis rotation during this process of removal of the 85 % solvent, even if this is not necessarily required for the ultimate strength, given the generally strong hydrogen bonds between the individual macromolecules of aramids (see for details Chap. 11 of this Volume).

In contrast with the processing of these lyotropic systems, the orientation of flexible macromolecules during processing is much more complicated. This is mainly due to the presence of the restoring entropic forces and the absence of possibilities to freeze in the ultimate flow-induced orientation. In this respect is it worthwhile remembering that the frozen-in orientation in, e.g., injection molding, where both high strain rates and high cooling rates prevail, is only of the order of 2 % of the maximum molecular orientation that is obtainable (see Sec. 1.2 of this Chapter). In injection molding, even the presence of this minor orientation proved to be relevant for long term dimensional stability, since it introduces anisotropic relaxation and physical ageing. Here we need to achieve the maximum orientation since, given the typical series character of amorphous and oriented structures, yielding rule-of-mixtures type behavior with emphasis on the enormous influence of the weakest component, even if only a few percent of unoriented material is present, this will ruin our ultimate properties, e.g., in terms of stiffness (see Irvine and Smith, 1986). Therefore almost without exception [a nice example thereof is the interlocking shish-kebab structure as obtained via a very well controlled, directed crystallization in supercooled melts, see Odell et al. (1985), Chap. 4 of this Volume] drawing in the solid state is the only way to approach maximum orientation. The reason is that two prerequisites for orienting flexible macromolecules exist: first, the product of the deformation rate and the relaxation time should be larger than one, in order to overcome the natural tendency of polymers to coil up, and second, the prod-

uct of the deformation rate and the deformation time, i.e., the total deformation, should be large enough to get full extension of the chains. In the solid state, the first requirement is easily met, given the long relaxation times below the melting temperature. However, the second requirement produces severe limitations, and naturally, there is a molecular weight dependent limit to the drawing, even at temperatures approaching the melting temperature. In apolar polymers with relatively weak van der Waals intermolecular interactions, even within the crystals, these constraints are caused by the presence of the entanglement network. They can be removed by the crystallization of polymers from dilute or semi-dilute solutions. Remarkable in this respect is the fact that the first strong PE fibers were made from stirred, seeded, supercooled solutions in which a gel was formed close to the rotor, from which a fiber was drawn using a seed that created a strong, elongational, orienting flow near its tip (Pennings et al., 1970; Zwijnenburg and Pennings, 1975).

As a consequence of the above, all oriented structures are (in practice) nowadays obtained in the solid state (see Chaps. 11 and 16 of this Volume). The most extreme example is the rather academic single-crystal-drawing, using coextrusion techniques with split billets, as developed by Kanamoto and co-workers [see, e.g., Kanamoto et al. (1983, 1984)]. High draw ratios are realized and the mechanical properties reach their upper limit in terms of the maximum crystal modulus as measured by X-ray scattering [see, e.g., Nakamae and Nishino (1991)]. A much more practical technique is the so-called gel-spinning process, where semi-dilute solutions of UHMWPE are continuously spun via a dry- or air-gap (dry–wet) spinning process, and the gel formed upon cooling, which is accompanied by crystallization, is the intermediate that arrests the disentangled state of the polymeric material [see, e.g., Smith et al. (1979), Smith and Lemstra (1980a, b, c, 1982), Smith et al. (1981), Lemstra et al. (1987)]. Even after removal of the solvent, the disentangled precursor fibers can be postdrawn in the solid state to HPPE (high performance polyethylene fibers). Impressive mechanical properties in terms of specific strength and modulus are today realized in continuous industrial processes.

In their final application, e.g., fishing lines, nets, wovens for impact protection, and composites, some of the properties of the original fibers are lost, but moreover, the heat resistance and especially the dimensionality of the fibers limits their applicability. This is mainly reflected in the poor compressive and shear strengths of some of the high performance fibers, which is directly related to their molecular structure. More specifically, to their secondary bonds. The sequence HPPE (1D), aramids (1.5D), carbon (2D), and glass (with 3D covalent bonds) reveals their compressive strength and creep resistance (Govaert, 1990; Bastiaansen, 1991; Peijs, 1993). As a consequence, only the latter fibers are generally used in structural applications, whereas the first ones give the best impact protection, and only limited adhesion to the matrix of the composite is necessary in this case. For further details, see Peijs (1993), De Kok (1995), De Kok and Meijer (1996), and De Kok and Peijs (1996). Especially in De Kok's thesis, the attention is focused on the transverse properties of composites, which often limit their applicability. Interestingly, the use of reactive solvents in composite applications with thermoplastic matrices offers new routes to design interfaces between the fibers and the matrix, and to tune both their thickness and their (eventually rubbery) properties (see Figs. 1-50 and 1-51).

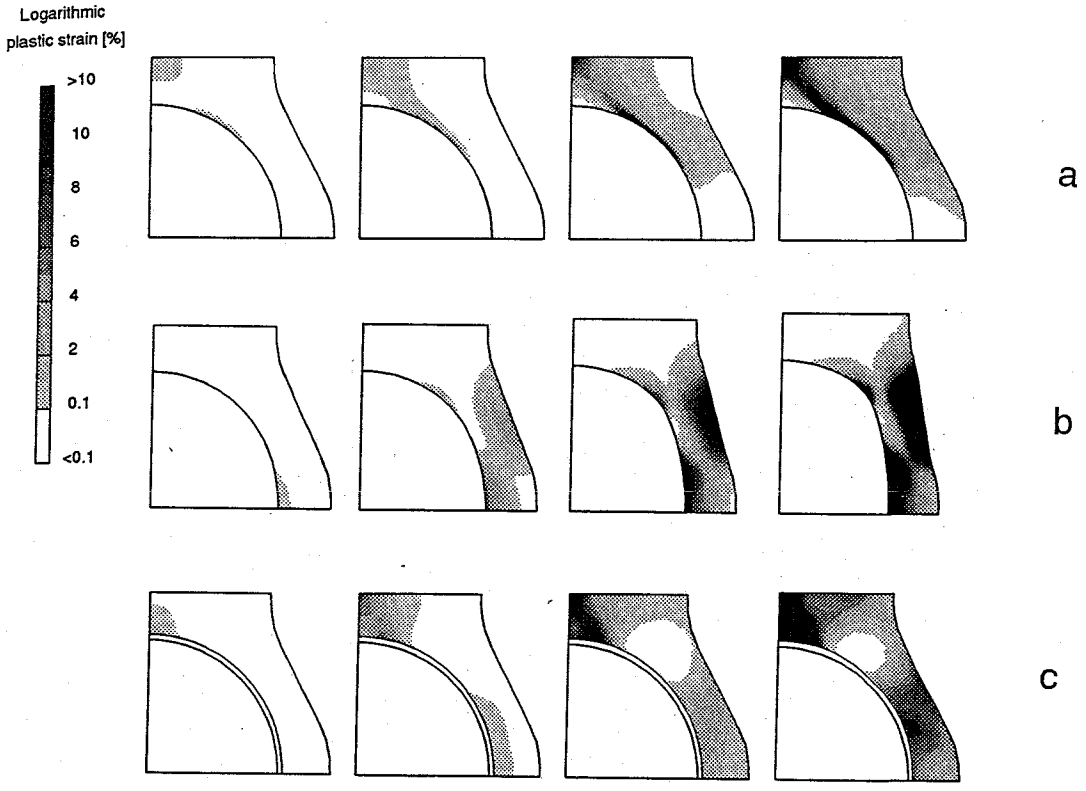

Figure 1-50. Plastically deformed areas in (a) carbon fiber, (b) rubber fiber, and (c) rubber-coated carbon fiber reinforced composites, with a hexagonal fiber array, at different percentages of the transverse strain (De Kok, 1995).

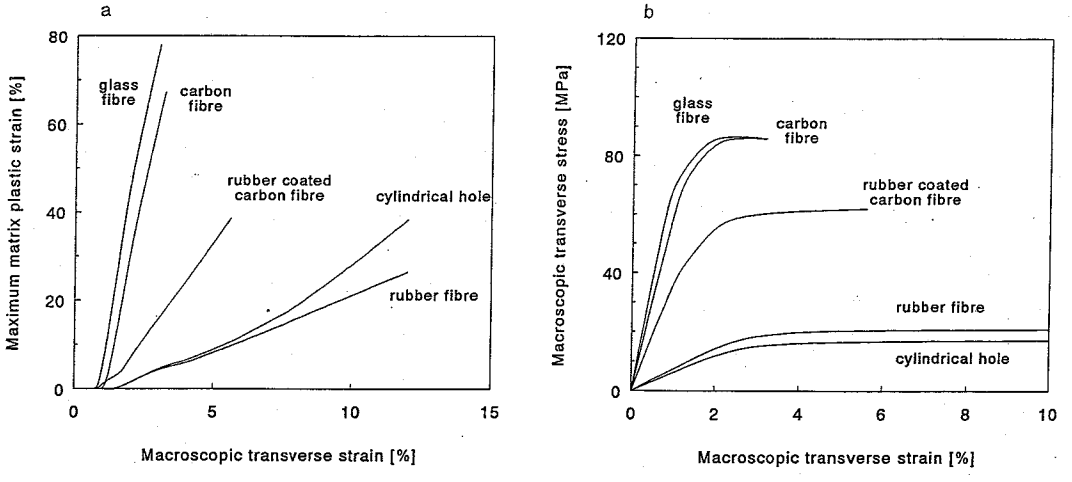

Figure 1-51. (a) Maximum local plastic strains in fiber composites as a function of the transverse strain applied, and (b) calculated stress-strain curves (De Kok, 1995).

The concept of (ultra)drawing of polymers via control of their entanglement structure proved to contain the key to the understanding of their mechanical properties, in general, and toughness, in particular, even for unoriented amorphous polymers. This brings us to a short review on toughness enhancement.

1.5.3 Ultimate Toughness

As stated above, product development at the large research laboratories of polymer manufacturers is often aimed at reaching the best compromise between processability and mechanical properties. To be more specific: to compromise between stiffness and strength on the one hand and impact properties on the other, especially in the development of engineering plastics that are used in structural applications. Various methods are used to control the molecular structure, by changing the flexibility of the polymer backbone and of the (sub)micron structure, or by blending different polymers, e.g., with a large difference in T_g. The general problem is that a large number of internal and external variables influence the toughness of the resulting system and, more seriously, that, as a result, experience obtained with one particular polymer system can rarely be used for another. Consequently, a lot of empirical knowledge exists which is difficult, if not impossible, to transfer to the next generation of researchers, and too many nonconclusive experiments are carried out. Hence the development time and the time-to-market increase unnecessarily. The main reason for this is that the problems met in "jumping scales" are not yet solved, i.e., it is relatively unknown how events on the molecular and microstructural scale influence the resulting properties on the macroscopic continuum level and vice versa. In retrospect, the secret of a material's behavior is contained in how the strong localizations of strain that naturally occur can be controlled prevented from developing into a catastrophic event, like a crack. The introduction of small rubbery particles, which should be able to cavitate, in, e.g., a glassy matrix, provides stress concentrations and, as a consequence, localized plastic flow occurs before the breaking stress of the matrix material is reached. Given the large number, typically 10^{10} per cm^3, of small, typically 1 μm in diameter, weak inclusions ("holes"), multiple crazing or shearing mechanisms are introduced which finally yield volume deformation rather than in-plane deformation (e.g., behind a macroscopic notch) with impact values of 10^5 J/m^2, as compared to the 1 J/m^2 which is roughly the theoretical work to break an interface made out of strong covalent bonds only.

It is the control of these mechanisms that contains the secret of successful product development in tough engineering polymer systems. Interesting in this respect is that, compared to a completely covalently bonded system, like diamond, the replacement of a large number of the strong covalent bonds by weak van der Waals bonds (with a bond strength that is typically only 10^{-5} that of the covalent bond), thus changing diamond into polyethylene for example, yields a 10^{10} times increase in the work-to-break. It is clear that volume deformation is the cause and that this is controlled by the fact that only the weak intermolecular secondary bonds are allowed to break, while the strong covalent bonds in the polymer backbone survive and give rise to "strain hardening" at some distance from the growing strain localization induced by the plastic flow. The oriented fibrils that occur in crazes, bridging the crack, give a good illustration of this principle, but similar arguments hold for the oriented molecules in shear bands. Basical-

ly it could be stated that the control of microdeformation in material systems, where mainly one bond type prevails, without exception should be realized via the introduction of surviving crack-bridging elements. Metal fiber reinforced metals, or ceramic fiber reinforced ceramics are the logical consequence, but even the stones added to concrete introduce a similar mechanism.

As an illustration, Fig. 1-52 shows the development of crazes in a polystyrene (PS) tensile bar tested at different deformation rates. The number of crazes that occur, before one of them develops into a macroscopic crack, increases with increasing deformation rate; however, their number is limited, and brittle behavior results. As an illustration of what might happen on a microscale, Figs. 1-53 and 1-54 show the deformations of (at least if unnotched) macroscopically tough polycarbonate (PC) plates with macroscopic holes of different sizes and in different packing orders. Clearly, localizations influence each other and the macroscopic response of the system depends on the threshold of percolation of the deformable areas. Figure 1-55 shows an example of the calculated deformation in one of these systems.

In order to model the deformation behavior in real systems in terms of the local deformation on the microscale, the number of mechanisms involved demand special numerical techniques where either a homogenization procedure is adapted, using a nonlocal constitutive model on the macroscopic level [see, e.g., Vosbeek (1994) and Vosbeek et al. (1997)], or the so-called "multi level finite element model" should be used (Smit, 1996; Smit et al., 1997). This is, however, still an area which requires a lot of research, and from now we will focus on the ultimate toughness concept, as introduced, amongst others, by Van der Sanden (1993), Van der Sanden et al. (1993 a, b, 1994 a, b) and Van der Sanden and Meijer (1993, 1994 a, b); Chap. 12 of this Volume.

A breakthrough in our understanding of the deformation and failure of polymer systems originated from the work of Kramer's group in Cornell, who carefully measured the maximum drawability realized in extremely localized deformation

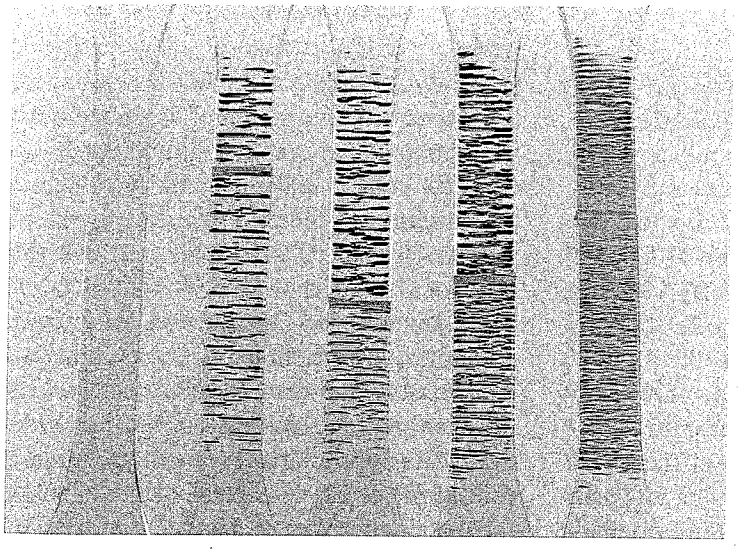

Figure 1-52. Crazes in a PS test bar, tested at (from left to right) 10^{-4}, 10^{-3}, 10^{-2}, and 10^{-1} s^{-1} (Smit, 1996).

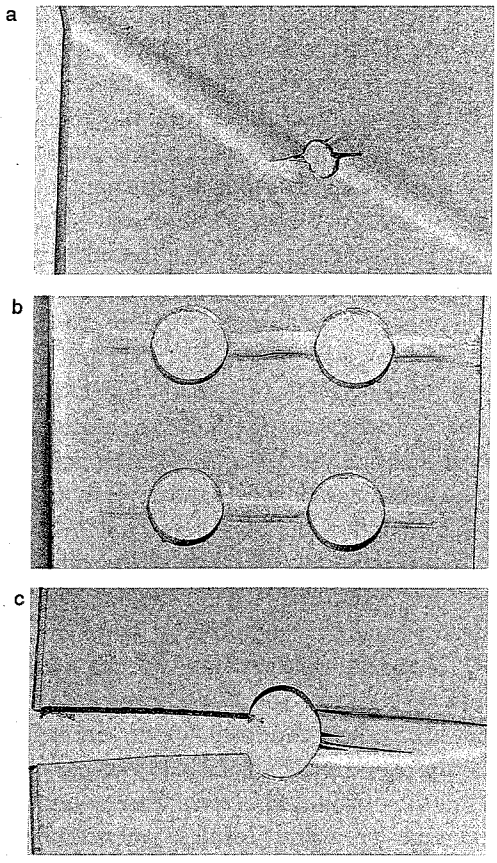

Figure 1-53. Macroscopic shear band development in a PC test plate with (a) one hole, (b) four holes, and (c) a rounded notch (Smit, 1996).

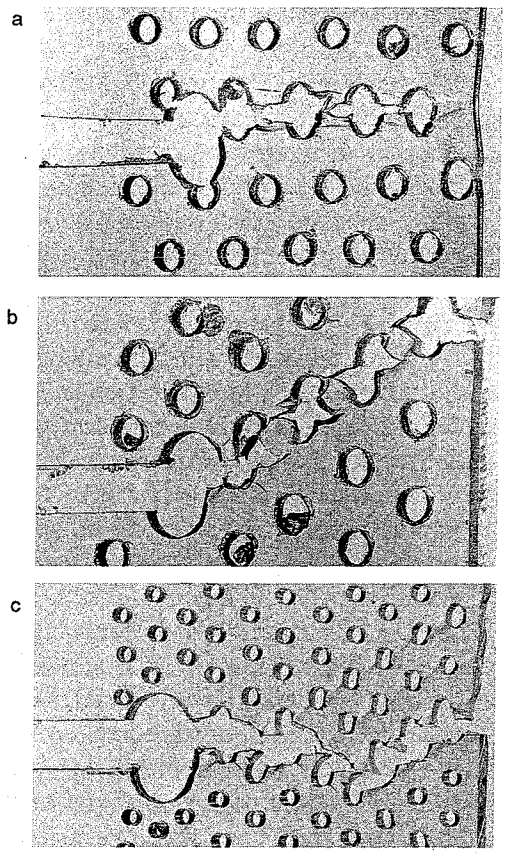

Figure 1-54. Deformation behavior in PC with holes beyond a rounded notch, with (a) a square (b) a hexagonal stacking, and (c) with more, smaller holes, but with an equal volume fraction of holes (Smit, 1996).

zones like crazes and shear bands [see Donald and Kramer (1982 a, b, c) and Henkee and Kramer (1984, 1986)]. A comparison of these results with those obtained on the constraints present for ultradrawability (a challenging discussion during a visit of Kramer to Smith and Lemstra in the early 1980s at the DSM central laboratories in Geleen, The Netherlands, proved to be useful for that purpose), revealed that locally the maximum drawability originating from the physical network was indeed realized. This maximum drawability of polymer networks can be measured by removing the secondary bonds by temperature rather than by stress, thus measuring the height of the rubber plateau modulus above the T_g and applying classical rubber elasticity theory to relate this modulus to the effective entanglement density (Tervoort, 1996). This density is the reciprocal of the molecular weight between entanglement points, M_e, or alternatively the molecular weight between crosslinks in thermosets, M_c, which directly determines the maximum drawability of the network; this scales approximately with the square root of M_e or M_c. As already stated above, this result completely changed the focus of

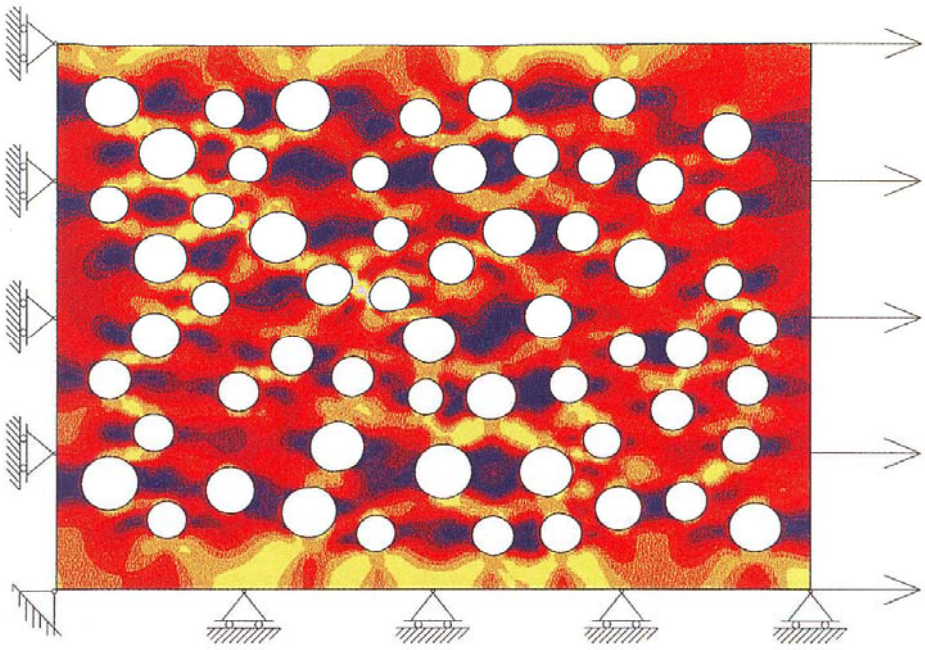

Figure 1-55. Calculated deformation in a PC plate containing holes (Smit, 1996).

research via a change of the general understanding of the deformation of polymer systems, and moreover, it changed the targets on material development, since the attention since then has been focused on the question: "How to avoid catastrophic localizations?" Exaggerating it could consequently be stated that all polymers can principally be characterized by only one parameter, their network density, and that, e.g., a polymer like polystyrene (PS) is so ductile, given its large M_e, that its localization is so pronounced that premature failure always occurs on too localized a scale (see Fig. 1-56).

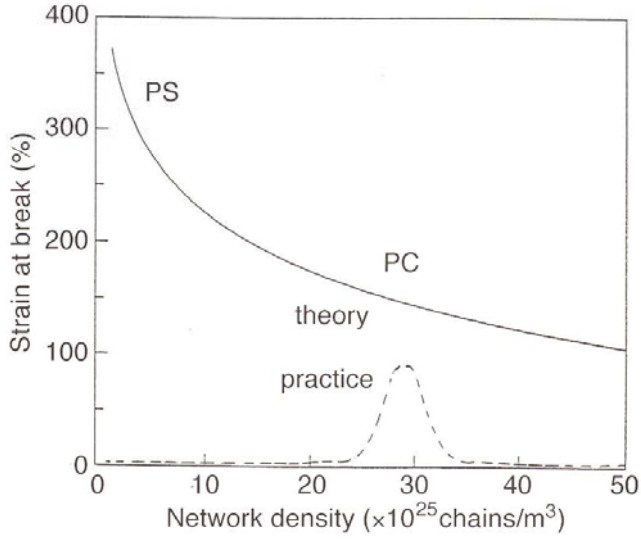

Figure 1-56. Macroscopic drawability (––) and theoretical maximum (–) drawability as a function of the network density of all polymers [after van der Sanden (1993)].

The solution to this problem was more or less straightforward: Make the material so thin, by controlling its microstructure, that its specific thickness (e.g., that of the ductile fibrils within the crazes) is reached throughout. The concept of the material specific thickness was, accordingly, proposed. Processing proved to be able to provide the necessary tools to reach this new goal. By making tapes of alternating nonadhering layers of decreasing thickness, applying the Multiflux technique, or by adding nonadhering core-shell rubbers of typically 200 and 100 nm diameter at increasing volume fractions, the macroscopic strain-to-break of the polymers suddenly increased when the local thicknesses went beyond a material-specific critical thickness and the ultimate toughness was reached. These results are summarized in Figs. 1-57 and 1-58 (see Chap. 12 of this Volume).

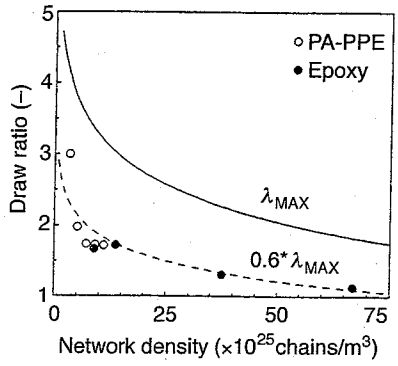

Figure 1-57. Macroscopic ductility reached, as a function of the network density, by decreasing the local material thickness to a value below the material-specific critical thickness (Van der Sanden, 1993).

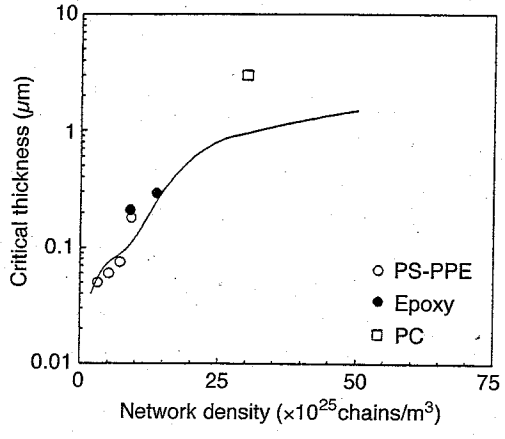

Figure 1-58. Material specific critical thickness as a function of the network density. Solid line: results of a first-order theory (Van der Sanden, 1993).

The goal of the present research in our laboratory is based on this critical thickness, D_{Ic}, between rubbery inclusions ("holes"), by realizing that the smaller "holes", which do not have to cavitate anymore and consequently do not have an "optimal" (read "minimum") size, yield the same critical interparticle distance, D_{Ic}, at much lower volume fractions of the dispersed phase. Consequently, in these polymer systems, called engineering foams (see Fig. 1-59), the ultimate toughness is realized as much as possible without degrading the other mechanical properties, so that the modulus and yield strength of the material are preserved.

The use of reactive solvents provides the necessary requirements to indeed realize these microstructures (Jansen 1996; Chap. 10 of this Volume).

1.5.4 Discussion

In this section it has been shown that, especially with respect to obtaining the ultimate properties of polymers, specific processing routes proved to be of utmost relevance. Basically, the same arguments hold for other nonstructural properties of polymers, such as those in functional applications, e.g., optical clarity, light emission, or intrinsic conductivity. The conjugated polymers developed for these last applications cannot generally be processed as such, but elegant processing methods have been developed, e.g., by Smith and Heeger at UCSB, California, and later at the Uniax Company [see Andreatta et al. (1988, 1990), Tokito et al. (1990, 1991), Moulton and Smith (1992 a, b, 1993), Motamedi et al. (1992), Cao et al. (1992, 1994), Cao and Smith (1993), Yang et al. (1993), and Westerweele et al. (1995)].

1.6 Extruder Modeling

1.6.1 Introduction

Although both this introductory Chapter and the rest of this Volume of this Series on Materials Science and Technology focus on a coupling of the material to be processed and the different processing techniques employed (via, e.g., the study of structure development during flow, reactive extru-

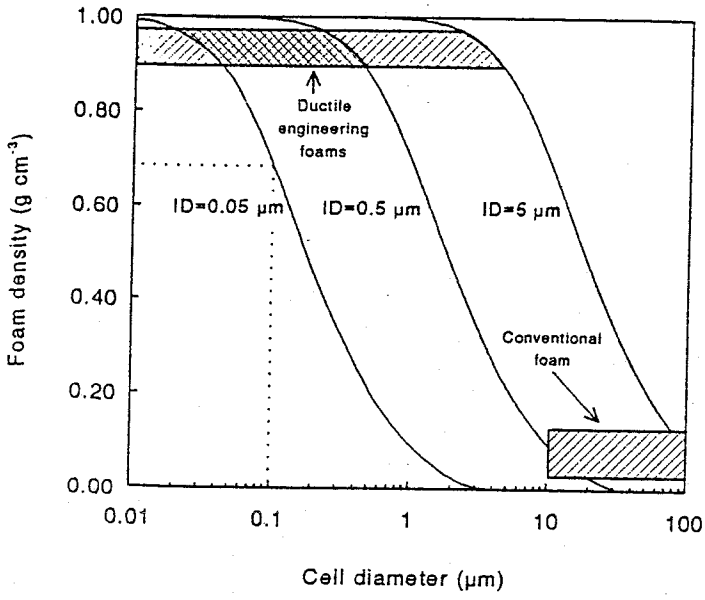

Figure 1-59. Foam density as a function of the size of the dispersed phase ("holes") for given material-specific critical (inter-hole) distances (Van der Sanden, 1993).

sion, phase separation, and crystallization), and aim at predicting product properties (e.g., the short and long term dimensional stability, modulus, strength, and toughness of polymeric systems), at least one section of this introductory chapter should deal with the aspects of extrusion modeling. The majority of practical polymer systems experience an extrusion operation either during the preparation process, e.g., the final devolatilization process following the polymerization reactors or a compounding step, or during the final shaping process. Extruders can be defined as viscosity independent drag pumps with a dramatically low pumping efficiency. The first part of this definition reveals why extruders are frequently used in polymer processing, given the generally high viscosities that prevail, while the second part of this definition elucidates some of the disadvantages of extruders, although in plasticating processes most of the heat generated can be used for melting the solid feedstock. Nevertheless, the dangers of unwanted local overheating and the occurrence of large temperature gradients always exist. This is why efficient mixing (homogenizing) elements are frequently employed or why, alternatively, gear pumps are sometimes introduced in the process to pressurize the melt at higher efficiency, thus avoiding too large temperature rises. In this section we will briefly review the developments in plasticating single screw extruders and in closely intermeshing, self-wiping, corotating twin screw extruders. These types of extruders are by far the most frequently used in practical polymer processing.

1.6.2 Single Screws

The theory of single screw extruders is now well established, and our understanding and modeling of the distinct zones, such as solids conveying, melting, melt pumping, and mixing, have finally led to the development of a functional screw design, where the distinct zones are geometrically separated (see Fig. 1-60).

Despite numerous improvements in the theory, developed over the years, the origi-

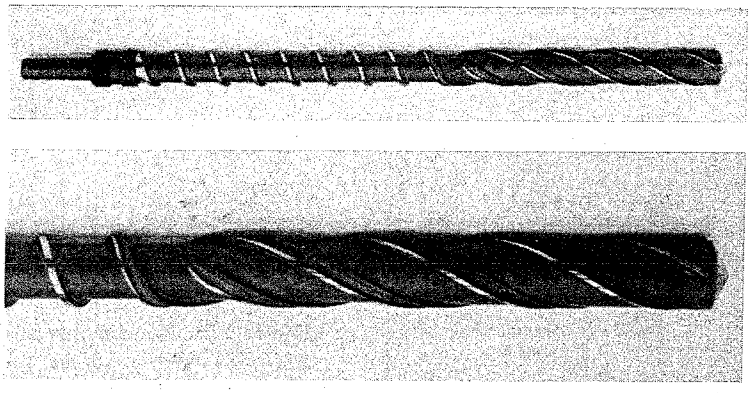

Figure 1-60. Functional screw design in plasticating single screw extruders showing the feed section with one channel, the optimal square pitch, and the three-channel-pair melting section with three solids conveying and melt channels separated by an extra flight (Meijer, 1980).

nal first-order models for the feed section (Darnell and Mol, 1956), the melting section (Tadmor, 1966), and the metering section (Anonymous, 1922; Rowell and Finlayson, 1928), are still useful for a general understanding. Based thereupon, axially and helically grooved feed sections have been developed, especially by the group of Menges at IKV, Aachen, Germany, during the 1970s and 1980s. Efficient multichannel melting sections with a larger (than the "square" screws which are optimal in the solid conveying section) pitch and obtaining complete phase separation via the addition of an extra flight, combined with maximum compression in the solid plug channels and decompression in the melt channels, were developed in the same period by the group of Ingen Housz in Twente, The Netherlands, and by Grünschloss at IKT, Stuttgart, Germany. These concepts of functional screw design should be combined with efficient homogenizers, e.g., the multichannel Maddock type mixers, or even better, the CTM (the cavity transfer mixer), as originally developed by Barmag, Germany, and later by Rapra, England, and improved with respect to its design in Twente, The Netherlands. For a detailed treatment, see, e.g., Meijer (1980), Ingen Housz and Mei-jer (1981 a, b), and Rauwendaal (1986), who copied these analyses in his book on extrusion, and Verbraak and Meijer (1989), who tested modern screw design in the practice of injection molding, including the CTM (Verheijen, 1988). It is interesting that these approaches are now gradually finding their way into practice, not least by the extra stimulation of the regular VDI courses on "Single Screw Extruders, Basic Principles and System Optimization", as organized by Wortberg [see Wortberg (1991)]. The simulation code REX, "Rechnerunterstützte Extrusions Auslegung", developed by Potente's group in a multi-sponsored research program, executed in Paderborn, Germany, summarizes the existing knowledge on screw design and can be considered as a simple, but user-friendly, development tool.

1.6.3 Twin Screws

Apart from the rotating and axially oscillating Buss-cokneader, which introduces a unique mixing operation, generated by the relative motion of the pins in the barrel wall that weave through the screw channel [see, e.g., Elemans (1989), Elemans and Meijer (1990), and Elemans (1994)], and which has found its characteristic applications in, e.g., food processing and polymer blending, especially of temperature-sensitive poly-

mers or reactive systems, the only frequently used compounding and devolatilization extruder is the closely intermeshing, self-wiping, corotating twin screw extruder [see e.g., White (1990 a) for an extended review]. These types of extruder are based on the building block principle and their variety is, consequently, enormous and they can in principle be designed for many different tasks. This flexibility in screw design and barrel choices evokes a large number of experiments in practice, in order to optimize the systems under consideration for their specific task. This fact provided the need for a comprehensive model, in order to predict some of the main aspects of the screw performance. Simple models were derived [see, e.g., Meijer and Elemans (1988), David et al. (1994), and White (1990 a)]. The basic outcome of models like these is that they can predict the lengths of those parts of the screw that are completely filled, dependent on the screw design chosen and the operating conditions, such as metered throughput and screw speed. Given the large difference in mechanical energy conversion in the partly filled channels compared with that of those that are completely filled, useful predictions are obtained for the critical screw speeds (below which vent ports overflow), the average residence time, the power requirements, the specific energy used, and as a consequence, the temperature rise of the melt during extrusion, provided that nonisothermal models are used [see, e.g., Meijer and Elemans (1988)].

As a result, a lot of the usual trial and error could in principle be avoided. More practical is the fact that, based upon these insights, elementary scaling concepts could be derived. These concepts reveal why in practice problems are often met if results from experiments on typical laboratory scale extruders must be transferred to the large scale of production plants and vice versa [see Elemans and Meijer (1994)]. In summary, the problems encountered stem in all but the rather rare adiabatic cases from the problems met in obtaining a similar temperature development in both the small and the large extruder and, consequently, in obtaining melt temperature control. Given their difference in surface-to-volume ratio, yielding a different heat exchange with the surroundings, specific scaling laws for equivalent temperature development exist which basically differ from the scaling laws for constant mixing, and generally lead to disappointing scaling factors for the attainable throughput on the larger machines. The different scaling strategies, following from different requirements, clearly elucidate the problems that can be expected and help engineers to make proper choices for their test conditions and plant layout. Of course, these results are only indicative. Quantitative predictions of the differences to be expected, and the effects of the different possible measures that can be adopted to overcome these problems, at least partly, can only originate from full nonisothermal modeling. Improvements in the basic models must still be strived for [see, e.g., White (1990 a) for a detailed survey].

An interesting consequence of the present understanding of the working principles of these kinds of extruders is that the variety of screw elements available only serves to change the pumping characteristics, locally, i.e. the throughput–pressure gradient relation, and thus helps to control the filled lengths and the overall residence time. Thus mixing is only indirectly controlled. This could have been concluded before, since the cross section of, e.g., positive or negative transport elements with different pitch angles, and positive, negative, and neutral kneading blocks, etc., is exactly the same and geometrically predicted by the self-wiping requirements. These requirements can

be combined with the urgent need for miniaturization in product development, eliminating this influence of screw design on the residence time, as occurs in every continuous extrusion operation, by designing a small, recirculating mixing device. Attempts to develop such useful devices were started in the early 1980s at DSM Central Laboratories in Geleen by Meijer and Martens, the last as the chief designer, using in the first instance a recirculating single screw extruder without (generation 1) and with (generation 2) an internal (Sulzer) static mixer. Independently, a similar device was constructed by Macosko's group in Minnesota. Since these types of extruder proved to seriously suffer from cleaning difficulties, it was decided to make use of the self-cleaning properties of corotating twin screw extruders. Martens proposed a basic design of a conical version in order to reduce the contents and still be able to design a bearing and thrust system, which was over the years improved by Martens and Bulters at DSM, Geleen (generation 3) and by Meijer and Garenfeld at CPC, Eindhoven (generation 4) (see Fig. 1-61).

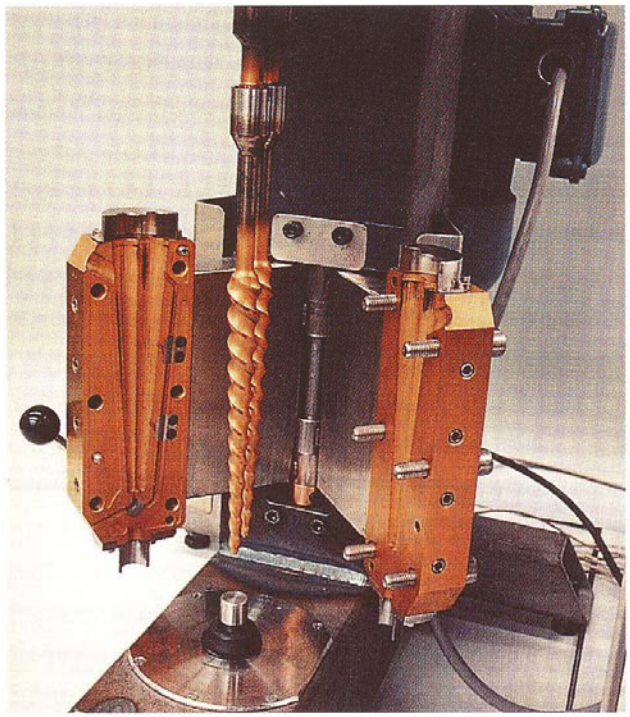

Figure 1-61. Mini-mixer, allowing for mixing or dissolving 1, 3, or 5 g of material (CPC Eindhoven, 1995).

A number of prototypes have been build today, and they are used by different research groups all over the world and prove to be successful and efficient, since only (at choice) 1, 3, or 5 g of material is needed, while the main characteristics of intensive mixing and/or dissolution are preserved. The small material samples from these devices can, subsequently, be molded into test plates or bars, or they can be spun directly into fibers. At DSM, Geleen, Bulters and Martens even designed a miniature injection molding device which can be combined with the mini-mixer, allowing for the production of a few test bars out of each batch.

1.6.4 Discussion

In the last few decades, a lot of attention has been paid to the modeling of extrusion processes, focusing on obtaining a qualitative and quantitative understanding of the (local) working principles. The theory of single screw extruders is relatively well established, but suffers from the uncertainties that naturally occur when the solid bed starts to be converted into a (initially highly viscous) liquid by pressure-, friction-, and temperature-induced melting. Between the pumping characteristics of the solids conveying zone, which are based on friction and consequently yield a wall shear stress that is proportional to the absolute value of the local pressure, and those of the melt conveying zone, large differences exist. In the latter the wall shear stress is only related to the viscosity and to the local velocity gradient (which is large in the initial stages of melting given the thin layers present), and not to the absolute pressure. As a consequence, a consistent model of the whole extruder screw is generally still

lacking. This is mainly due to the large pressure gradients that can practically be realized just at the end of the solid conveying section, especially if grooved feed sections are used, yielding the characteristic and unique pressure build-up capacity of these sections. A small misjudgement in the exact axial position of the solid-to-melt transition at the barrel wall gives rise to a substantial change in the pressure gradients and thus to the pressure build-up capacity, and gives a large error in the predicted absolute pressure. Thus the pumping characteristics of the plasticating extruder (as a whole) cannot generally be predicted well. This basic problem is unsolved, even in useful computer models like REX (Rechner unterstützte EXtruder Auslegung) (Wortberg, 1991), which are currently being improved, e.g., by Potente in Paderborn. A second, more scientific, problem is the missing knowledge of the exact deformation of the solid bed which contains large temperature gradients and is subjected to large shear and pressure forces, and might even break up under tension. This deformability determines the pressure gradient in the melting section and the melting length required to a great extent (Meijer, 1980). This, again, prevents a prediction of the accurate total pumping characteristics of plasticating extruders.

The theory of corotating twin screw extruders and oscillating and reciprocating single screw extruders with pins through the barrel wall should be improved by adapting a full 3D model. In particular in the intermeshing section, where one screw takes over the material from the neighboring screw, the details of the flow are extremely important, not only for predicting the local transport characteristics, and thus the pressure gradients, but more with respect to the exact folding and stretching that occurs here, which is of the utmost importance for efficient mixing. Moreover, these models should necessarily be nonisothermal, and sometimes it is important to incorporate the details of micro-mixing and/or devolatilization into the overall analysis.

1.7 Concluding Remarks

In this introductory chapter it has been demonstrated that polymer processing is an interesting, broad, and multidisciplinary area of research. Especially if the focus is on predicting product properties and not solely on the description of process parameters and the prediction of typical process-related parameters such as the pressure, torque, and power requirements, or clamping forces, the position and number of gates to control those of weld lines, etc. The reason is that in this case the necessary coupling with typical material parameters, such as described by their constitutive behavior, and with local processes that occur, such as micro-mixing or (the opposite) phase separation and coalescence, requires that the normal methods of the researchers in this area (advanced 3 D, nonisothermal, non-Newtonian, transient, mathematical models) have to be extended to those of the polymer physicists (theoretical and practical rheology and rheometry, composition and prediction of phase diagrams, inclusion of the kinetics in the local processes), yielding interesting challenges for coupling the macroscopic flow field with the microscopic processes. The basic reason for this is that in polymer technology neither the chemistry, nor the production technology, nor the final design solely determine the product properties. The whole trajectory from polymer synthesis, via polymer physics, polymer processing, and design proves to be relevant, and each discipline has its own input in the final result. A newly synthesized polymer that cannot be processed will find lim-

ited applications. More important, however, is that during processing most of the final material properties can often be obtained, or the materials themselves can be polymerized, given the large flexibility of the intermediate fluid state of matter that is often present at intermediate temperatures during processing. Besides, the two basic types of bond present in polymers, with their strong intramolecular covalent bonds in the main chain and weak secondary intermolecular bonds in between the chains, make these materials unique, not only during processing (the physical network of chains provides the melt strength necessary for drawing, spinning, blowing, or vacuum forming operations), but also in their final applications. The ultimate properties of polymers in terms of modulus, strength, and impact resistance are often uniquely obtained via specific processing routes and clearly illustrate this particular behavior and the opportunities that polymers provide. Basically, nature is built up from polymers. Only, nature uses much more advanced synthesis routes, is mainly based on hydrogen bonding, and makes maximum use of the self-organizing possibilities of macromolecules.

In the successive chapters of this Volume, the details of the different aspects of processing for properties, as introduced in this Chapter, are elucidated in more detail. The Volume basically consists of four distinct parts: 1) Introduction, 2) Structure Development during Flow, 3) Reactive Processing, and 4) Applications. Of course, many limitations were necessary during the composition of this Volume, but the contents cover the total area of interest to a great extent.

1.8 References

Abid, S. (1993), Ph. D. Thesis, Inst. Fluid Mech., Toulouse, France.

Abid, S., Chesters, A. K. (1994), *Int. J. Multiphase Flow., 20,* 613.

Agassant, J. F. (1991), *Polymer Processing, Principles and Modeling.* Munich: Hanser.

Allan, P. S., Bevis, M. J. (1992), SCORTEC pat. GB 2170-140-B.

Andreatta, A. Cao, Y., Chiang, J. C., Smith, P., Heeger, A. J. (1988), *Synth. Met. 26,* 383.

Andreatta, A., Heeger, A. J., Smith, P. (1990), *Polym. Commun. 31,* 249.

Anonymous (1922), *Engineering, 114,* 606.

Arnold, F. E., Tsai, T. T., Hwang, W. F. (1989), *J. Polym. Sci., Polym. Chem. Ed. 27,* 2839.

Arnold, F. E., Wallace, S. J., Tan, L. S. (1990), *Polymer 31,* 2411.

Astarita, G., Marrucci, G. (1974), *Principles of Non-Newtonian Fluid Mechanics.* New York: McGraw-Hill.

Baaijens, F. P. T. (1991), *Rheol. Acta 30,* 284.

Baaijens, F. P. T. (1993), *J. Non-Newtonian Fluid Mech. 48,* 147.

Baaijens, F. P. T. (1994a), *J. Non-Newtonian Fluid Mech. 51,* 141.

Baaijens, F. P. T. (1994b), *J. Non-Newtonian Fluid Mech. 52,* 37.

Baaijens, J. P. W. (1994c), Ph. D. Thesis, Eindhoven.

Baaijens, F. P. T., Douven, L. F. A. (1990), in: *Integration of Theory and Applications in Applied Mechanics:* Dijksman, J. F., Nieuwstadt, F. (Eds.). Dordrecht: Kluwer, pp. 73–90.

Baaijens, F. P. T., Baaijens, J. P. W., Peters, G. W. M., Meijer, H. E. H. (1994), *J. Rheol. 38 (2),* 351.

Baaijens, J. P. W., Peters, G. W. M., Baaijens, F. P. T., Meijer, H. E. H. (1995), *J. Rheol. 39,* 1243.

Bastiaansen, C. W. M. (1991), Ph. D. Thesis, Eindhoven.

Berger, W., Kummerlöwe, C., Henze, A. (1993), *Polym. Adv. Technol. 4,* 385.

Berghmans, S. (1995), Ph. D. Thesis, KUL, Leuven.

Bernhardt, E. C. (1974), *Processing of Thermoplastic Materials.* New York: Reinhold.

Bevis, M. J. (1994), *Polymer 35,* 2480.

Bevis, M. J., Allan, P. S., Holden, A., Busse, B., Diener, L. (1992), *Kunststoffe 82,* 135.

Bird, R. B., Stewart, W. E., Lightfoot, E. N. (1960), *Transport Phenomena.* New York: Wiley.

Bird, R. B., Curtiss, C. F., Armstrong, R. C., Hassager, O. (1987), *Dynamics of Polymeric Liquid, Vol. 1: Fluid Mechanics, Vol. 2: Kinetic Theory.* New York: Wiley.

Boshouwers, G., van der Werf, J. (1988), Ph. D. Thesis, Eindhoven.

Braun, D., Hartwig, C., Reubold, M., Soliman M., Wendorff, J. H. (1993), *Macromol. Chem. Rapid Commun. 14,* 663.

Brook, A. N., Hughes, T. J. R. (1982), *Comput. Methods Appl. Mech. Eng. 32,* 199.

Brown, R. A., McKinley, G. H. (1994), *J. Non-Newtonian Fluid Mech. 52,* 407.

Brucato, V., Piccarolo, S., Titomanlio, G. (1993), *Macromol. Chem., Macromol. Symp. 68,* 245.
Cao, Y., Smith, P. (1993), *Polym. Commun. 34,* 3139.
Cao, Y., Smith, P., Heeger, A. J. (1992), *Synth. Met. 48,* 91.
Cao, Y., Colaneri, N., Heeger, A. J. Smith, P. (1994), *Appl. Phys. Lett. 65,* 2001.
Caspers, L. W. (1995), Ph. D. Thesis, Eindhoven.
Cheng, L. P. (1993), Ph. D. Thesis, Columbia University of New York.
Cheng, L. P., Soh, Y. S., Dwan, A. H., Gryte, C. C. (1994), *J. Polym. Sci.: Part B, Polym. Phys. 32,* 1413.
Chesters, A. K. (1975), *Int. J. Multiphase Flow 2,* 191.
Chesters, A. K. (1988), in *Euromech, Int. Conf. on Turbulent Two Phase Flow Systems,* Toulouse, France, p. 234.
Chesters, A. K. (1991), *Trans. IChemE 69A,* 259.
Chesters, A. K., Hofman, G. (1982), *Appl. Sci. Res. 38,* 353.
Chiang, H. H., Himasekhar, K., Santhanam, N., Wang, K. K. (1991 a), *Heat and Mass Transfer of Solids Proc.,* ASME, HTD 175/MD 25, pp. 133–146.
Chiang, H. H., Hieber, C. A., Wang, K. K. (1991 b), *Polym. Eng. Sci. 31,* 116.
Cintra, J. S. Jr., Tucker, III, C. L. (1994), in: *Proc. 10th Annual Meeting of the Polymer Processing Society* Akron, OH, pp. 208–209.
Corbey, R. M. (1992), WFW Report 91.015, Eindhoven.
Couniot, A., Dheur, L., Dupret, F. (1993), in: *Proc. of the IMA Conference on Mathematical Modeling for Materials Processing 1991:* Cross, M., Pittman, J. F. T., Wood, R. D. (Eds.). Oxford: Oxford University Press, pp. 381–398.
Crevecoeur, G. (1991), Ph. D. Thesis, KUL, Leuven.
Crevecoeur, G., Groeninckx, G. (1990 a), *Bull. Soc. Chim. Belg. 11–12,* 1031.
Crevecoeur, G., Groeninckx, G. (1990 b), *Polym. Eng. Sci. 30,* 532.
Creveoceur, G., Groeninckx, G. (1990 c), *Mater. Res. Symp. Proc. 171,* 165.
Crevecoeur, G., Groeninckx, G. (1991), in: *Integration of Fundamental Polymer Science and Technology-5:* Lemstra, P. J., Kleintjes, L. A. (Eds.). London: Elsevier.
Crochet, M. J., Legat, V. (1992), *J. Non-Newtonian Fluid Mech. 42,* 283.
Crochet, M. J., Davies, A. R., Walters, K. (1984), *Numerical Simulation of Non-Newtonian Flow.* Amsterdam: Elsevier.
Dang, T. D., Evers, R. C. (1991), *J. Polym. Sci., Polym. Chem. Ed. 29,* 121.
Darnell, W. H., Mol, E. A. J. (1956), *SPE J. 12,* 4.
David, B., Sapir, T., Nir, A., Tadmor, Z. (1994), in: *Mixing and Compounding of Polymers.* Manas-Zloczower, I., Tadmor, Z. (Eds.). Munich: Hanser, Chap. 11.
De Kok, J. M. M. (1995), Ph. D. Thesis, Eindhoven.
De Kok, J. M. M., Meijer, H. E. H. (1996), *Composites,* in press.
De Kok, J. M. M., Peijs, A. A. J. M. (1996), *Composites,* in press.
Dell'Aversana, P., Banavar, J. R., Koplik, J. (1996), *Phys. Fluids 8 (1),* 15
Demarmels, A., Meissner, J. (1985), *Rheol. Acta 24,* 253.
Doi, M. (1981) *J. Polym. Sci., Polym. Phys. Ed. 19,* 229.
Doi, M., Edwards, S. F. (1986), *The Theory of Polymer Dynamics.* Oxford: Clarendon.
Donald, A. M., Kramer, E. J. (1982 a), *J. Polym. Sci., Polym. Phys. Ed. 20,* 899.
Donald, A. M., Kramer, E. J. (1982 b), *Polymer 23,* 461.
Donald, A. M., Kramer, E. J. (1982 c), *Proc. 5th Int. Conf. on the Deformation, Yield and Fracture of Polymers,* Cambridge, p. 15.1.
Dotrong, M., Dotrong, M. H., Evers, R. C. (1992), *ACS Polym. Prepr. 33,* 319.
Douven, L. F. A. (1991), Ph. D. Thesis, Eindhoven.
Douven, L. F. A., Baaijens, F. P. T., Meijer, H. E. H. (1995), *Prog. Polym. Sci. 20,* 403.
Dupret, F., Vanderschuren, L. (1988), *AIChE J. 34,* 1959.
Eisenbach, C. D., Fischer, K., Hofmann, J. (1995), *ACS Polym. Prepr. 36,* 795.
Eisenberg, A., Molnar, A. (1992), *Macromolecules 25,* 5774.
Elemans, P. H. M. (1989), Ph. D. Thesis, Eindhoven.
Elemans, P. H. M. (1994), in: *Mixing and Compounding of Polymers:* Manas-Zloczower, I., Tadmor, Z. (Eds.) Munich: Hanser.
Elemans, P. H. M., Meijer, H. E. H. (1990), *Polym. Eng. Sci. 30,* 893.
Elemans, P. H. M., Meijer, H. E. H. (1994), in: *Mixing and Compounding of Polymers:* Manas-Zloczower, I., Tadmor, Z. (Eds.). Munich: Hanser.
Fan, Y., Crochet, M. J. (1995), *J. Non-Newtonian Fluid Mech. 57,* 283.
Fenner, R. T. (1970), *Extruder Screw Design.* London: Illiffe.
Fenner, R. T. (1979), *Principles of Polymer Processing.* London: Macmillan.
Ferry, J. D. (1980), *Viscoelastic Properties of Polymers,* 3rd ed. New York: Wiley.
Fischer, H., Windle, A. H., Keller, A. (1996), *J. Non-Newtonian Fluid Mech. 67,* 241.
Flory, P. J. (1953), *Principles of Polymer Chemistry.* New York: Cornell University Press.
Flory, P. J. (1969), *Statistical Mechanics of Chain Molecules.* New York: Wiley-Interscience.
Fortin, M., Fortin, A. (1989), *J. Non-Newtonian Fluid Mech. 32,* 295.
Franck, A., Meissner, J. (1984), *Rheol. Acta 23,* 117.
Fuller, G. G., Cathey, C. A., Hubbard, B., Zebrowski, B. E. (1987), *J. Rheol. 31,* 235.
Funt, J. M. (1976), *Mixing of Rubber.* Rubber and Plastics Research Association.

Goossens, J. G. P., Rastogi, S., Meijer, H. E. H. (1997), unpublished.
Govaert, L. E. (1990), Ph. D. Thesis, Eindhoven.
Grace, H. P. (1982), *3rd Eng. Found. Conf. Mixing,* Andover, NH, U.S.A. (1971); republished in *Chem. Eng. Commun. 14,* 225.
Graham, T. (1866), *Phil. Mag. 32,* 401.
Grizaud, N., Moldenaers, P., Mortier, M., Mewis, J. (1993), *Rheol. Acta 32,* 218.
Guénette, R., Fortin, M. (1995), *J. Non-Newtonian Fluid Mech. 60,* 27.
Haagh, G. A. A. V. (1996), Internal Report TUE, CPC.
Harra, M., Chen, W. (1996), *ACS Polym. Prepr. 37/1,* 388, 390.
Hayes, R. E. (1991), *Polym. Eng. Sci. 31,* 842.
Helminiak, T. E., Hwang, W.-F., Wiff, D. R., Benner, C. L. (1983), *J. Macromol. Sci., Phys. B22,* 221.
Hendriks, M. A. N., Oomens, C. W. J., Janssen, J. D. (1990), in: *Mechanical Identification of Composites:* Vautrin A., Sol, H. (Eds.). Amsterdam: Elsevier Applied Science, pp. 75–81.
Henkee, G. S., Kramer, E. J. (1984), *J. Polym. Sci., Polym. Phys. Ed. 22,* 721.
Henkee, G. S., Kramer, E. J. (1986), *J. Mater. Sci. 21,* 1398.
Hieber, C. A., Shen, S. F. (1980), *J. Non-Newtonian Fluid Mech. 7,* 1.
Hieber, C. A., Socha, L. S., Shen, S. F., Wang, K. K., Isayev, A. I. (1983), *Polym. Eng. Sci. 23,* 20.
Hinrichsen, G., Rötting, O. (1993), *Angew. Macromol. Chem. 200,* 193.
Hudson, N. E., Jones, T. E. R. (1993), *J. Non-Newtonian Fluid Mech. 46,* 69.
Ingen Housz, J. F., Meijer, H. E. H. (1981 a), *Polym. Eng. Sci. 21 (6),* 352.
Ingen Housz, J. F., Meijer, H. E. H. (1981 b), *Polym. Eng. Sci. 21,* 1156.
Irvine, P. A., Smith, P. (1986), *Macromolecules 26,* 240.
Isayev, A. I. (Ed.) (1987), *Injection and Compression Molding Fundamentals.* New York: Marcel Dekker.
Isayev, A. I. (Ed.) (1990), *Progress in Polymer Processing.* Munich: Hanser.
Janeschitz-Kriegl, H. (1983), *Polymer Melt Rheology and Flow Birefringence.* Berlin: Springer.
Jansen, B. J. P. (1996), Internal Report, CPC, Eindhoven.
Jansen, B. J. P., Meijer, H. E. H., Lemstra, P. J. (1997), unpublished.
Janssen, J. M. H. (1993), Ph. D. Thesis, Eindhoven.
Janssen, J. M. H., Meijer, H. E. H. (1993), *J. Rheol. 37 (4),* 597.
Janssen, J. M. H., Meijer, H. E. H. (1995), *Polym. Eng. Sci. 35,* 1766.
Janssen, J. M. H., Peters, G. W. M., Meijer, H. E. H. (1993), *Chem. Eng. Sci. 48,* 255.
Janssen, L. P. B. M. (1978), *Twin Screw Extrusion.* Amsterdam: Elsevier.
Johnson, C. (1987), *Numerical Solution of Partial Differential Equations by the Finite Element Method.* Cambridge: Cambridge University Press.
Joseph, D. D. (1990), *Fluid Dynamics of Viscoelastic Liquids.* New York: Springer.
Kanamoto, T., Tsurata, A., Tanaka, M., Porter, R. S. (1983), *Polym. J. 15,* 327.
Kanamoto, T., Tsurata, A., Tanaka, M., Takeda, M. (1984), *Polym. J. 16,* 75.
Keller, A., Muller, A. J., Odell, J. A. (1987), *Progr. Colloid Polym. Sci. 75,* 179.
Kennedy, P. (1993), *Flow Analysis Reference Manual,* Moldflow Pty. Ltd., Australia.
Kesting, R. E. (1985 a), in: *Synthetic Polymeric Membranes.* New York: McGraw-Hill.
Kesting, R. E. (1985 b), *ACS Symp. Ser. 269,* 131.
Kesting, R. E., Fritzsche, A. K. (1993), in: *Polymeric Gas Separation Membranes.* New York: Wiley-Interscience.
Koros, W. J., Fleming, G. K. (1993), *J. Membr. Sci. 83,* 1.
Kovacs, A. J., Aklonis, J. J. Hutchinson, J. M., Ramos, A. R. (1979), *J. Polym. Sci., Polym. Phys. Ed. 17,* 1097.
Krasnopolskaya, T. S., Meleshko, V. V., Peters, G. W. M., Meijer, H. E. H. (1996), *Quarterly J. Mech. Appl. Math. 49 (4),* 593.
Krasnopolskaya, T. S., Meleshko, V. V., Peters, G. W. M., Meijer, H. E. H. (1997), *J. Fluid Mech. 538,* 119.
Kummerlöwe, C., Kammer, H.-W. (1990), *Acta Polym. 41,* 269.
Larson, R. G. (1988), *Constitutive Equations for Polymer Melts and Solutions.* Boston, MA: Butterworths.
Lemstra, P. J., Kirschbaum, R., Ohta, T., Yasuda, H. (1987), in: *Developments in Oriented Polymers 2:* Ward, I. M. (Ed.). New York: Elsevier Appl. Sci., p. 39.
Li, L. et al. (1990), *J. Rheol. 34,* 103.
Liang, E. W., Wang, H. P., Perry, E. M. (1993), *Adv. Polym. Technol. 12,* 243.
Lodge, A. S. (1964), *Elastic Liquids.* London: Academic.
Loeb, S., Sourirajan, S. (1962), *Adv. Chem. Ser. 38,* 117.
Macosko, C. W. (1989), *RIM, Fundamentals of Reaction Injection Molding.* Munich: Hanser, p. 246.
Macosko, C. W. (1994), *Rheology, Principles, Measurements and Applications.* Weinheim: VCH.
Maffetone, P. L., Marrucci, G., Mortier, M., Moldenaers, P., Mewis, J. (1994), *J. Chem. Eng. 180,* 7736.
Manas-Zloczower, I. (1994), in: *Mixing and Compounding of Polymers:* Manas-Zloczower, I., Tadmor, Z. (eds.). Munich: Hanser, Chap. 3.
Manas-Zloczower, I., Nir, A., Tadmor, Z. (1982), *Rubber Chem. Technol. 55,* 1250.
Manas-Zloczower, I., Nir, A., Tadmor, Z. (1984), *Rubber Chem. Technol. 57,* 583.

Marrucci, G., Greco, F. (1993), in: *Advances in Chemical Physics.* Vol. 86: Prigogine, I., Rice, S. A. (Eds.). New York: Wiley, p. 331.
Marrucci, G., Maffetone, P. L. (1993), in: *Liquid Crystalline Polymers:* Carfagna, C. (Ed.). New York: Pergamon, pp. 127–131.
McKelvey, J. M. (1962), *Polymer Processing.* New York: Wiley.
McKinley, G. (1995), private communications.
Meijer, H. E. H. (1980), Ph. D. Thesis, UT, Enschede, The Netherlands.
Meijer, H. E. H., Elemans, P. H. M. (1988), *Polym. Eng. Sci. 28(5),* 275.
Meijer, H. E. H., Janssen, J. M. H. (1994), in: *Mixing and Compounding of Polymers. Theory and Practice:* Manas-Zloczower, I., Tadmor, Z. (Eds.). New York: Hanser, pp. 85–148.
Meijer, H. E. H., Venderbosch, R. W., Goossens, J. G. P., Lemstra, P. J. (1996), *High Perform. Polym. 8,* 1.
Meissner, J. (1969), *Rheol. Acta 8,* 78.
Meissner, J. (1971), *Rheol. Acta 10,* 230.
Meissner, J. (1992), *Macromol. Chem. Symp. 56,* 25.
Meissner, J., Hostettler, J. (1992), in: *Theoretical and Applied Rheology:* Moldenaers, P., Keunings, R. (Eds.). Amsterdam: Elsevier, p. 938.
Meissner, J., Raible, T., Stephenson, S. E. (1981), *J. Rheol. 25 (1),* 673.
Meissner, J., Stephenson, S. E., Demarmels, A., Portman, P. (1982), *J. Non-Newtonian Fluid Mech. 11,* 221.
Meleshko, V. V., Peters, G. W. M. (1996), *Phys. Lett. A216,* 87.
Meleshko, V. V., Grinchenko, V. T., Isaeva, T. L. (1991), *Dokl. Akad. Nauk Ukr. SSR Ser. A N8,* 64 (in Ukrainian).
Middleman, S. (1968), *The Flow of High Polymers.* Munich: Hanser.
Middleman, S. (1977), *Fundamentals of Polymer Processing.* New York: McGraw-Hill.
Mikkelsen, K. J., Macosko, C. W., Fuller, G. G. (1988), in: *Proc. 10th Int. Congress on Rheology,* Vol. 2: Uhlherr, P. H. T. (Ed.). Sydney, p. 125.
Moldenaers, P., Fuller, G., Mewis, J. (1989), *Macromolecules 22,* 960.
Moldenaers, P., Yanase, H., Mewis, J., Fuller, G. G., Lee, C. S., Magda, J. J. (1993), *Rheol. Acta 32,* 1.
Motamedi, F. et al. (1992), *Polym. Commun. 33,* 1102.
Moulton, J., Smith, P. (1992a), *Polymer 33,* 2340.
Moulton, J., Smith, P. (1992b), *J. Polym. Sci., Polym. Phys. Ed. 30,* 871.
Moulton, J., Smith, P. (1993), in: *Handbook of Fiber Science and Technology,* Vol. III, Part C: Lewin, C. M., Preston, J. (Eds.). New York: Dekker, pp. 275–315.
Mulder, M. H. V. (1991), in: *Principles of Membrane Technology.* Dordrecht, The Netherlands: Kluwer.
Munstedt, H. (1975), *Rheol. Acta 14,* 1077.
Munstedt, H. (1979), *J. Rheol. 23,* 421.
Nakamae, K., Nishino, T. (1991), in: *Integration of Polymer Science and Technology.* Oxford: Elsevier, Part 5, p. 121.
Nguyen, K. T., Kamal, M. R. (1993), *Polym. Eng. Sci. 33,* 665.
Noolandi, J., Shi, A.-C. (1996), *ACS Polym. Prepr. 37/1,* 387.
Odell, J. A., Keller, A., Miles, M. J. (1985), *Polymer 26,* 1219.
Oomens, C. W. J., Hendriks, M. A. N., Ratingen, M. R., Janssen, J. D., Kok, J. J. (1993), *J. Biomechanics 26 (4/5),* 617.
Ottino, J. M. (1989), *The Kinematics of Mixing: Stretching, Chaos and Transport.* Cambridge: Cambridge Univ. Press.
Ottino, J. M. (1990), *Annu. Rev. Fluid Mech. 22,* 207.
Ottino, J. M. (1991), *Phys. Fluids A 3,* 1417.
Papathanasiou, T. D., Kamal, M. R. (1993), *Polym. Eng. Sci. 33,* 400.
Pearson, J. R. A. (1985), *Mechanical Principles of Polymer Melt Processing.* London: Elsevier.
Pearson, J. R. A., Richardson, S. M. (Eds.) (1983), *Computational Analysis of Polymer Processing.* London: Applied Science.
Peijs, A. A. J. M. (1993), Ph. D. Thesis, Eindhoven.
Pennings, A. J., van der Mark, J. M. A. A., Booij, H. C. (1970), *Koll. Z. Z. Polym. 236,* 99.
Peters, G. W. M., van der Velden, P. J. L., Meijer, H. E. H., Schoone, P. (1994), *Int. Polym. Proc. 9,* 258.
Petrie, C. J. S. (1979), *Elongational Flows.* London: Pittman.
Piccarolo, S. (1992), *J. Macromol. Sci. B31 (4),* 501.
Piccarolo, S., Sain, M., Brucato, V., Titomanlio, G. (1992), *J. Appl. Polym. Sci. 46,* 625.
Potente, H. (1981), *Auslegen von Schneckenmaschinen Baureihen.* Munich: Hanser.
Rauwendaal, C. (1986), *Polymer Extrusion.* Munich: Hanser.
Reijnierse, C. (1995), WFW Report 95-160, ISBN 90-5258-568-8, Eindhoven.
Rowell, H. S., Finlayson, D. (1928), *Engineering* 126; 249; 385.
Saiu, M., Brucato, V., Piccarolo, S., Titomanlio, G. (1992), *Int. Polym. Proc. 7,* 267.
Schowalter, W. R. (1978), *Mechanics of Non-Newtonian Fluids.* Oxford: Pergamon.
Schunk, P. R., Scriven, L. E. (1990), *J. Rheol. 34,* 1085.
Schunk, P. R., deSantos, J. M., Scriven, L. E. (1990), *J. Rheol. 34,* 387.
Selen, J. H. A. (1995), WFW Report 95.141, ISBN 90-5282-559-9, Eindhoven.
Sitters, C. W. M. (1988), Ph. D. Thesis, Eindhoven University of Technology, The Netherlands.
Smid, J., Albers, J. H. M., Kusters, A. P. M. (1991), *J. Membr. Sci. 64,* 121.
Smit, R. (1996), Internal report WFW, Eindhoven.

Smit, R., Brekelmans, W. A. M., Meijer, H. E. H. (1997), unpublished.
Smith, P., Lemstra, P. J. (1980a), *Polymer 21,* 1341.
Smith, P., Lemstra, P. J. (1980b), *Colloid Polym. Sci. 258,* 891.
Smith, P., Lemstra, P. J. (1980c), *J. Polym. Sci., Phys. Ed. 19,* 1007.
Smith, P., Lemstra, P. J. (1982), *J. Polym. Sci., Phys. Ed. 20,* 2229.
Smith, P., Lemstra, P. J., Kalb, B., Pennings, A. J. (1979), *Polym. Bull. 1,* 733.
Smith, P., Lemstra, P. J., Booij, H. C. (1981), *Polym. Sci., Phys. Ed. 19,* 877.
Spoelstra, A. B. (1992), WFW Report 92.098, ISBN 90-5282-201-8, Eindhoven.
Stone, H. A., Leal, L. G. (1989a), *J. Fluid Mech. 198,* 399.
Stone, H. A., Leal, L. G. (1989b), *J. Fluid Mech. 206,* 223.
Stone, H. A., Leal, L. G. (1990), *J. Fluid Mech. 220,* 161.
Stone, H. A., Leal, L. G. (1994), *Annu. Rev. Fluid Mech.,* 26.
Stone, H. A., Bentley, B. J., Leal, L. G. (1986), *J. Fluid Mech. 173,* 131.
Tadmor, Z. (1966), *Polym. Eng. Sci. 6,* 185.
Tadmor, Z., Gogos, C. E. (1979), *Principles of Polymer Processing.* New York: Wiley.
Tadmor, Z., Klein, I. (1971), *Engineering Principles of Plasticating Extrusion.* New York: Van Nostrand Reinhold.
Takayanagi, M., Ogata, T., Morikawa, M., Kai, T. (1980), *J. Macromol. Sci., Phys. B17,* 591.
Tanner, R. I. (1985), *Engineering Rheology,* London: Oxford University Press.
Tas, P. P. (1994), Ph. D. Thesis, Eindhoven.
Taylor, G. I. (1932), *Proc. R. Soc. (London) A 138,* 41.
Taylor, G. I. (1934), *Proc. R. Soc. (London) A 146,* 501.
Tervoort, T. A. (1996), Ph. D. Thesis, Eindhoven.
Thomson, R. D., Wood, O. C., Zienkiewicz, A. (Eds.) (1989), *Numerical Methods in Industrial Forming Processes.* Rotterdam: Balkema.
Tjahjadi, M., Ottino, J. M. (1991), *J. Fluid Mech. 232,* 191.
Tjahjadi, M., Stone, H. A., Ottino, J. M. (1992), *J. Fluid Mech. 243,* 297.
Tjahjadi, M., Stibe, H. A., Ottino, J. M. (1994), *AIChE J.* 1.
Tokito, S., Smith, P., Heeger, A. J. (1990), *Synth. Met. 36,* 183.
Tokito, S., Smith, P., Heeger, A. J. (1991), *Polymer 32,* 464.
Tomotika, S. (1935), *Proc. R. Soc. (London) A 150,* 322.
Tomotika, S. (1936), *Proc. R. Soc. (London) A 153,* 302.
Tucker III, C. L. (Ed.) (1989), *Fundamentals of Computer Modeling for Polymer Processing.* Munich: Hanser.
Turng, L. S., Wang, V. W. (1991), in: *In Search of Excellence, ANTECH Conference Proceedings,* Vol. 37. SPE, pp. 297–300.
Turng, L. S., Wang, V. W., Wang, K. K. (1993), *J. Eng. Mater. Technol. 115,* 48.
Van der Sanden, M. C. M. (1993), Ph. D. Thesis, Eindhoven.
Van der Sanden, M. C. M., Meijer, H. E. H. (1993), *Polymer 34,* 5063.
Van der Sanden, M. C. M., Meijer, H. E. H. (1994a), *Polymer 35,* 2774.
Van der Sanden, M. C. M., Meijer, H. E. H. (1994b), *Polymer 35,* 2991.
Van der Sanden, M. C. M., Meijer, H. E. H., Lemstra, P. J. (1993a), *Polymer 34,* 2148.
Van der Sanden, M. C. M., Meijer, H. E. H.,. Tervoort, T. A. (1993b), *Polymer 34,* 2961.
Van der Sanden, M. C. M., Buijs, L. G. C., de Bie, F. O., Meijer, H. E. H. (1994a), *Polymer 35,* 2783.
Van der Sanden, M. C. M., de Kok, J. M. M., Meijer, H. E. H. (1994b), *Polymer 35,* 2995.
Van Nieuwkoop, J., Muller von Czernicki, M. M. O. (1997), *J. Non-Newtonian Fluid Metch.,* in press.
Venderbosch, R. W. (1995), Ph. D. Thesis, Eindhoven.
Venderbosch, R. W., Meijer, H. E. H., Lemstra, P. J. (1994), *Polymer 35,* 4349.
Venderbosch, R. W., Meijer, H. E. H., Lemstra, P. J. (1995a), *Polymer 36,* 1167.
Venderbosch, R. W., Meijer, H. E. H.,. Lemstra, P. J. (1995b), *Polymer 36,* 2903.
Verbraak, C. P. J. M., Meijer, H. E. H. (1989), *Polym. Eng. Sci. 29 (7),* 479.
Verheijen, J. (1988), DSM Research Report, NC 88.12566, Geleen (in Dutch).
Vinogradov, G. V., Fikman, V. D., Radushkevich, B. V., Malkin, A. Y. (1970), *J. Polym. Sci. A-2 (8),* 657.
Vleeshouwers, S., Meijer, H. E. H. (1996), *Rheol. Acta, 35,* 391.
von Wrobleski (1879), *Wied. Ann. Phys. 8,* 29.
Vos, E., Meijer, H. E. H., Peters, G. W. M. (1991), *Int. Polym. Proc. 6,* 42.
Vosbeek, P. H. J. (1994), Ph. D. Thesis, Eindhoven.
Vosbeek, P. H. J., Schreurs, P. J. G., Meijer, H. E. H. (1997), unpublished.
Wagner, M. H. (1994), *Rheol. Acta 33,* 506.
Wagner, M. H. (1996), *Polym. Eng. Sci. 36,* 925.
Walters, K. (1992), in: *Proc. XI Int. Cong. on Rheology, Theoretical and Applied Rheology:* P. Moldenaers, R. Kennings (Eds.). Amsterdam: Elsevier.
Westerweele, E., Smith, P., Heeger, A. J. (1995), *Adv. Mater. 7,* 788.
White, J. L. (1990a), *Twin Screw Extrusion, Technology and Principles.* Munich: Hanser.
White, J. L. (1990b), *Principles of Polymer Engineering Rheology.* New York: Wiley.
Wimberger Friedl, R. (1991), Ph. D. Thesis, Eindhoven.

Wortberg, J. (1991), *Einschneckenextruder, Grundlagen und Systemoptimierung,* Düsseldorf: VDI-Gesellschaft Kunststofftechnik.
Yanase, H., Moldenaers, P., Mewis, J., Abetz, V., van Egmond, J., Fuller, G. G. (1991), *Rheol. Acta 30,* 89.
Yang, C. Y., Cao, Y., Smith, P., Heeger, A. J. (1993), *Synth. Met. 53,* 293.
Ziabicki, A. (1976), *Fundamentals of Fibre Formation.* New York: Wiley.
Zoetelief, W. F. (1995), Ph. D. Thesis, Eindhoven.
Zoetelief, W. F., Douven, L. F. A., Ingen Housz, A. J. (1996), *Polym. Eng. Sci.,* in press.
Zwijnenburg, A., Pennings, A. J. (1975), *Colloid Polym. Sci. 452,* 253.

General Reading

Agassant, J. F. (1991), *Polymer Processing, Principles and Modeling.* Munich: Hanser.
Astarita, G., Marrucci, G. (1974), *Principles of Non-Newtonian Fluid Mechanics.* New York: McGraw-Hill.
Bird, R. B., Stewart, W. E., Lightfoot, E. N. (1960), *Transport Phenomena.* New York: Wiley.
Bird, R. B., Curtiss, C. F., Armstrong, R. C., Hassager, O. (1987), *Dynamics of Polymer Liquids, Vol. 1: Fluid Mechanics; Vol. 2: Kinetic Theory.* New York: Wiley.
Crochet, M. J., Davies, A. R., Walters, K. (1984), *Numerical Simulation of Non-Newtonian Flow.* Amsterdam: Elsevier.
Fenner, R. T. (1979), *Principles of Polymer Processing.* London: Macmillan.
Ferry, J. D. (1980), *Viscoelastic Properties of Polymers,* 3rd ed. New York: Wiley.
Isayev, A. I. (Ed.) (1987), *Injection and Compression Molding Fundamentals.* New York: Marcel Dekker.
Isayev, A. I. (Ed.) (1990), *Progress in Polymer Processing.* Munich: Hanser.
Janeschitz-Kriegl, H. (1983), *Polymer Melt Rheology and Flow Birefringence.* Berlin: Springer.
Joseph, D. D. (1990), *Fluid Dynamics of Viscoelastic Liquids.* New York: Springer.
Larson, R. G. (1988), *Constitutive Equations for Polymer Melts and Solutions.* Boston, MA: Butterworths.
Macosko, C. W. (1994), *Rheology, Principles, Measurements and Applications.* Weinheim: VCH.
Middleman, S. (1977), *Fundamentals of Polymer Processing.* New York: McGraw-Hill.
Pearson, J. R. A. (1985), *Mechanical Principles of Polymer Melt Processing.* London: Elsevier.
Pearson, J. R. A., Richardson, S. M. (Eds.) (1983), *Computational Analysis of Polymer Processing.* London: Applied Science.
Rauwendaal, C. (1986), *Polymer Extrusion.* Munich: Hanser.
Schowalter, W. R. (1978), *Mechanics of Non-Newtonian Fluids.* Oxford: Pergamon.
Tadmor, Z., Gogos, C. E. (1979), *Principles of Polymer Processing.* New York: Wiley.
Thomson, R. D., Wood, O. C., Zienkiewicz, A. (Eds.) (1989), *Numerical Methods in Industrial Forming Processes.* Rotterdam: Balkema.
Tucker III, C. L. (Ed.) (1989), *Fundamentals of Computer Modeling for Polymer Processing.* Munich: Hanser.
White, J. L. (1990), *Twin Screw Extrusion, Technology and Principles.* Munich: Hanser.
White, J. L. (1990), *Principles of Polymer Engineering Rheology.* New York: Wiley.
Ziabicki, A. (1976), *Fundamentals of Fiber Formation.* New York: Wiley.